Department of Electrical and Computer Systems Engineering

Technical Report
MECSE-10-2004

Fibre Design for Dispersion Compensation and Raman Amplification

T.L. Huynh and L.N. Binh

MONASH
UNIVERSITY

MONASH UNIVERSITY

DEPARTMENT OF ELECTRICAL AND COMPUTER SYSTEMS ENGINEERING

TECHNICAL REPORT 2004

DISPERSION IN PHOTONIC SYSTEMS

Part I: Fibre Design for Dispersion Compensation and Raman Amplification

Candidate: Thanh Liem Huynh

Supervisor: Le Nguyen Binh

Email: thanh.huynh@eng.monash.edu.au

Department of Electrical and Computer Systems Engineering

Monash University, Clayton 3168 Australia.

I.   Summary

This report presents Part I of three parts of the thesis project "Dispersion in Photonic Systems" which is planned for the degree of Master of Engineering Science with the intention of conversion to the candidature of Doctor of Philosophy in January 2005.

Dispersion issues are critical in optical fibre communications and photonic signal processing systems. In particular, in ultra-long haul and ultra-high speed multi-wavelength transmission (DWDM), the demands for low dispersion and low dispersion slope are very high for transmission bit rate of 40 Gbps and higher. Furthermore, in photonic systems, e.g. phase control array antenna processing using optical fibre as the transmission medium for distribution of phase dependent signals, the fibre dispersion becomes a critical factor. Thus the field of research for the thesis project is named as "Dispersion in Photonic Systems".

The first part of this thesis concentrates on the design of optical fibres with very high and negative dispersion so as to compensate for non-zero dispersion caused by the optical transmission fibres. This type of fibre is called dispersion compensation fibres (DCF). Thus the combined transmission and compensation fibres can be employed in ultra-long haul DWDM optical communications systems.

Further in order to compensate for the attenuation of optical channels transmission over long reach fibre distance, optical amplifiers which are either Erbium-doped fibres amplifiers (EDFA) or Raman optical fibre amplifiers can be utilised. The later type is normally used in conjunction with EDFA and would be implemented in either distributed or lumped configurations. The fibres act as the amplification medium in Raman optical amplifiers. The main issue is which type of fibres should be used, the transmission or the compensation type?

From optical engineering point of view, if optical amplification can be combined with dispersion compensation in the same fibre, savings of optical components and ease of system design would add a significant advantage to long haul optical transmission systems. This is

the main motivation that we select the DCF as the Raman optical amplification medium. We thus present in this Part I report a novel design approach for optical fibres with highly negative and matched dispersion slope for DWDM dispersion compensation and optimization of the fibre parameters for Raman amplification.

A summary of all design parameters and propagation constants is described and employment of different refractive index profiles are considered in the design for DCF such as the W- and triple-clad index profiles with 4 and 7 degree of freedom respectively. The unique and interesting property of non-zero cut off wavelengths of W-fibre is thoroughly discussed. The sensitivity of fibre profiles to the variation of chromatic dispersion in triple clad is also carefully investigated. We define RDS and Kappa value as the figure of merit for the design of combined dispersion - DCF spans. Several profiles designed for upgrading the current system using single-mode fibre (SMF) as well as the modern systems using non zero dispersion shifted fibre (NZ-DSF) are also shown. The matching of dispersion and dispersion slope allows us to conclude that transmission of DWDM channels in the C-band can be implemented over several spans (or thousands of kms of transmission and compensation fibres) without difficulties. Hence the transmission distance is only limited by the total cascaded optical amplification noise.

The design methodology of DCF for discrete Raman amplifier (DCF-DRA) is also comprehensively shown in this study. The doping concentration of an optical fibre influences the refractive index distribution and hence its dispersion characteristics. It also results in different amplification gain via the Raman scattering process. We model the gain coefficient with the approach of using the actually experimental gain and zero-Kelvin Raman cross-section/absorption Raman cross section and the asymptotic approximation of the Raman gain within C-band. In addition, the mode spot-size of an optical fibre contributes to the total average absorption and coupling of the pump and signal power respectively. This aspect has been taken into the design of the DCF fibres. An optimization process has been extensively studied. A quadratic relationship between the dispersion and gain tilt has been formed to permit the optimization of the design of DCF for Raman amplification.

TABLE OF CONTENTS

II. Introduction

For over the last decade, long-haul and high-capacity dense-wavelength-division-multiplexed (DWDM) optical systems have been widely deployed as the result of the rapidly increasing demands for high-speed commercial services and global-network research and military applications. Such the DWDM systems operate at 10 Gbps, 40 Gbps or even higher over transmission fibers of 2000 to 6000 km [1, 2]. With this long-haul distance of signal transmission and the availability of optical amplifiers, dispersion characteristics of the transmission fibers become most critical over other conventional effects such as the attenuation problem in the old systems. It is also inevitable for those high-speed systems to compensate the dispersion slope simultaneously with the dispersion. Besides, nowadays, signals are optically amplified by use of Raman amplifiers (RA) which are based on the Stimulated Raman Scattering (SRS) non-linear phenomenon.

Therefore, the necessity of the compensation for the cumulative dispersion of the long-haul transmission simultaneously with controlling, maximising and flattening the Raman gain are the essential requirement for system design. The dispersion compensation fibre (DCF) is a critical component in every long-haul transmission system, which helps to prevent severe penalties of interference due to anomalous dispersion as well as reducing the nonlinearity effects such as Self-Phase Modulation (SPM) and Cross-phase Modulation (XPM). The properties of DCF such as small effective area and high Germanium (Ge) doping concentration give higher Raman gain efficiency and lower threshold power to excite Raman Amplification. It also gives additional flexibility in system, saves space and low cost. It is thus advantageous to integrate RA on DCF and hence, minimizing the additional gain required on Erbium dope-fibre amplifier (EDFA). The report is structured as follows:

The first part of this report – section III aims to outline the theoretical background of dispersion in photonic systems. The following section (section IV) introduces the equivalent step-index (ESI) method to transform complicated fibre profiles to the well-known step-index profile, which eases the computation of critical fibre characteristics. In section V, the

design methodology of multi-clad DCF for dispersion management will be systematically addressed. The next part - section VI addresses the fibre design for Raman amplification. A new and simple design algorithm DCF for Raman amplification has been developed and summarised. The focus is on the effective Raman gain to maximise and flatten the gain. Finally, in section VII , the plan for future works is outlined. Impacts of dispersion to photonic modulation formats in high-speed and long-haul DWDM systems is the next phase in the task list. The final achievement is expected to be on Photonic signal processors (PSP) and its application in phase-controlled array antennas.

III. Background of Dispersion in Photonic Systems

This section briefly presents the key theoretical concepts describing the properties of chromatic dispersion in a single-mode fibre. Another aim of this section is to introduce the key parameters which will be commonly mentioned in the design sections later on.

A step-index optical fiber with core radius notation, a, is considered. The refractive indices of the core and cladding are noted to be n_1 and n_2 respectively. The significant transverse propagation constants of guided lightwaves u and v in the core and cladding regions are formulated as

$$u = a\sqrt{k^2 n_1^2 - \beta^2} \qquad\qquad\qquad (\text{III-1})$$

$$v = a\sqrt{\beta^2 - k^2 n_2^2} \qquad\qquad\qquad (\text{III-2})$$

where $k^2 n_1^2$ and $k^2 n_2^2$ are the plane-wave propagation constants in the core and second cladding layers respectively. β is the longitudinal propagation constant of the guided waves along the optical fiber, which can be expressed as

$$\beta = \sqrt{k^2 (b(n_1^2 - n_2^2) + n_2^2)} \qquad\qquad\qquad (\text{III-3})$$

where b is the notation of the critical normalized propagation constant whose value for guided modes fall within the range of [0,1] and it is formulated as

$$b = \frac{\dfrac{\beta}{k} - n_2}{n_1 - n_2} \qquad\qquad\qquad (\text{III-4})$$

The normalised frequency is then mathematically expressed as

$$V = ak\sqrt{n_1^2 - n_2^2} \qquad\qquad\qquad (\text{III-5})$$

It is very important to clearly address that the above propagation constants are defined as the basis for understanding the properties of the step-index fiber profile and will be redefined for the core-cladding regions in the design of the multiple-cladding DCF (MC-DCF) in section V.

The first parameter when addressing the effect of the dispersion in optical fibre is the group velocity. The group velocity v_g can be related to the phase (propagation) constant β of the guided mode by [3] [4]

$$v_g^{-1} = \frac{d\beta}{d\omega} \tag{III-6}$$

A pulse having the spectral width of $\Delta\omega$ is broadened by:

$$\Delta T = \beta_2 L \Delta\omega \tag{III-7}$$

where β_2 is the well-known group velocity dispersion (GVD) which is the second order derivative of β.

The dispersion slope, $S(\lambda)$, which is an essential dispersion factor for high-speed DWDM transmission can be obtained from the higher order derivatives of the propagation constant as

$$S = \frac{dD}{d\lambda} = \left(\frac{2\pi c}{\lambda^2} \right)\beta_3 + \left(\frac{4\pi c}{\lambda^3} \right)\beta_2 \tag{III-8}$$

where β_3 is defined as

$$\beta_3 = \frac{d\beta_2}{d\omega} = \frac{d^3\beta}{d\omega^3} \tag{III-9}$$

The total dispersion factor which is actually the chromatic dispersion, D (ps/nm.km), of a single mode optical fibre is given by:

$$D = -\left(\frac{2\pi c}{\lambda^2} \right)\beta_2 \equiv D_M + D_W \tag{III-10}$$

D_M and D_W are the material and waveguide dispersion parameters respectively. Although these factors are well-known, a brief outline of their background is essential.

The material dispersion in an optical fibre is due to the wavelength dependence of the refractive index (RI) of the core and cladding. The RI $n(\lambda)$ is approximated by the well-known Sellmeier's equation:

$$n^2(\lambda) = 1 + \sum_{i=1}^{M} \frac{B_i \lambda^2}{\left(\lambda^2 - \lambda_i^2 \right)} \tag{III-11}$$

where λ_j indicates the ith resonance wavelength and B_j is its corresponding oscillator strength. n stands for n_1 or n_2 for core or cladding regions. These constants are tabulated in Table IX-1 in the Appendix for several material types [5]. The first three Sellmeier terms, B_1, B_2 and B_3, are normally used. These tabulated coefficients are then used to find material dispersion factor, D_M which can be obtained by

$$D_M = -\frac{\lambda}{c}\left(\frac{d^2 n(\lambda)}{d\lambda^2}\right) \qquad \text{(III-12)}$$

where c is the velocity of light in vacuum. For pure silica and over the spectral range of 1.25 μ m-1.66 μm, D_M can also be approximated by an empirical relation [3]

$$D_M = 122\left(1 - \frac{\lambda_{ZD}}{\lambda}\right) \qquad \text{(III-13)}$$

where λ_{ZD} is the zero material dispersion wavelength[1]. For instance, λ_{ZD} = 1.276 μm for pure silica. λ_{ZD} can vary according to various doping concentrations in the core and cladding of different materials such as Germanium (Ge) or Fluorine (F).

The waveguide dispersion D_W can be calculated as [3, 4]:

$$D_W = -\left(\frac{n_1 - n_2}{c\lambda}\right)V\frac{d^2(Vb)}{dV^2} \qquad \text{(III-14)}$$

where b and V is the normalised propagation constant and normalized frequency as defined in (III-4) and (III-5) respectively. $Vd^2(Vb)/dV^2$ is defined as the normalised waveguide dispersion parameter, which will be redefined in the design of MC-DCF profile as it has significant contribution to the characteristics of the total chromatic dispersion.

It is also of significance to firmly understand the Equivalent Step-Index methods which are used to transform complicated profiles of SMF and DCF to the well-known simple SI profile. The ESI methods ease the calculation of critical parameters which describe fibre properties such as the mode-field radius or spotsize, effective area, the normalized frequency V-parameter..etc. The most effective ESI method, up to the awareness of the author, which is based on pertubationary theory and also known as the method of moments, is discussed. These results are very useful for design simulations of not only DCF but other various types of fibres.

---

[1] λ_{ZD} is defined as the wavelength at which the material dispersion factor $D_M(\lambda) = 0$

IV. Step-Index Fibre and ESI Methods

In the manufacture of optical fibre, it is impossible to achieve a truly perfect step-index profile. In addition, modified index-profile fibres such as graded-profile fibres and especially, multiple-cladding fibre are utilised for dispersion management and non-linearity control of the optical system. It therefore results in a significant concern to simplify these fibre profiles back to the simple and well-known step-index for the convenience of design calculations.

There are several approaches for deriving the solutions of arbitrary profiles of the fibres such as Numerov method, resonance method and variational or pertubationary or best known as the method of moments. Although the first two methods are capable of giving good results for the ESI models, it is far complicated in aspect of design. The method of moments has been proven as the most effective method to achieve the ESI model of a fibre with arbitrary profile[4]. Several research efforts for determining the ESI of a SMF fibre with arbitrary profiles such as graded-index or central-dip profiles [6-9] as well as the multi-clad fibres [4, 10-13] were published.

The results of the ESI model derived from the momentum method for a SMF with graded-index and central-dip profile can be summarised as follows [4, 14]:

V_e = effective or equivalent V-parameter

a_e = ESI core radius

λ_{ec} = ESI cut-off wavelength

Δ_e = Equivalent relative index difference

The refractive index profile of the fibre is defined as follows:

$$s(R) = \frac{n^2(r) - n_{clad}^2}{n_0^2 - n_{clad}^2}$$

(IV-1)

where $R = \dfrac{r}{a}$ and $0 \leq R \leq 1$ n_0, n_{clad} and $n(r)$ are the core, cladding and the index distribution respectively.

A. ESI model for power-law graded-index profile:

The parameter *s(R)* is determined by: $s(R) = 1 - R^{\alpha}$ where α defines the power index of the profile. The power-graded index profile is illustrated in Fig. IV-1 with various values of exponential index α
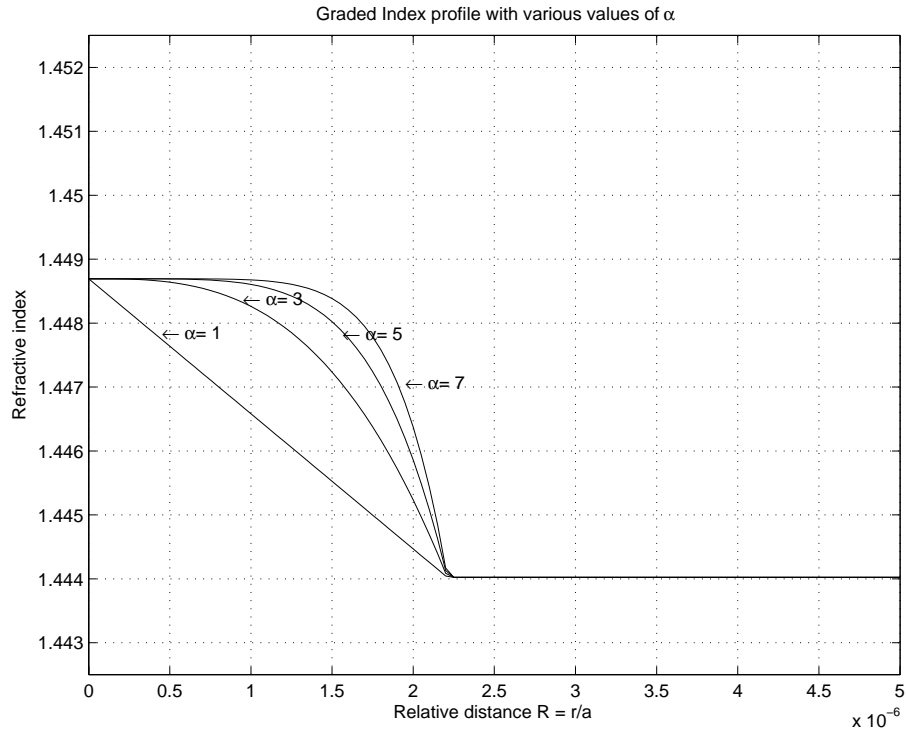
Figure IV-1: Power-law graded-index profile

The accurately approximation of ESI parameters of this kind fibre have been derived and formulated as [4]:

$$\frac{V_e}{V} = \left(\frac{\alpha}{\alpha + 2}\right)^{1/2} \tag{IV-2}$$

$$\frac{a_e}{a} = \frac{\alpha + 2}{\alpha + 3} \tag{IV-3}$$

where *Ve* and a_e are defined as above. These parameters are the most critical factors in determining the fibre properties such as spot size, the effective area, the attenuation, the effect of non-linearity, etc.

11

B.   ESI model for central-dip index profile

The profile of the fibre is expressed as: $s(R) = 1 - \gamma(1-R)^{\alpha}$ where γ corresponds to the relative depth of the central dip. Fig IV-2 shows the shape of this profile
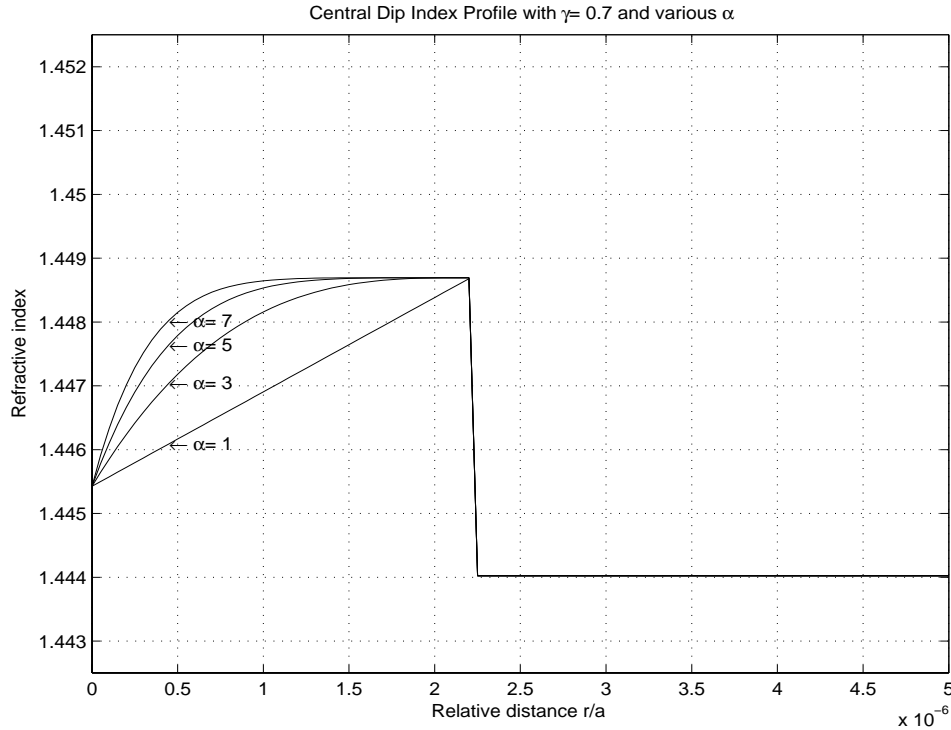
Figure IV-2: Central-Dip index profile

The ESI parameters of this fibre can be derived as:

$$\frac{V_e}{V} = \left(1 - \frac{2\gamma}{(\alpha+1)(\alpha+2)}\right)^{1/2} \tag{IV-4}$$

$$\frac{a_e}{a} = \frac{(\alpha+1)(\alpha+2)(\alpha+3) - 6\gamma}{(\alpha+3)\left[((\alpha+1)(\alpha+2) - 2\gamma)\right]} \tag{IV-5}$$

It is important to address the limitation of the ESI models. The ESI models do not give an accurate approximation for the waveguide dispersion hence, inaccurate to chromatic dispersion. However, this problem can resolved with the introduction of enhanced ESI method of moments (E-ESI).

C. Enhancement of ESI method in Dispersion Computation

The E-ESI method with the addition of enhancement factors was published in Ref. [8]. The method can be summarised as follows:

The normalized propagation constant $b(V)$ of the normal ESI model is now adjusted by the factor of $\Delta\bar{\Omega}_4$ and the enhancement function $f(\bar{V})$:

$$b(V)_e = \left(\frac{\Omega_0}{\bar{\Omega}_2}b(\bar{V})\left[1+\left|\Delta\bar{\Omega}_4\right|f(\bar{V})\right]\right) = b(V) + b(V) \times Enhancement\ Factor \qquad \text{(IV-6)}$$

where $\qquad Enhancement\ Factor = b(\bar{V})\left(\dfrac{\Omega_0\left|\Delta\bar{\Omega}_4\right|f(\bar{V})}{\bar{\Omega}_2}\right)$ $\qquad$ (IV-7)

and $\Omega_M = \displaystyle\int_0^1 s(R)R^{M+1}dR \qquad$ where $s(R) \approx \dfrac{n(r)-n_{clad}}{n_{core}-n_{clad}}(as\ defined\ above)\ ; M = 0,1,2...$

$\bar{\Omega}_M = \dfrac{\Omega_M}{\Omega_0}$; $\qquad \Delta\bar{\Omega}_4 = \dfrac{(3/4)\bar{\Omega}_4 - \bar{\Omega}_2}{\bar{\Omega}_2}$ $\quad$ and $f(\bar{V})=0.313\bar{V}-0.013\bar{V}^2$ with $\bar{V}=\sqrt{(2\Omega_0)V}$

The data for the enhancement factor $\Delta\bar{\Omega}_4$ and for the first two moments ($\Omega_0\ and\ \Omega_2$) according to several values of the exponential index α of the graded-index profile are given in Table IV-1 [8]

α	Ω_0	Ω_2	$\Delta\bar{\Omega}_4$
∞	0.500	0.500	0.000
16	0.444	0.450	0.010
8	0.400	0.417	0.029
4	0.333	0.375	0.067
2	0.250	0.333	0.125
1	0.167	0.3	0.190

Table IV-1: Enhancement Factors for improving accuracy of ESI models

V.   Fibre Design for Dispersion Management

Key strategies and design steps of multi-clad single mode fibres with modified dispersion characteristics for dispersion-management have been revised in numerous papers [15-23]. However, the drawback of these strategies is normally the level of complication due to derivation of numerical solutions from the boundary wave equations and hence, they are not straight forward for engineering design practice. In addition, they were inadequately showing the sensitivity of the dispersion property to variations of critical fibre parameters. In addition, the desire for dispersion management on the long-haul DWDM optical system has dramatically increased for the last decade. Hence, it is essential to have a systematic review of the fibre design for dispersion management with focus on dispersion compensating fibres (DCF).

During 1980s, standard SMF (SSMF) was optimized for operation at wavelengths about the window of 1310 nm, where they exhibit the zero dispersion property. In early 1990s, with the debut of EDFAs together with the low loss characteristic in the 3rd window around 1550 nm, the modern optical communication systems have largely shifted the operation to C-band, whose wavelengths range from 1530 nm to 1565nm. However, as several millions of kms of installed SSMF have been widely utilized, the 1310 nm-wavelength optical systems are still extensively deployed as the communication backbones in most of the countries in the world and they can not be soon replaced with the modern systems. Besides, at the wavelength of 1550 nm, the SSMF suffers a moderately large dispersion of approximately 17 ps/nm.km. It is therefore very essential to upgrade these systems by means of compensation for the dispersion. In addition, DCFs are always one of the most concerning factors in planning the long-haul and high-speed system.

By modifying the fibre properties, it is possible to design the fibres with special characteristics such as very low dispersion (Dispersion Flattened Fibre - DFF) or large negative dispersion (Dispersion Compensating Fibre - DCF). These types of fibres are utilized for dispersion management purposes throughout the system. As the result, the transmission length of the system can be expanded considerably without severe penalties caused by distortion or inter-symbol interference. Another significant advantage of DCF is the easy implementation of

dispersion management in WDM system. No adjustment is required when the light source is varied. However, fine tuning or also known as mobbing for the residual dispersion at the end of the system is still inevitably necessary since the compensation of the dispersion can not be perfectly achieved for all the operational wavelengths in the C-band.

The key factor of modifying the SI fibre is the addition of another outer layer to the profile. In order to achieve a high negative dispersion value, the inner clad is highly depressed and controlled in order that the higher order modes do not exist in the operating wavelength range [24]. By doping with Germanium, the core material index can reach to a high refractive index value. In the other hand, Fluorine doping is employed to create depressed inner-claddings which allows zero-dispersion to be obtained with a small amount of GeO_2 in core. The spectral-loss characteristics of fluorine-silicate glass in the $1.0\mu m$ -$1.7\mu m$ range are superb and thus suitable for long wavelength applications [25, 26].

It is also significant to investigate the situation of multi-dopant fibre e.g the profile of GeO_2-doped SiO_2 core and P_2O_5/F-doped SiO_2 cladding). As described in [27], P_2O_5 allows a reduction of drawing temperature and is always introduced with a very small quantities(< 0.2 mole percent). Hence, P_2O_5 has little influence on the dispersion calculation.

This section presents the design methodology for simultaneous compensation of both dispersion and dispersion slope using multi-clad index profile of SMF: W-fibre or double-clad fibre and triple-clad fibre. These two profiles are the most commonly profiles deployed for the DCF fibre due to their capability and special dispersion characteristics giving anomalous negative dispersion. The organization of this section is as follows:

- The first part of this section describes the key operational fibre parameters which need to be obtained as the results of the design. The significant parameters give information about the characteristics of the designed fibre.
- W-fibre considered to be the basis of the modified SMF designed for dispersion management purposes, will be thoroughly investigated in the second part. The design methodology, the effect of the fibre profile parameters on the design as well as the

obtained results will be discussed in detail. Several sample design profiles for W-shaped DCF fibre have been achieved, which demonstrates the feasibility of this kind of fibre for dispersion compensation schemes.

- A more favourable option for the design of a DCF is the triple-clad fibre profile, in which a new and fast algorithm that locates saddle points of the waveguide dispersion factor has been developed in part 3. This technique simplifies the design of triple-clad fibre. Sensitivities of key design parameters and their impacts to the design are also discussed.

A. Operational Fibre Parameters

A.1 Spot size r_o:

With the assumption of Gaussian mode field distribution, the spot size is analytically approximated for *V>1* as: [3, 28]

$$r_0 = \sqrt{\frac{a_0^2}{\ln V_{eff}^2}}$$

(V-1)

Hence the effective area can be calculated:

$$A_{eff} = \pi r_0^2$$

(V-2)

A.2 Figure of Merit (FOM)

The FOM evaluates the amount of Dispersion per unit Loss as an indication to the trade-off between the dispersion and the attenuation in the design of the fibre. It is a useful parameter to ensure that a desired amount of large dispersion is not obtained with excessive fibre loss. Large dispersion is desirable only when the design shows an increase in amount of dispersion per dB loss.

$$M = \frac{|D_c|}{\alpha_c}$$

(V-3)

A.3 Relative Dispersion Slope (RDS):

The desire in the design of DCF is to obtain the same RDS as that of the transmission optical line in order to achieve a simultaneous compensation for both dispersion slope and dispersion.

$$RDS = \frac{Dispersion \ \text{Slope}}{\text{Dispersion}} = \frac{D_s{}'}{D_s} \tag{V-4}$$

At 1550 nm, D_s and D_s' for SSMF are typical 17 ps/nm.km and 0.07 ps/nm^2.km respectively, which gives the nominal value of RDS to be approximately 0.004 to 0.006 nm^{-1}. The efficiency of the dispersion compensation utilising DCF can be further evaluated based on the Slope-Compensating Rate(S-CR) [29] and the Kappa parameter, which are defined as follows:

$$S - CR = \frac{RDS_{DCF}}{\text{RDS}_{SMF}} \tag{V-5}$$

$$Kappa = \frac{1}{RDS} \tag{V-6}$$

The length of a DCF span due to adispersion compensation can be calculated from the following equation

$$D_{SMF} L_{SMF} = D_{DCF} L_{DCF} \tag{V-7}$$

where D is the dispersion level, L is the fibre length in km. The typical dispersion value of SMF at 1550 nm is approximately +17 ps/nm.km and the SMF span length is 80 km–100 km.

Since the RDS of SMF and DCF are desirably the same, the above equation can be rewritten as

$$\frac{L_{SMF}}{L_{DCF}} = \frac{D_{DCF}}{D_{SMF}} = \frac{S_{DCF}}{S_{SMF}} \tag{V-8}$$

A.4 Non-Linear Phase Shift (NLPS)

NLPS is created due to Self-Phase Modulation (SPM) accumulated along the span.[30]

$$\phi_{NL} = \frac{2\pi}{\lambda} \int_0^L \frac{P(z)}{A_{eff(z)}} n_2(z) dz \tag{V-9}$$

where L is the span length, P is the average optical power, z is the longitudinal position and n_2 is the non-linear refractive index (about 2 to 3*10^{-20})

A.5 Attenuation

To model fibre attenuation, actual data for fibre losses as measured in fabrication [31] are used for approximation of a linear increase of loss with growing level of anomalous dispersion, as followed

$$\alpha \; = 0.12 - 3000D + L_R \qquad\qquad\qquad (\text{V-10})$$

where D is dispersion in ps/nm/km, L_R is the Rayleigh scattering loss approximated by fitting to experimental curves for loss in fibres doped with variable amount of GeO$_2$, and can be expressed in *dB/km* by a linear relationship with index difference as [14, 32]

$$L_R = (0.75 + 4.5\Delta)\lambda^{-4} \qquad\qquad\qquad (\text{V-11})$$

where Δ is the index difference and λ is in *um*.

Two sources of loss caused by the bending of the fibre are:

- *Macro-bending Loss*: the plane wavefronts associated with the guided mode are pivoted at the centre of the curvature and their longitudinal velocity along the fibre axis increaseas. The is a critical bending radius, beyond which there will be a large phase difference compared to that in the cladding and hence, a large amount of loss due to radiation will occur.

- *Micro-bending Loss* of SM is a function of the fundamental mode spot size. Therefore, it is desirable to have a small spot size to minimize micro-bending loss. Hence, microbending can be negligible in DCF with very small spot size.

The design methodology of Multi-clad fibre which consists of W-shape or Double Clad fibre and Triple-Clad fibre are discussed in the next section.

B. W-Fibre

The profile of W-fibre is illustrated in Fig. V-1
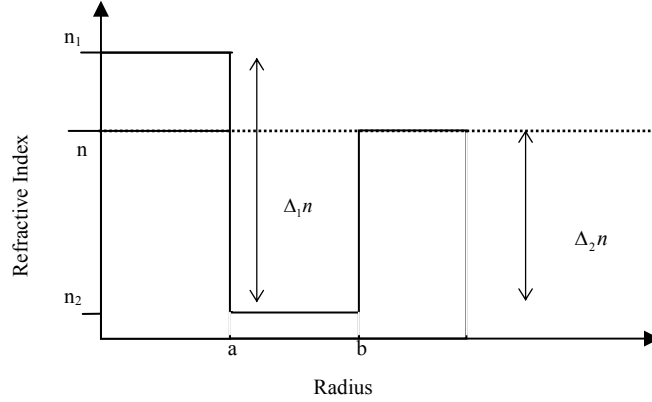
Figure V-1: Profile of refractive indices of W-fibre or Double Clad fibre

Where the significant profile parameters are defined as follows:

$$\Delta_1 n = n_1 - n_2 \qquad \Delta_2 n = n_2 - n$$
$$\Delta_1 = \frac{\Delta_1 n}{n} \quad \text{and} \quad \Delta_2 = \frac{\Delta_2 n}{n} \qquad \text{(V-12)}$$

The ratio of the core and the cladding radii (R) and the ratio between the relative indices (δ) are the critical design aids and defined as:

$$\delta = \frac{\Delta_2}{\Delta_1} \qquad \text{and} \qquad R = \frac{b}{a} \qquad \text{(V-13)}$$

The special characteristics of W-fibre was first investigated in early 1970s [33]. It then became the fundamental modified structure for dispersion-shifted fibre, DFF and DCF. Optical fibers with this type of structure have some interesting properties that are very different from the properties of conventional step-index fibers. The properties listed below were first described in [33]

- W-fibers can be designed to have anomalous dispersion in the single mode frequency region.

- Single-mode operation in W-fibers can be maintained over relatively large core sizes.

- In the single-mode regime, in comparison with standard SM fibers, the W-fiber 's fundamental mode is more tightly confined within the core of the fiber.

In W-fibre, there are actually five degrees of freedom in designing a W-Fibre which can be clearly seen as the core radius *(a)*, the cladding radius *(b)*, the RI of the core, the inner cladding and the outer cladding which are n_1, n_2 and n respectively. These five parameters are not always directly used for the design but commonly lead to the design parameters defined in (V-12) and (V-13).

B.1 Cut-off conditions

One of the first significant concerns when designing a fibre with W-profile is the cut-off wavelength of the fundamental - LP_{01} mode. Unlike the step-index profile where the fundamental mode faces always mathematically exists i.e faces no cut-off, the W-profile fibre has been reported in [11, 33-36] about the interesting characteristic of the *mathematical* LP_{01} finite/non-zero cut-off wavelength or frequency. These cut-offs start to appear when the longitudinal propagation constant becomes equally weighted with the plane wave constant of the outer cladding: $\beta = kn$ or in other words, the mode field remains constant in the outer cladding. *When the frequency decreases below the cut-off of LP_{01} or equivalently, when the wavelength exceeds the LP_{01} cut-off, the mode field becomes oscillating (or radially traveling) in the outer cladding and the mode suffers the power leakage.*

However, it should be understood that the mathematical cut-off of LP_{01} does not imply the case of none mode is guided along the fibre, but it rather means that the fundamental mode is no longer completely guided in the core and a large portion of the field hence the power is now oscillating in the outer cladding.

The cut-off frequency of the fundamental mode can be analytically and numerically determined from the dispersion equations in terms of the Bessel functions for the eigen fields of the weakly guided LP_{01} [11, 33-37], with the cut-off condition $\beta = kn$. The condition for which the LP_{01} cut-off occurs is given by the equation: [4, 11, 33]

$$\frac{b}{a} = \frac{1}{\sqrt{|\delta|}} \qquad (V\text{-}14)$$

which defines the limit for the LP_{01} mode to be guided or leaky. The curve is obtained and plotted in Fig. V-2 [11], for which

$$LP_{01} \text{ mode is guided when } \frac{b}{a} \le |\delta|^{-\frac{1}{2}}, \quad \text{ie when } \beta > kn \qquad (V\text{-}15)$$

$$LP_{01} \text{ mode is leaky when } \frac{b}{a} > |\delta|^{-\frac{1}{2}}, \quad \text{ie when } \beta < kn \qquad (V\text{-}16)$$
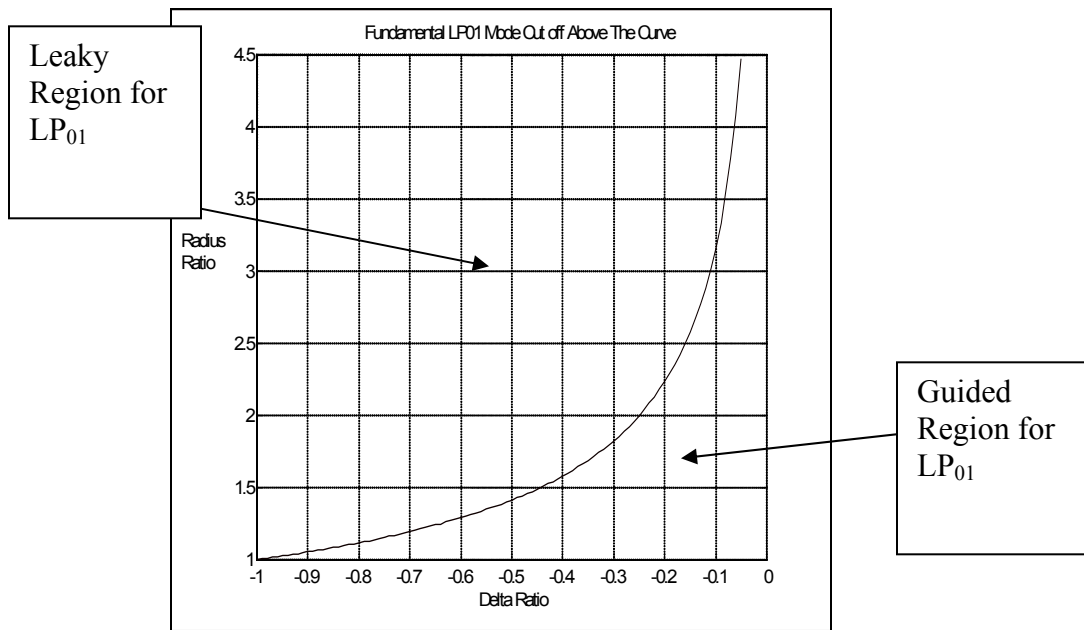
Figure V-2: Cut-off Limit for the LP_{01} mode determined by radius and index ratios.

In the leaky mode, the inner cladding plays a role of a tunnel through which the power is trapped in the core and the outer cladding. In this leaky mode, the abrupt power leakage loss above the LP_{01} cut-off wavelength can be considerably reduced by the increase of the thickness of inner cladding [4, 36].

It is significant to understand the physical insight of the finite cut-offs in W-profile fibre. The discussion is based on the normalized propagation constant characteristics which are demonstrated in Fig. V-3. At short wavelengths or large value of V, the LP_{01} mode behaves as if the profile has an infinite inner cladding and does not "see" the outer cladding yet. The

propagation constant b(V) (known as B(V) in V-3) is gradually rolling off to zero until it realizes the existence of the outer cladding at longer operating wavelengths (smaller V value) when the condition (V-14) occurs or $\beta = kn$. The b(V) then needs to abruptly steer its curve to zero, which produces the finite cut-off value of LP_{01} mode. Another notable characteristic of the phenomenon is the capability of high negative or anomalous dispersion due to the abrupt variation in the curve b(V) and the hence, its second-order derivative gives a sharp peak shape of the waveguide parameter.
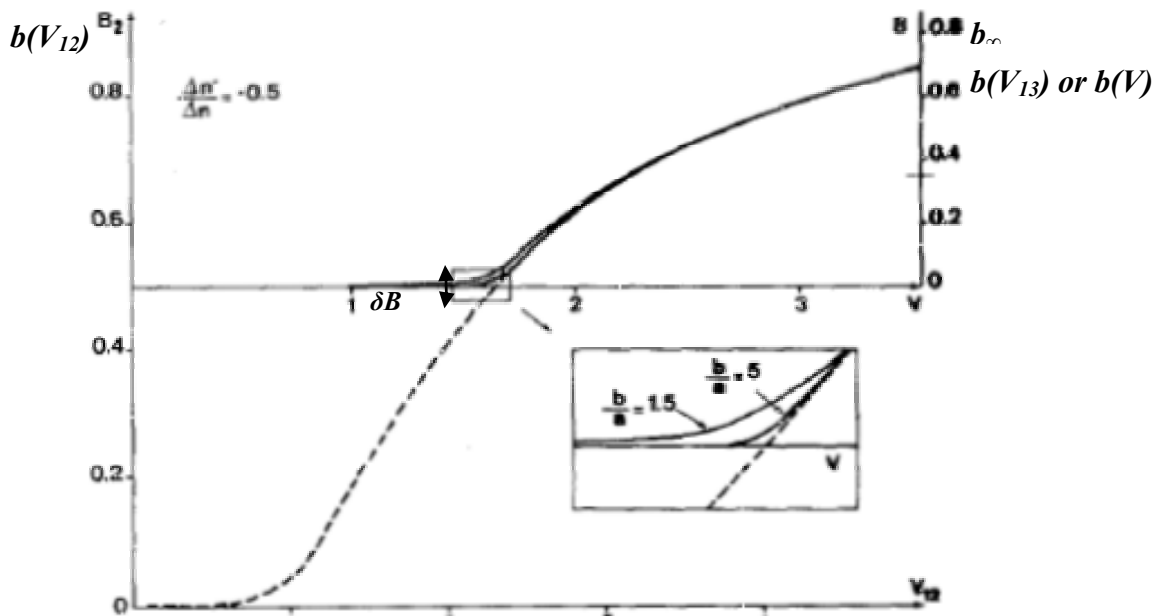
Figure V-3: Analytical approximation of b(V) shown

Ref [38] has shown the ability for high-dispersion of the W-DCF fibre. Furthermore, it has been shown in Ref [39] that triple-clad (TC) and quadruple-clad (QC) fibres can be synthetically designed from W-fibre.

A method allowing the approximation of the fundamental-mode cut-off was developed in Ref [11, 35], which is utilized in the simulation. *Apart from the mathematical cut-offs, the effective cut-off wavelength is also important for consideration. It is determined when the profile has been converted to be the ESI profile.*

B.2 Design Equations:

Adapted and modified from Ref [4, 11, 34-36], the following equations form the backbone of the simulation in designing the W-fibre DCF. The notations in the equations can be referenced from (V-12) and (V-13). The first part of this section will describe the methodology and the critical equations used in the simulation to obtain the total chromatic dispersion and property parameters of the DCF fibre. The second part shows the key equations for computing the cut-off wavelengths and cut-off normalized frequency V-parameters for both LP_{01} and LP_{11} modes, in which LP_{01} can experience a non-zero cut-off frequency.

B.2.a.   *Wave numbers of guided modes in W-fibre*

As seen in section III, the normalized propagation constants play critical roles influencing the chromatic dispersion characteristics of the fibre. Hence, in this section, those constants are again introduced but redefine or modified according to the special properties of W-profile fibre.

Starting the analysis of W-fibre is the formulation of the normalised propagation constant $b(V_{12})$ defining the propagation the field in the region limited by the core and the inner cladding:

$$b(V_{12}) = \frac{\dfrac{\beta^2}{k_0^2} - n_2^2}{n_1^2 - n_2^2} \qquad\qquad (V\text{-}17)$$

where

$$V_{12} = k_0 a n \sqrt{2\Delta_1} \qquad\qquad (V\text{-}18)$$

Based on Fig. V-3, the dashed curve represents the gradual roll off of $b(V_{12})$ vs the normalized frequency V_{12} defined by the core and inner cladding when the field does not yet "see" the existence of outer cladding as if the inner cladding spreads out indefinitely from the core. However, at longer wavelengths or smaller V, the LP_{01} mode starts to spread out and "see" the outer cladding, the propagation constant is quickly steered to zero on the V_{13} horizontal axis. *For convenience, V_{13} is short-written as V.*

$b_\infty(V_{13}) \equiv b_\infty(V)$ is denoted as the solution of the usual dispersion equation for step-index fibre constructed by the core and the outer cladding and computed as [34]:

$$b_\infty(V_{13}) = \frac{1}{1+\delta}\big(b(V_{12}) + \delta\big) \tag{V-19}$$

The effective normalised frequency between the core and the two claddings is given as follows[4]:

$$V_{13} \equiv V = \frac{2\pi}{\lambda} an\sqrt{2(\Delta_1 + \Delta_2)} \approx V_{12}(1+\delta)^{\frac{1}{2}} \tag{V-20}$$

by which

$$V_{12} = \frac{V}{\sqrt{1+\delta}} \tag{V-21}$$

The key strategy of the approximation is to find an analytical equation for the complete curve of the propagation constant for W-shaped profile [11, 34], whose curve can be expressed as

$$b(V_{13}) \equiv b(V) = b_\infty(V) + \delta b(V) \tag{V-22}$$

$\delta b(V_{13})$ is defined in Fig.V-3 implying the offset of $b(V)$ from $b(V_{12})$ at the position closely to the cut-off boundary, which is caused by the abrupt steering of the curve. By expressing the dispersion equation in term of δb and using approximations for the Bessel functions in the equation, δb is found to be

$$\delta b(V) = \frac{Y(V)}{V}\big(1 + X(V)\big) \tag{V-23}$$

where

$$Y(V) = 1.4\Big(-\delta + \sqrt{-\delta(1+\delta)}\Big)\exp\left[-2V_{12}\sqrt{-\delta}\left(\frac{b}{a}-1\right)\right] \tag{V-24}$$

$$X(V) = \frac{-2}{\dfrac{\delta}{1+\delta}+b_\infty+\dfrac{5Y}{V}}\left\{b_\infty + \frac{2Y}{V} - \sqrt{-\frac{\delta}{1+\delta}\left(b_\infty+\frac{Y}{V}\right)-\frac{Y}{V}\left(2b_\infty+\frac{Y}{V}\right)}\right\} \tag{V-25}$$

An analytical approximation to the single clad equivalent b(V₁₂) is given in [40] to less than 2% error over the range *1.3 ≤V₁₂≤2.8* as

$$b_{12}(V_{12}) = \left(1.1428 - \frac{0.996}{V_{12}}\right)^2 \tag{V-26}$$

and over the range *2.8 ≤V₁₂≤6* as [40]

$$b_{12}(V_{12}) = 1.01 - \frac{1 + 2\log V_{12}}{V_{12}^2} \qquad \text{(V-27)}$$

The first derivative of $V_{13}\, b(V_{13})$ is computed analytically as

$$\frac{d(V_{13}b)}{dV_{13}} = \frac{1}{1+\delta}\frac{d(V_{12}b_{12})}{dV_{12}} + \frac{d(V_{13}\delta b)}{dV_{13}} \qquad \text{(V-28)}$$

and the second derivative can be derived as follows

$$V_{13}\frac{d^2(V_{13}b)}{dV_{13}^2} = \frac{1}{1+\delta}V_{12}\frac{d^2(V_{12}b_{12})}{dV_{12}^2} + V_{13}\frac{d^2(V_{13}\delta b)}{dV_{13}^2} \qquad \text{(V-29)}$$

The first term on the right hand side can be considered as the chromatic dispersion in the case of single clad step index fibre over the range $1.3 \le V_{12} \le 2.8$, which can been calculated with less than 5% relative error as:

$$V_{12}\frac{d^2(V_{12}b_{12})}{dV_{12}^2} = 0.080 + 0.549\left(2.834 - V_{12}\right)^2 \qquad \text{(V-30)}$$

For the range $2.8 \le V_{12} \le 6$, it is better approximated by

$$V_{12}\frac{d^2(V_{12}b_{12})}{dV_{12}^2} = -0.14 + \frac{0.29}{\left(V_{12} - 1.56\right)^2} \qquad \text{(V-31)}$$

The same waveguide dispersion equation for single clad fibre is used

$$D_W = -\frac{n(\Delta_1 + \Delta_2)}{\lambda c}V_{13}\frac{d^2(V_{13}b)}{dV_{13}^2} \qquad \text{(V-32)}$$

B.2.b.   Equations for cut-off conditions of Double-Clad fibre

The cut-off wavelength and the cut-off normalized frequency V-parameter of the fundamental mode LP_{01} are calculated based on the equations in [35]

$$V_c(\delta, R) = V_c(\infty)\left[1 - 2.008(1+\delta) \times \exp\left(\frac{-1.992(R-1)\sqrt{|\delta|}}{1.1428 - \sqrt{|\delta|}}\right)\right] \qquad \text{(V-33)}$$

with

$$V_c(\infty) = 1.075(1-\delta) \qquad \text{(V-34)}$$

where δ and R are defined in (V-13).

The accuracy of (V-33) is better than 0.5% for $-0.8 < \delta < -0.25$ and better than 1% for $-0.85 < \delta < -0.2$

Based on Ref [37] and by interpolating method, the cut-off V-parameter (V_{c11}) for LP$_{11}$ has been shown to be linearly related to the ratio of the two relative index differences (δ) and can be approximated to be:

$$V_{c11} = 2.405 - 1.385\delta \qquad \qquad \text{(V-35)}$$

It is notable that in the design of DCF fibre, δ is negative which is resulted from the low refractive index of the depressed inner cladding. According to [4], δ stays within the range of interest of $-1 < \delta < -0.2$.

The effective cut-off wavelength is determined from the ESI profile of the W-fibre as

$$\lambda_c = \lambda \times \frac{V_{eff}}{2.405} \qquad \qquad \text{(V-36)}$$

B.3 Design Results:

B.3.a.   Effects of δ and R on the Waveguide Parameter:

Fig.V-4, V-5, V-6 and V-7 show the shape and the peak value of the waveguide parameters which are determined according to the variations of the ratio between the core and cladding radii (R) as well as the relative index ratio (δ). These figures are obtained based on Eq.V-29 and the derivations shown in Eqs V-17 to V-31.

Core radius = 2e−006; rradii(R) = 2

$\delta = -0.35$

$\delta = -0.3$

$\delta = -0.25$

$\delta = -0.2$

Waveguide Parameter $d^2(Vb)/d(V^2)$

Normalised Frequency V
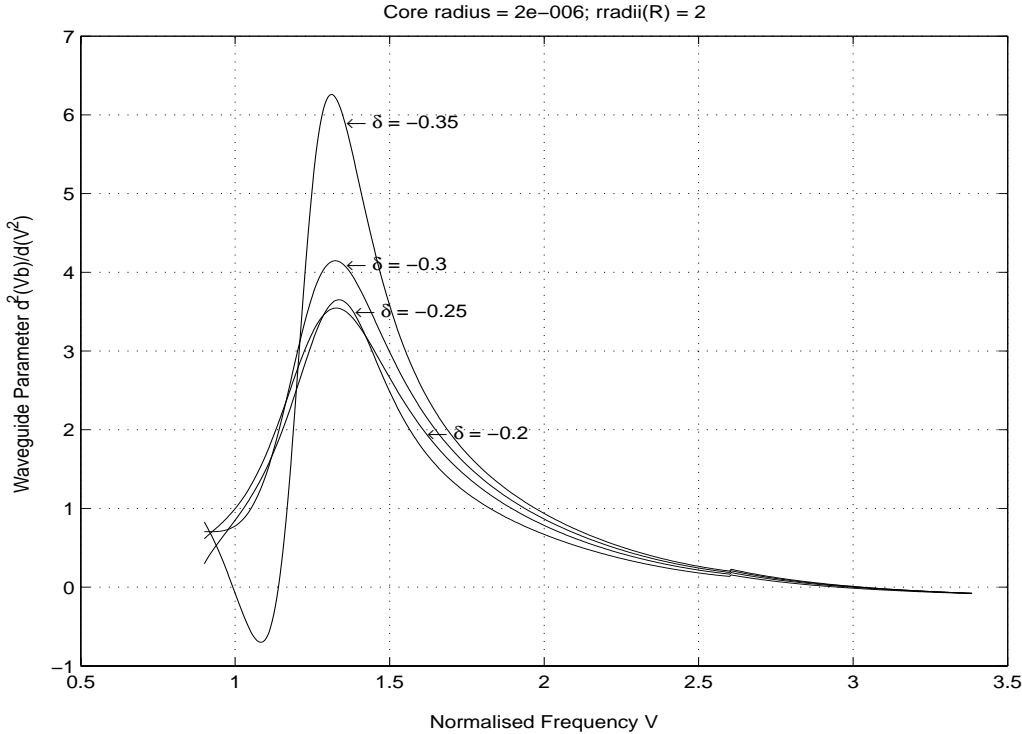
Figure V-4: Waveguide Parameters with R =2 and variation of δ

Core radius1 = 2e−006; rradii = 2.5

$\delta = -0.3$

$\delta = -0.25$

$\delta = -0.2$

Waveguide Parameter $d^2(Vb)/d(V^2)$

Normalised Frequency V
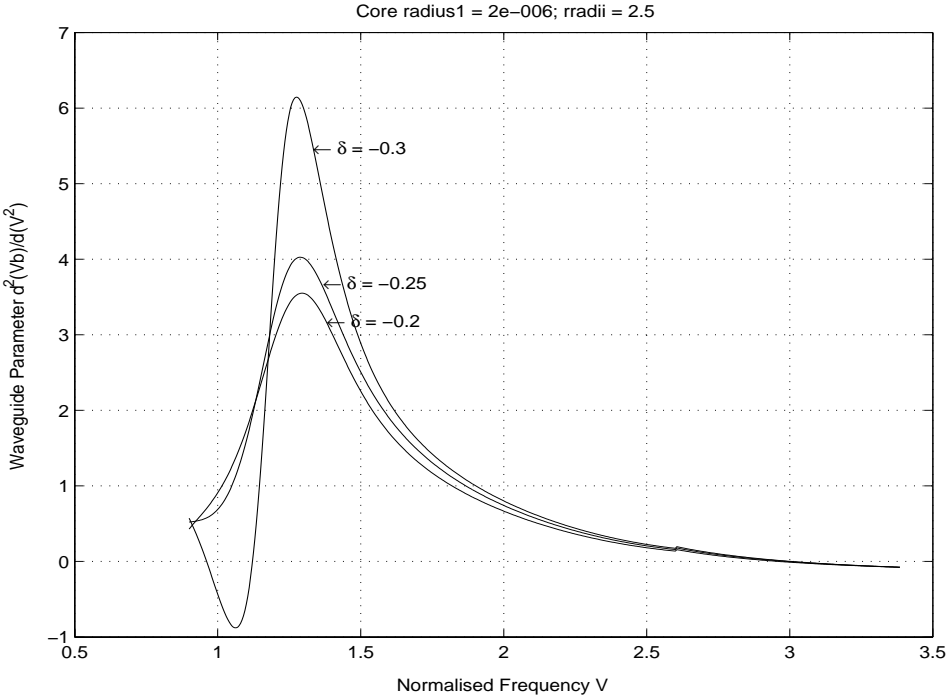
Figure V-5: Waveguide Parameters with R = 2.5 and variation of δ
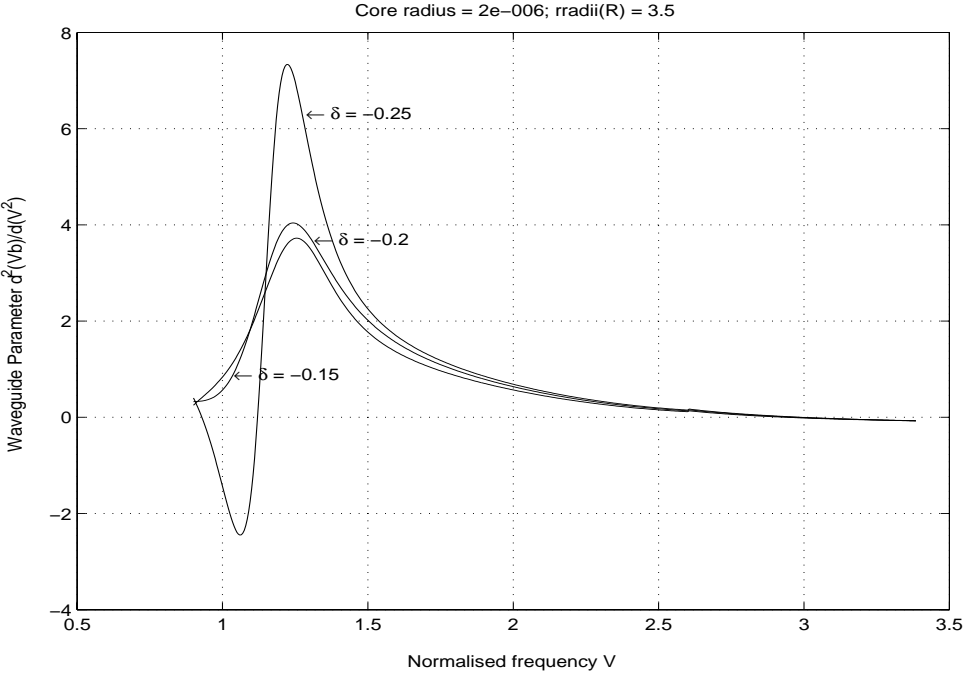
Figure V-6: Waveguide Parameters with R =3.5 and variation of δ
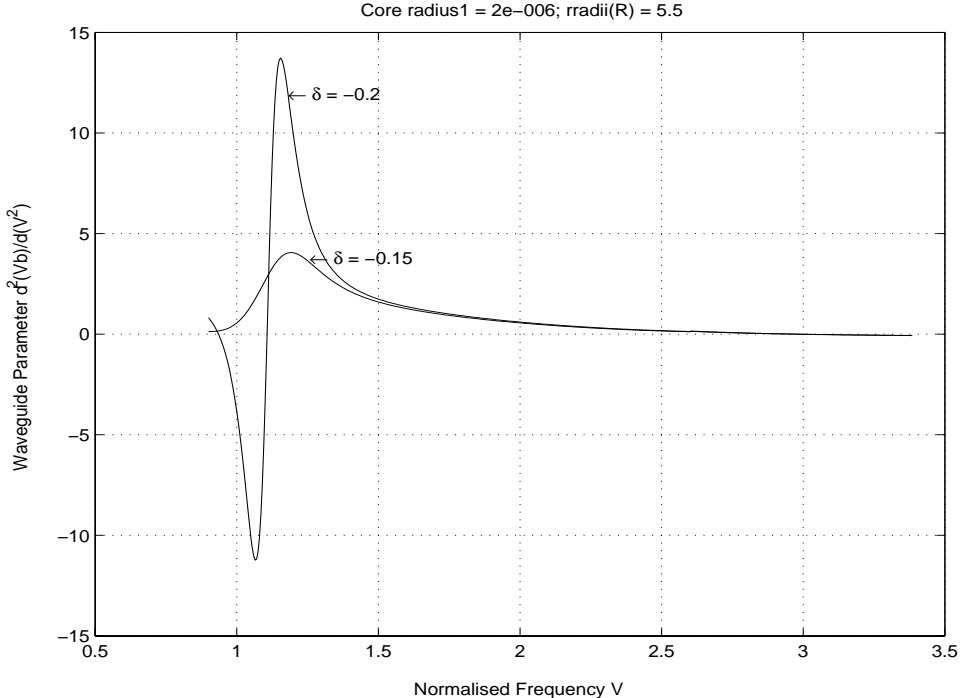
Figure V-7: Waveguide Parameters with R = 5.5 and variation of δ

Significant discussion points are noted as follows:

- The peak value of the waveguide parameter is increased when δ becomes more negative, i.e either the inner cladding is highly depressed or the RI of the outer cladding is rising to the RI level of the core.

- In addition, the value of the radii ratio ($R=b/a$) between the core and the cladding also plays a significant role to the peak value. As R grows from 3.5 in Fig.V-6 to 5.5 in Fig.V-7, the peak value of the waveguide parameter corresponding to $\delta = $ -0.2 increases significantly from 4 to approximately 13.5, which potentially gives a high negative value for the chromatic dispersion of the DCF.

- However, the draw back caused by the high peak value of the waveguide parameter is the steep slope of the waveguide parameter, which implies a high sensitivity of the fibre design to the bending loss.

- Large negative in value of δ leads to the shift of the waveguide parameter and therefore the peak value towards the smaller values of normalized frequency V. As shown later in Figure V-11, this implies the shift of the high negative dispersion to longer operating wavelengths, which might fall outside the operating C,L-band of interest.

B.3.b.   *Effects of δ and R on the cut-off conditions*

Figures V-8, V-9 and V-10 comprehensively demonstrate the variation of the finite cut-off normalized frequency V-parameter and the cut-off wavelengths as the result of changing design values of δ and R. These cut-offs start to appear when the condition (V-16) occurs i.e

$R > |\delta|^{1/2}$.

As addressed in section B.1 , w*hen the frequency decreases below the cut-off of LP$_{01}$ or equivalently, when the wavelength exceeds the cut-off LP$_{01}$, the mode field becomes oscillating (or radically traveling) in the outer cladding and the mode suffers the power leakage.* Besides,

the cut-offs for $LP1_1$ are the boundaries for the second higher mode to appear. It is therefore desirable to have the operating normalized frequency V and wavelength to operate in the region of single mode and completely guided mode, i.e $V_{c01} < V < V_{c11}$ and $\lambda_{c11} < \lambda < \lambda_{c01}$.
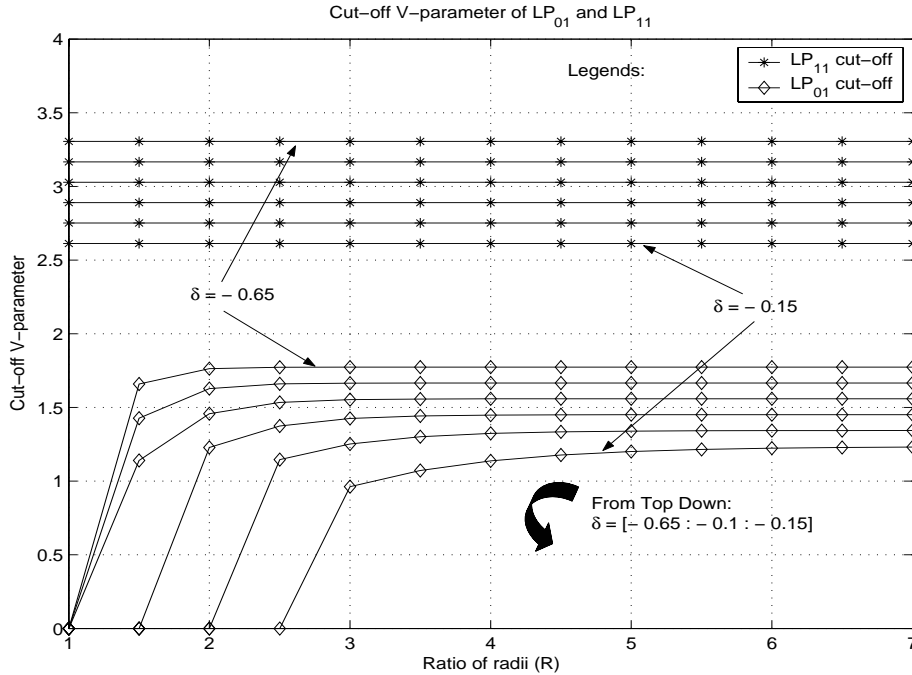
Figure V-8: Cut-off normalized frequency of LP_{01} and LP_{11} modes

- In Fig.V-8, going down from the top, higher values of V_{C01} and V_{C11} are obtained accordingly to the negative increase of δ from -0.65 to -0.15. As being inversely proportional to the V_{C01} and V_{C11}, in Fig V-9 and V-10, the values of λ_{C01} and λ_{C11} are expected to be reduced correspondingly with more negative value of δ.

- The results are verified with [4], [11] in which the value of LP_{01} V-cut-off also increase with $|\delta|$ whereas, inversely, the cut-off wavelength decreases.

- Therefore, small δ is desirable which gives smaller V_{C01} and larger λ_{C01}.

- For a given level of δ, small b/a is desirable which gives values close to zero for the cut-off V_{C01} and hence the cut-off wavelength may approach to large values.

- If $R < |\delta|^{\frac{1}{2}}$ or the fundamental mode is totally guided in the core, W-fibre now has infinite cut-off wavelength or zero cut-off frequency likely to the step-index fibre.

Cut−off wavelengths of LP_{01} and LP_{11}
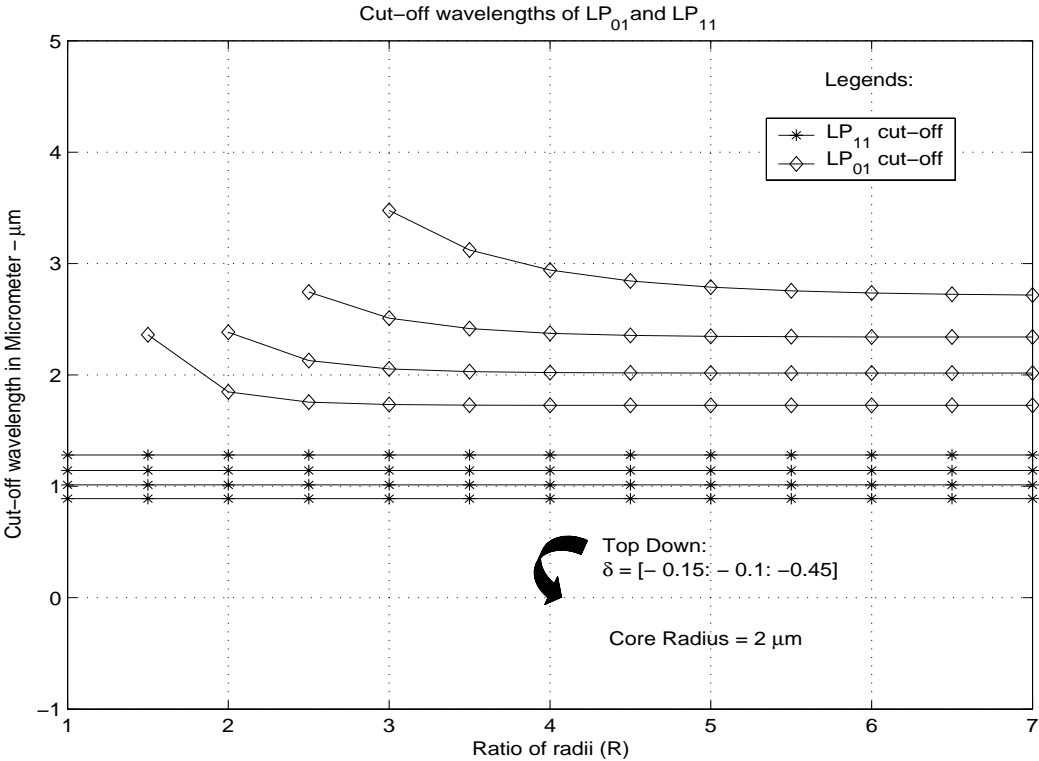
Figure V-9: Cut-off wavelengths of LP_{01} and LP_{11} modes with core radius to be 2 μm

Cut−off wavelengths of LP_{01} and LP_{11}
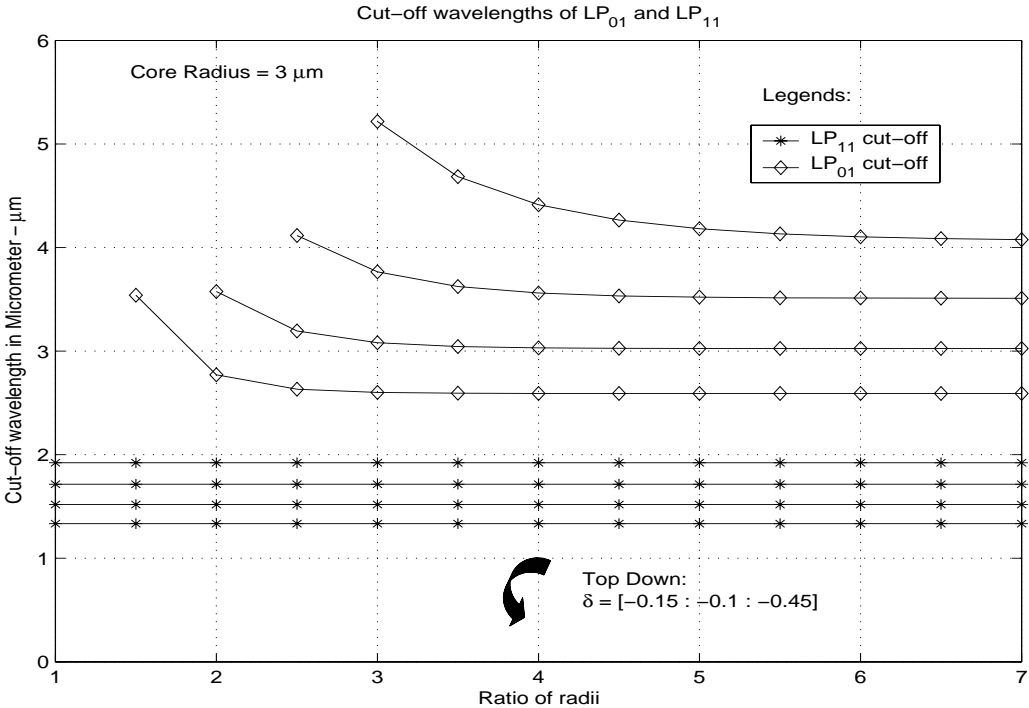
Figure V-10: Cut-off wavelengths of LP01 and LP11 modes with core radius to be 3 μm

- Large b/a causes V_{C01} to approach the asymptotic steady state value.

- It can also be noted that the core rand the cladding radius plays a significant role in the design consideration of the cut-off parameters. Reducing the size of the core or increasing the cladding radius results in the lower values of cut-off wavelengths of both LP_{01} and LP_{11} modes. Hence, it is necessary to consider an adequately large core radius in order to guarantee the guiding of LP_{01} mode in the DCF and to increase the value λ_{C11}, which helps reduce the leakage and bending losses of the LP_{01} mode.

B.3.c.   *Effects of Core and Cladding Radius on Total Chromatic Dispersion*

The shifting of the operating V values and hence, the total dispersion shift versus the wavelengths are clearly illustrated in Fig.V-11, V-12 and V-14. In Fig V-11 and V-12, the core radius of 1.4 µm or 1.5 µm are of the design interest due to the proper position within the operating C-band.

However, it is essential for the design no to let the operating V value to be lower than the cut-off of the fundamental mode - V_{C01} as discussed above. This is demonstrated in Fig. V-13 and V-14.
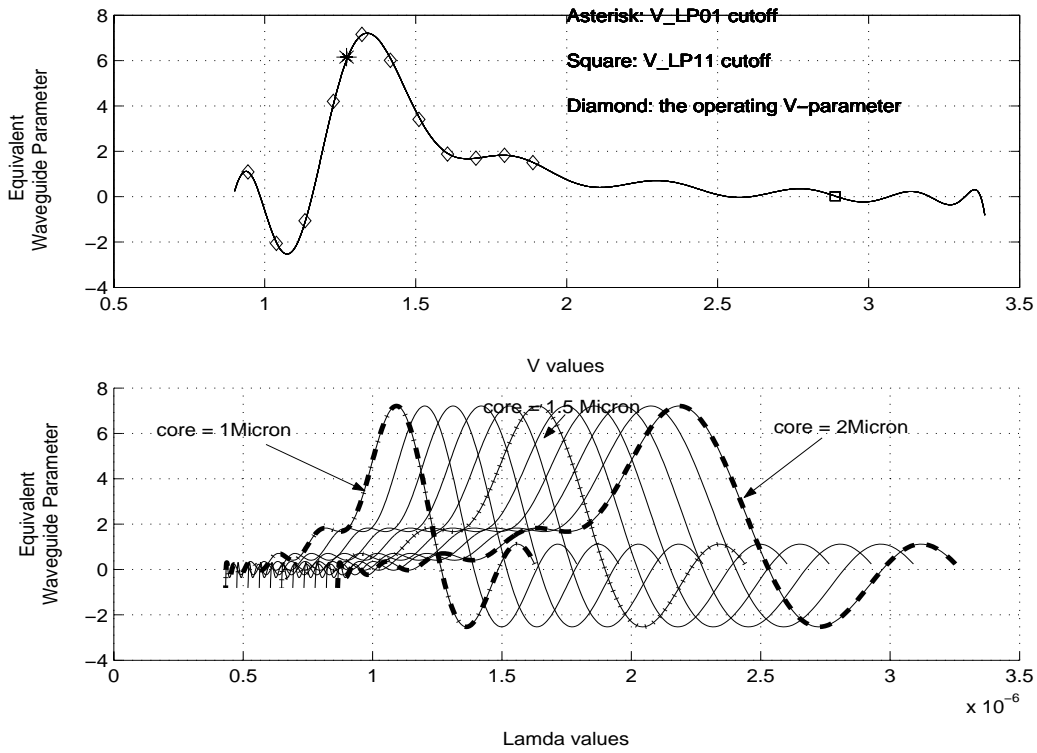
Figure V-11: a) Operating, cut-off V-parameters on Waveguide Parameter
b) Illustration of shifting of Waveguide Parameters with variation of core radius
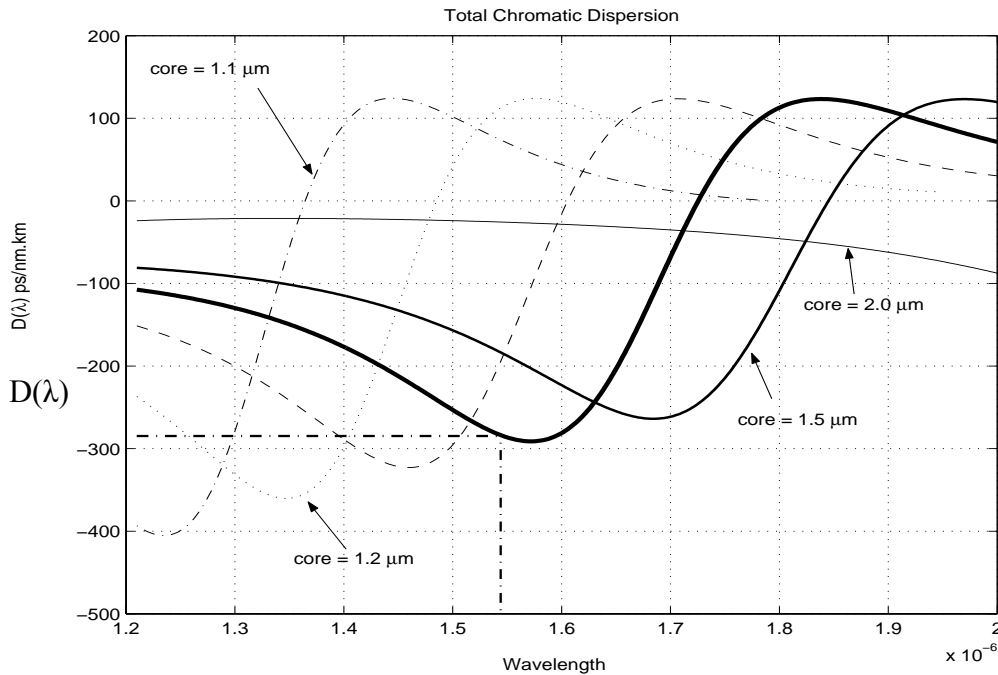
Figure V-12 Illustration of shifting of Waveguide Parameters with variation of core radius

To investigate the effect of cladding radius on the chromatic dispersion, the core radius is kept fixed at 1.3 µm and the cladding radius is investigated according to the variation of the R which ranges from 1.5 to 4.5.
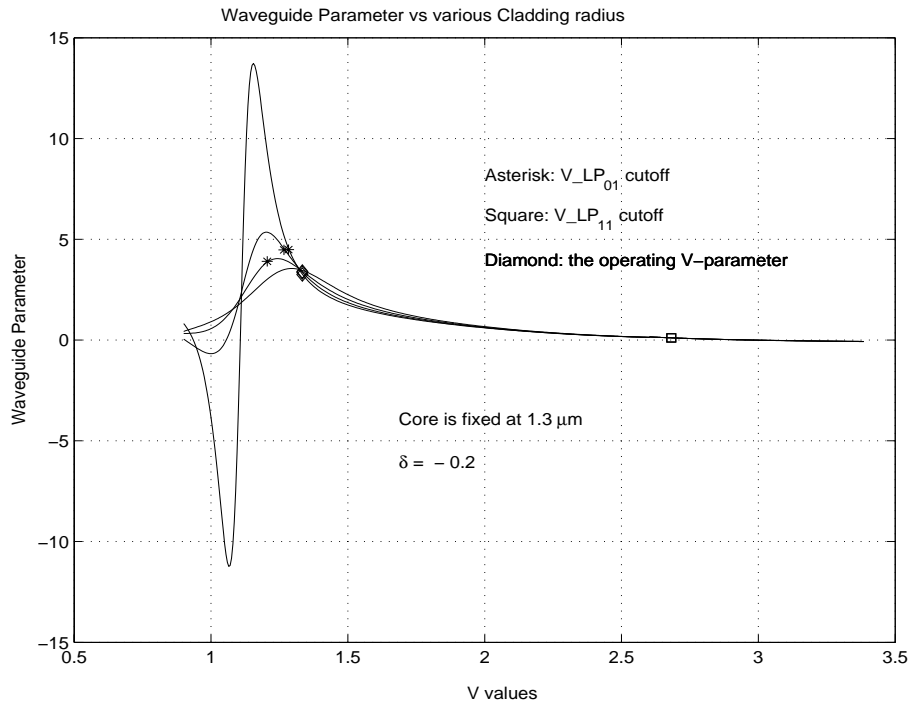
Figure V-13: Waveguide Parameters with variation of cladding radius

- The asterisks and the square markers show the values of V_{C01} and V_{C11} respectively. As shown in Fig. V-13, the operating V value is higher than the cut-off of LP_{01} mode. Therefore, the single mode propagation is conserved.

- It is significant to understand the dependence of the cut-off values on the design parameters. In terms of Eq.V-33, it can be drawn that the cut-off V_{C01} and V_{C11} depend only on the ratio of the radii and δ. In addition, as discussed in the previous sections, these two parameters play the critical roles in determining the shape of the waveguide factor. Therefore the first step in the design is to consider the proper combination of these two design parameters.

- The desire of shifting the operating V or V_{13} to the proper position on the right steep slope of the waveguide parameter, i.e to lower V-values, which correctly corresponds to the operating band of interest: C, L - band, can be achieved by reducing the core radius or increasing the inner cladding's refractive index. V_{13} can also be shifted by changing the value of δ. However, this variation will affect to the waveguide parameter which has already been properly selected. These points can be verified with the following equations : $\quad V_{12} = k_0 an\sqrt{2\Delta_1}$; $V_{12}\sqrt{1+\delta} = V_{13}$
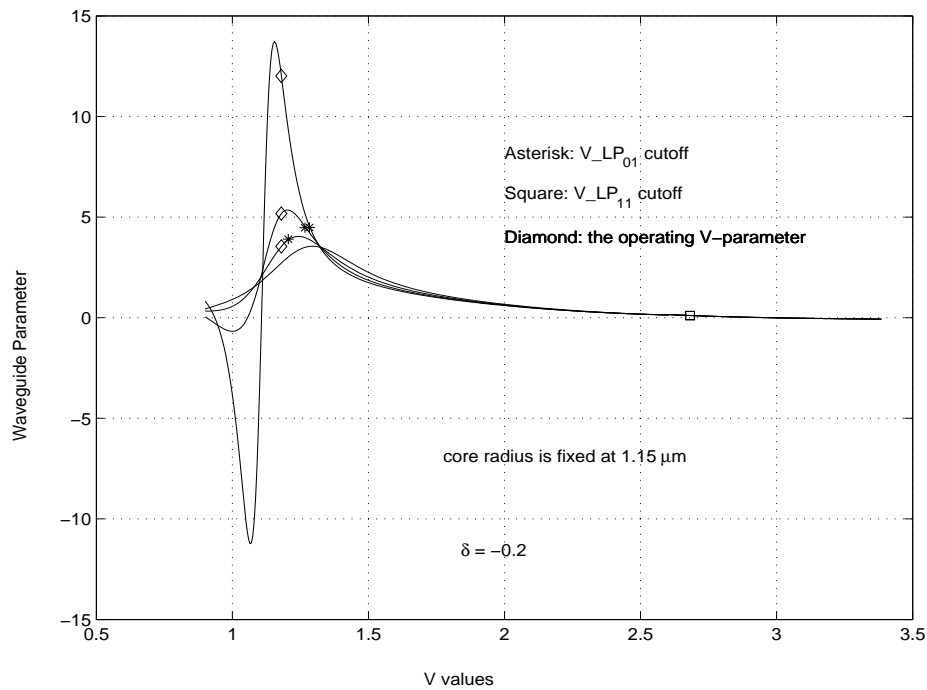
Figure V-14: Illustration of the case when operating V-parameter is lower than the cut-off V-parameter of LP$_{01}$

B.3.d.   *Effects of core, inner and outer cladding RI on total chromatic dispersion and other properties*

Since the RI of the core and the inner cladding are mainly influent on the shifting of the waveguide factors and hence the total dispersion of the interested operating spectrum, C-L-band, it is of more significance to thoroughly investigate the effect of the variation of the outer cladding RI on the design of the W-fibre. This can be achieved by keeping the the RIs of core and inner-cladding to be constant and varying the δ, hence the RI of the outer-cladding.

The radii and RIs of core and inner-cladding are kept constant as follows:

Core radius a (µm)	Inner-cladding radius b (µm)	Core RI (n_1)	Inner-cladding RI (n_2)	Outer-cladding RI (n_3)
1.6	2.56	1.4503 (4.1%Ge-doped)	1.4208 (5.05%F-doped)	Varied from 1.4261 to 1.4341

Table V-1: Profile for investigation with variation of outer-cladding RI.

Outer-cladding RI (n_3) varied from 1.4261 to 1.4341 is equivalent to the variation of δ in the range of -0.21 to -0.44 in the same sequence. Based on the condition for completely guiding the fundamental mode in the core shown in (V-16), the profile conserves the single mode within the range of δ of [-0.21 to -0.4]. When δ is more negatively increased, the leaky mode is triggered to occur.

The graphical results of key properties of the designed W-fibre with various values of cladding radius n_3 are shown in Fig.V-15 to V-24.
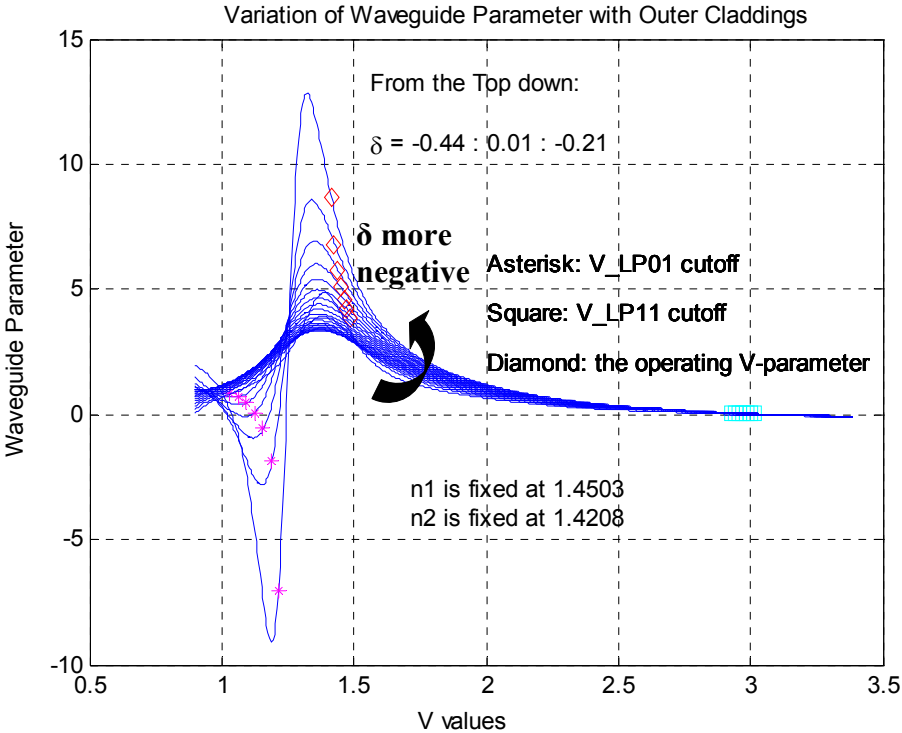
Figure V-15: Waveguide Parameters vs normalised frequency V
with variation of outer-cladding RI
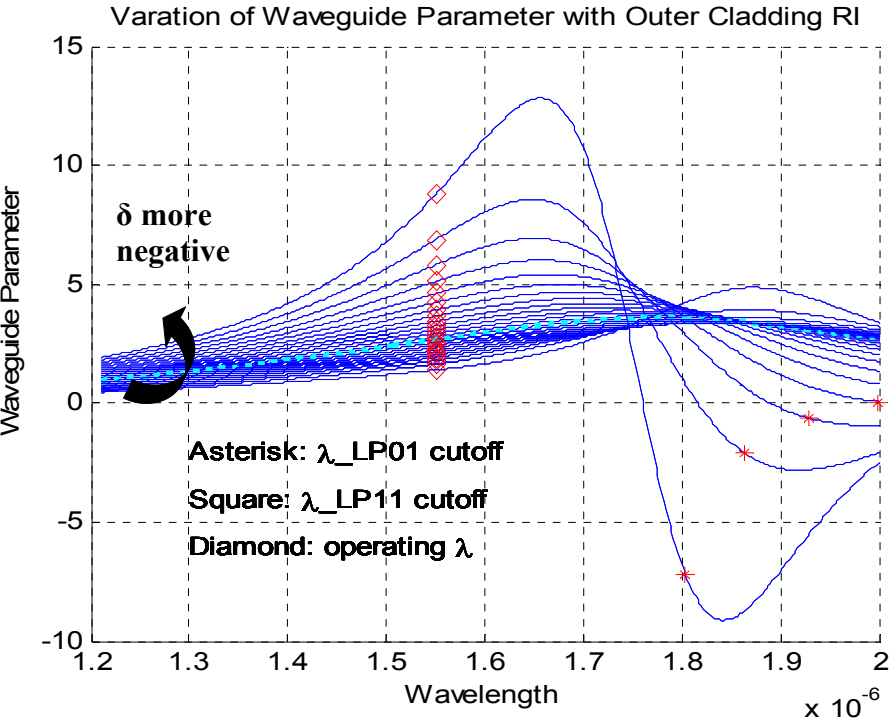
Figure V-16: Waveguide Parameters vs wavelengths with variation of outer-cladding RI
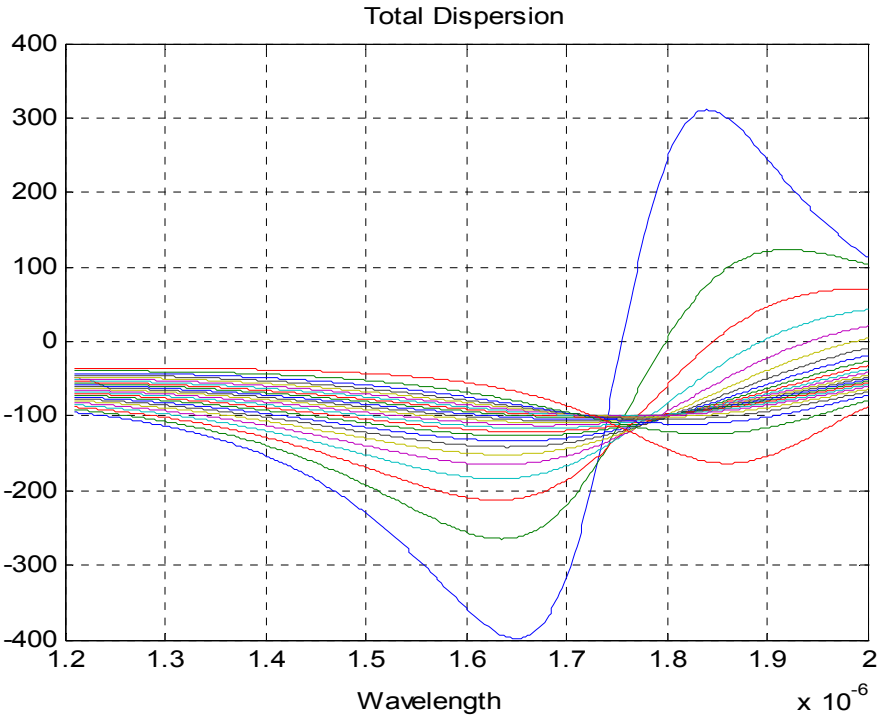
Figure V-17: Total Chromatic Dispersion vs wavelengths
with variation of outer-cladding RI
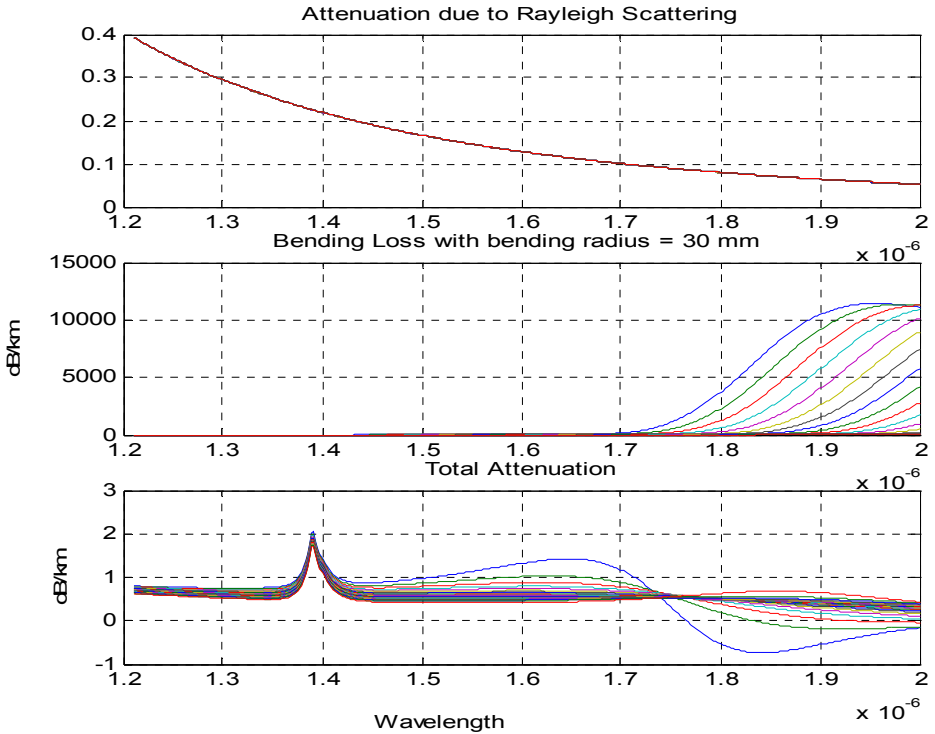
Figure V-18: Total Attenuation with variation of outer-cladding RI
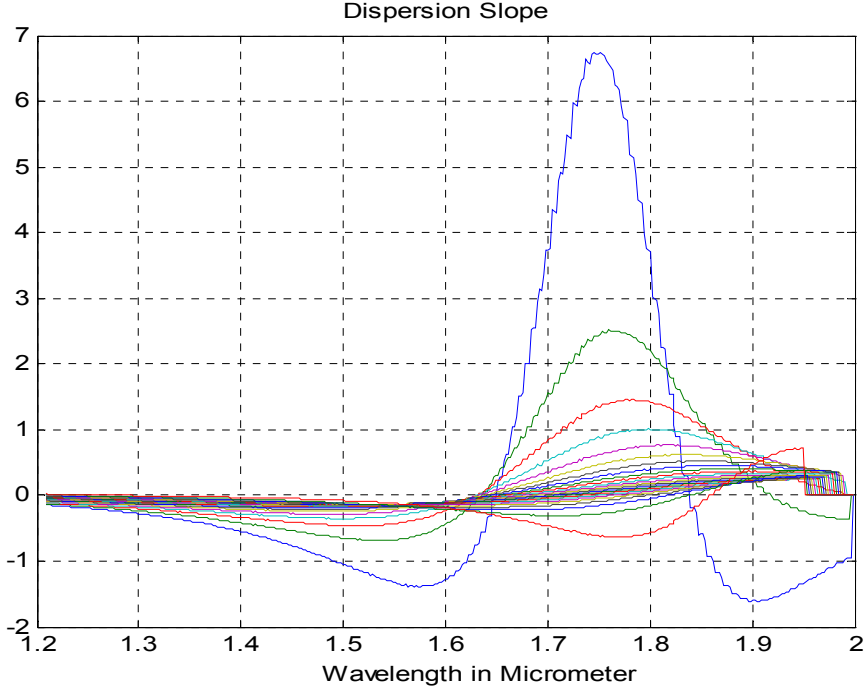
Figure V-19: Dispersion Slope with variation of outer-cladding RI
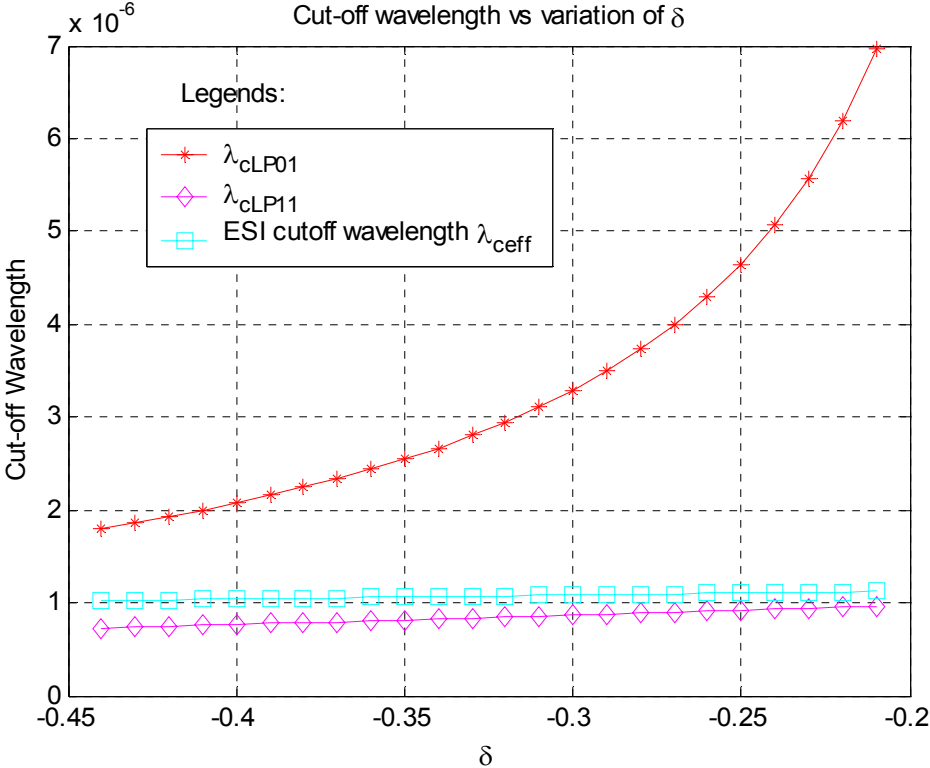
Figure V-20: Cut-off wavelengths with variation of outer-cladding RI
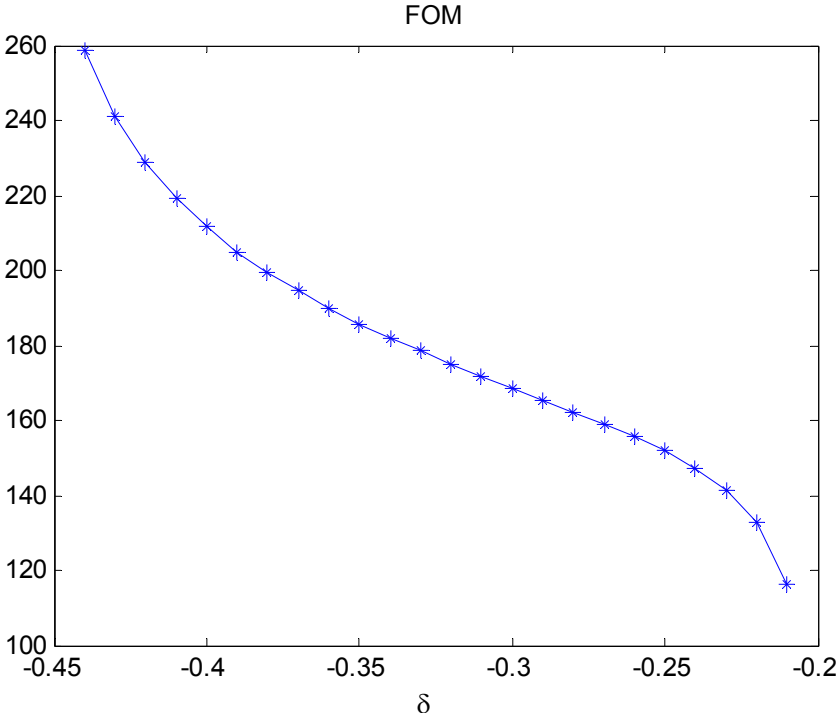
Figure V-21: FOM with variation of outer-cladding RI
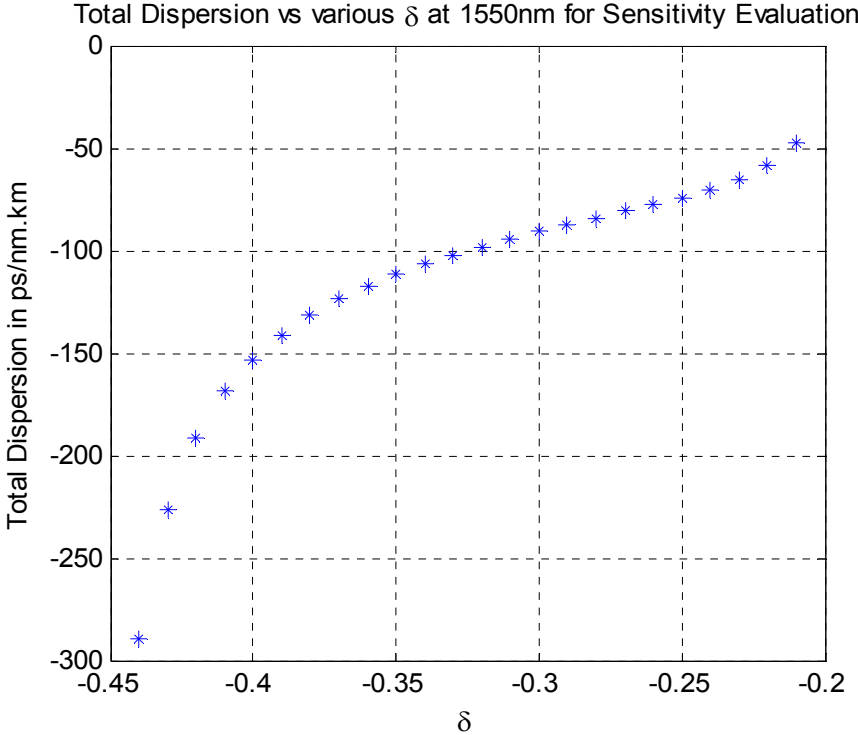
Figure V-22: Sensitivity of W-fibre with variation of outer-cladding RI
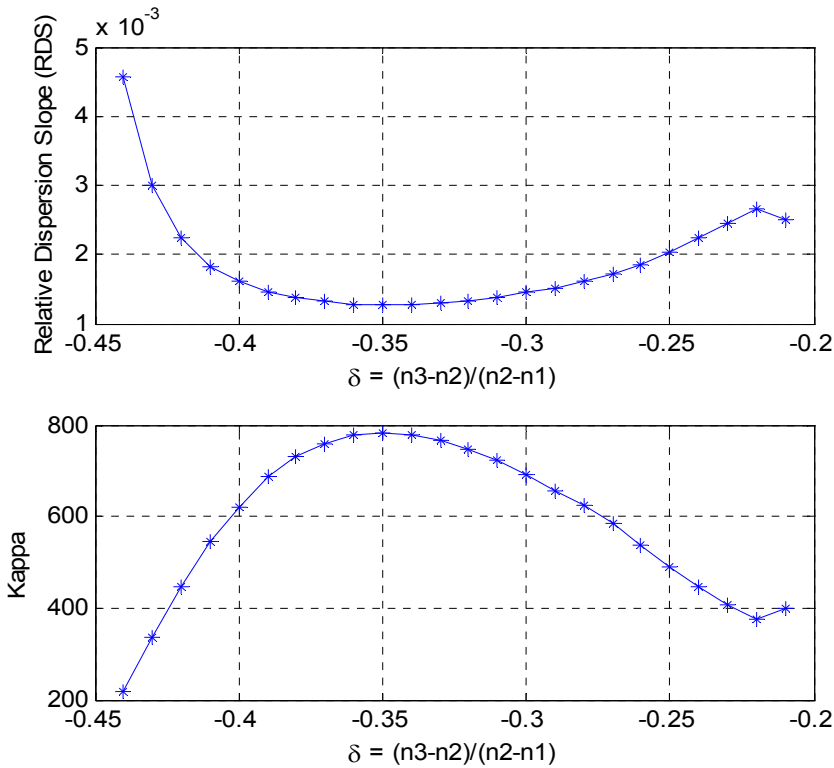
Figure V-23: RDS and Kappa with variation of outer-cladding RI
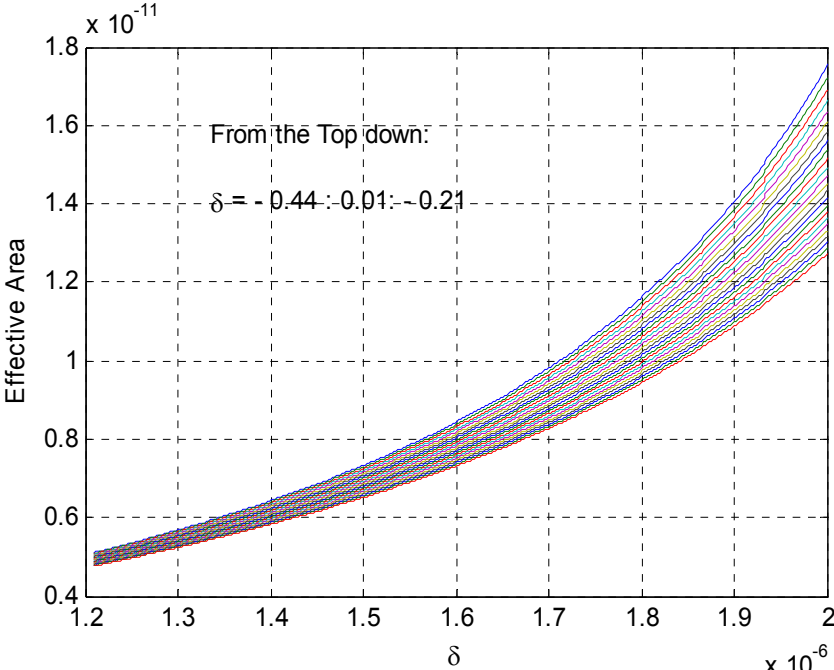
Figure V-24: Effective area with variation of outer-cladding RI

B.4 Discussion on the optimization and the validity of the results

The case of $\delta = -0.44$ or $n_3 = 1.4341$ is considered to be the optimized as it enables both large anomalous negative dispersion and high dispersion slope with large RDS and FOM. Although, a relatively high attenuation at the window about 1550 nm wavelength of 1.1344 dB/km might be seen as the trade-off the design, the large figure of FOM (up to 260 ps/nm.dB in Fig.V-21) and the short length of this DCF W-fibre will overcome this limitation.

This design is aiming for the compensation of the standard SMF fibre operating in the window of 1310 nm. With the dispersion value about 17 ps/nm.km and the dispersion slope of about 0.057 ps/nm^2.km at 1550 nm wavelength, SMF fibre produce the RDS and Kappa figures of approximately 0.0034 nm^{-1} and 298 nm respectively. Compared to the design results with $\delta = -0.44$, the designed RDS may obtain a high value up to 0.0047 nm^{-1} (Fig. V-23) which is due to the dispersion of -300 ps/nm.km and the slope of -1.3199 approximately (Fig. V-17 and V-22). In contrast, the Kappa value of this result, can reach to a low value of 200 nm. This DCF W-fibre can be suitably used in compensation management for several types of standard SMF fibres such as SMF-28 of Corning or Furukawa SM332 .etc or even the low-slope NZ-DSF for DWDM transmissions: FutureGuide^{TM} - USS of Fujikara.

For relatively high slope NZ-DSF fibres such as FutureGuide^{TM} – ULA of Fujikara which has RDS value of 0.0062 nm^{-1}, the following design profiles may be best suitable for the compensating management scheme.

B.5 Design profiles for NZ-DSF fibre

Profile 1

Core radius a (µm)	Inner-cladding radius b (µm)	Core RI (n_1)	Inner-cladding RI (n_2)	Outer-cladding RI (n)
1.35	2.835	1.4487 (3.1% Ge-doped)	1.4208 (5.05% F-doped)	1.42566

Table V-2: Fibre parameters of profile 1

Disper-sion (ps/nm. km)	Dispersion Slope (ps/nm². km)	RDS (nm⁻¹)	Attenuation (dB/km)	FOM (ps/nm. dB)	λ_{C11} (µm)	Effective Area (µm²)	Critical curvature (mm)
-165.42	-1.0321	0.00624	0.7615	220.4	1.0412	6.8597	9.92

Table V-3: Design results of fibre properties of profile 1

The profile in Table V-2, gives the design parameters to be : *R = 2.1 and δ = -0.174*, which implies the infinite cut-off wavelengths and the completely guided mode within the core. Hence, the designed fibre does not experience the loss of power due to leaky mode

The graphical plots obtained in the simulation are demonstrated in Figs. V-25 to Fig.V-26.
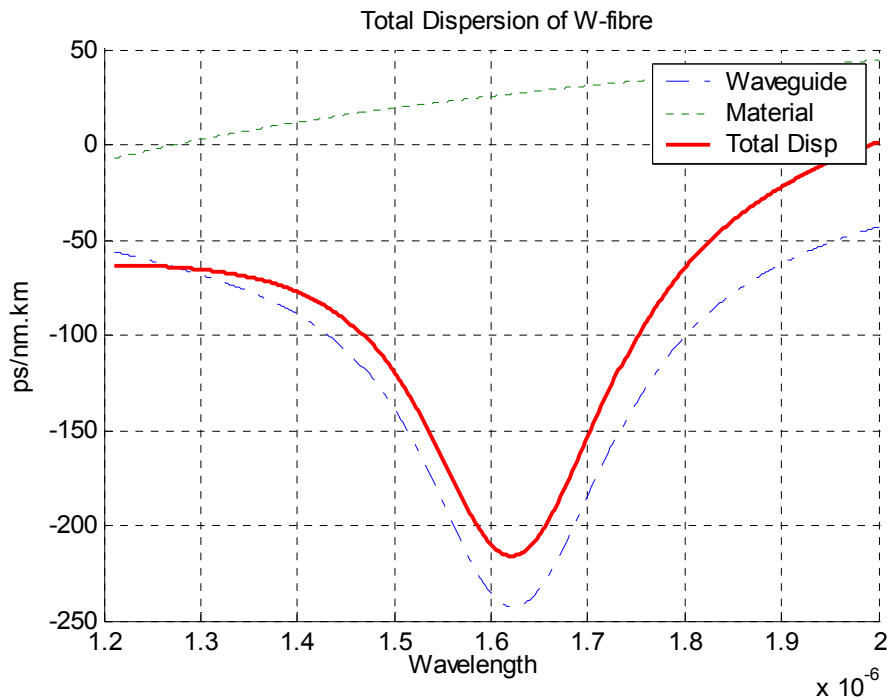
Figure V-25: Total Dispersion of W-fibre for NZ-DSF (Profile 1)
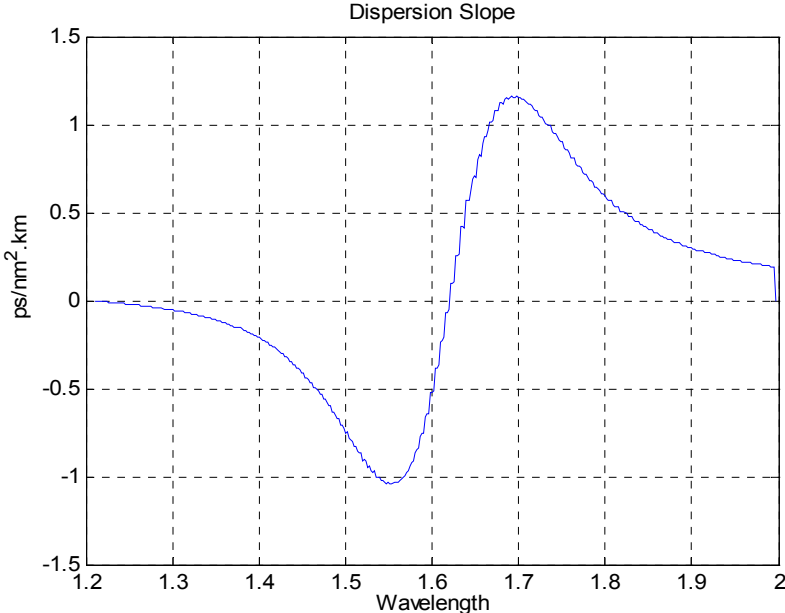
Figure V-26: High dispersion slope achieved for W-fibre for NZ-DSF (Profile 1)
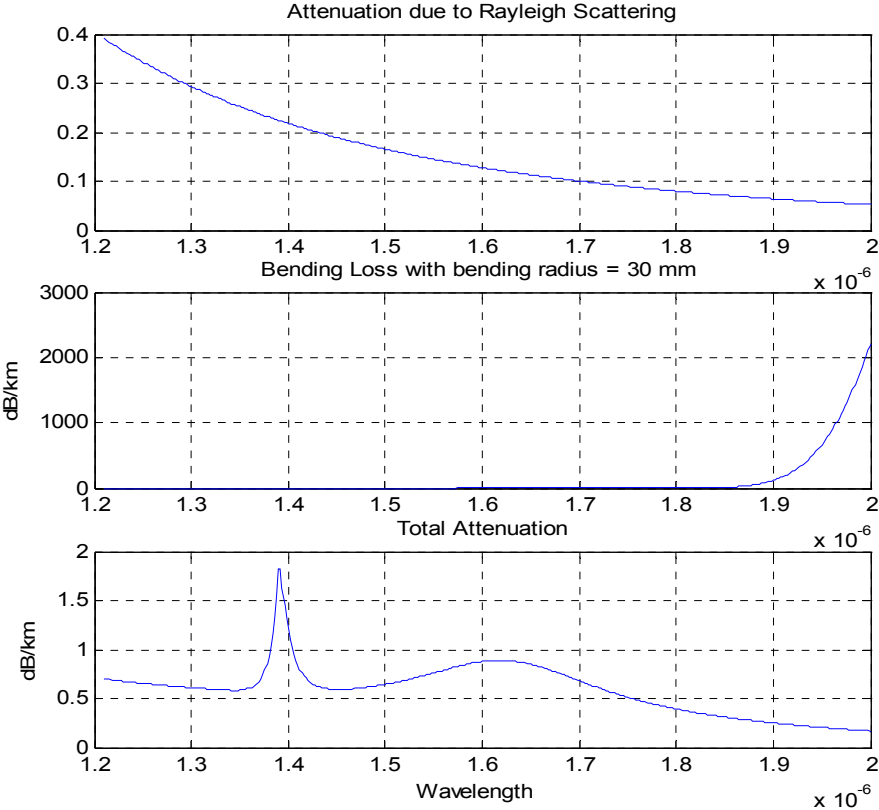
Figure V-27: Total Attenuation of W-fibre for NZ-DSF (Profile 1)

However, several types of very high slope NZ-DSF long-haul transmission fibres such as LEAF® or TrueWave-RS fibres which have been widely deployed always pose challenges to the simultaneous compensation for the dispersion and dispersion slope. The LEAF® fibres has a high value of RDS of 0.0202 (nm^{-1}) and that for the TrueWave-RS fibre is 0.01 (nm^{-1}) [2, 41].

The following profiles of the DCF W-fibre are specifically designed for those sorts of fibres.

B.6 Design profiles for very high slope NZ-DSF fibres

Profile 2

Core radius a (µm)	Inner-cladding radius b (µm)	Core RI (n_1)	Inner-cladding RI (n_2)	Outer-cladding RI (n)
1.31	2.62	1.4487 (3.1% Ge-doped)	1.4208 (5.05% F-doped)	1.42566

Table V-4: Fibre properties of profile 2

Dispersion (ps/nm.km)	Dispersion Slope (ps/nm^2.km)	RDS (nm^{-1})	Attenuation (dB/km)	FOM	λ_{C11} (µm)	Effective Area (µm^2)	Critical curvature (mm)
-546.14	-13.646	0.025	1.9036	316.54	1.0463	7.049	12.15

Table V-5: Fibre parameters of profile 2

The profile in Table V-4, gives the design parameters to be : *R = 2 and δ = -0.174*, which implies the infinite cut-off wavelengths and the completely guided mode within the core. Hence, the designed fibre does not experience the leaky mode
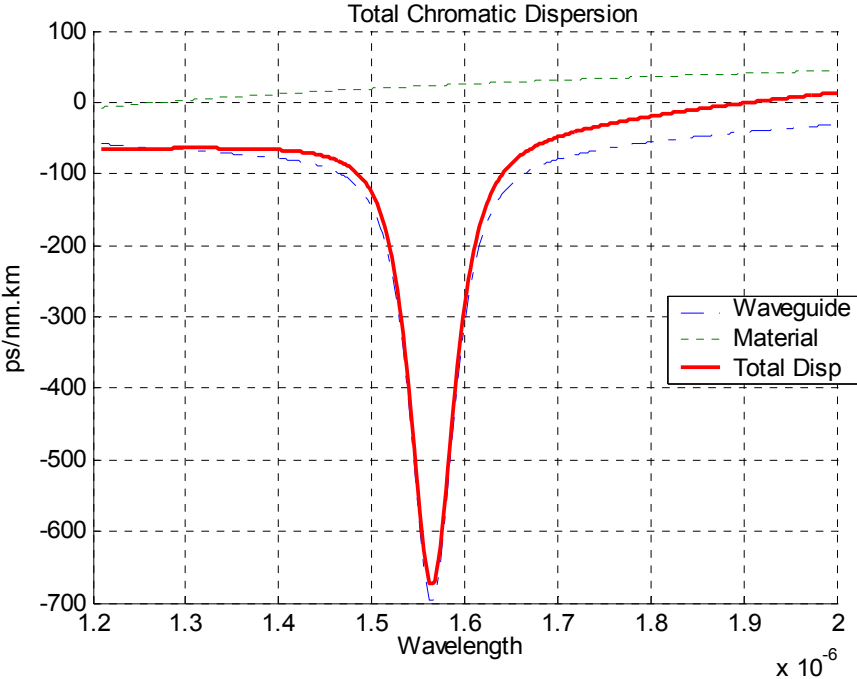
Figure V-28: Large negative Chromatic Dispersin of W-fibre (Profile 2) designed for compensation of high slope NZ-DSF
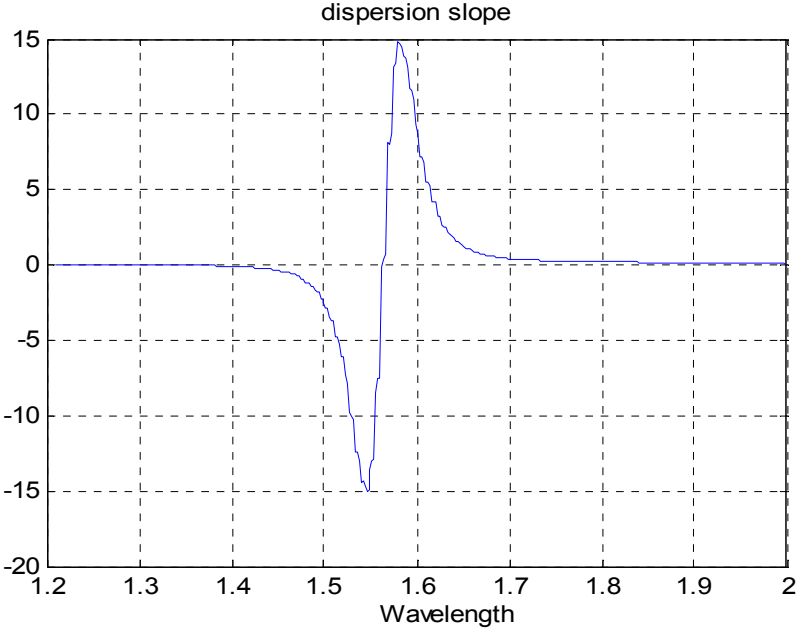
Figure V-29: High Dispersion Slope of W-fibre (Profile 2) designed for compensation of high slope NZ-DSF
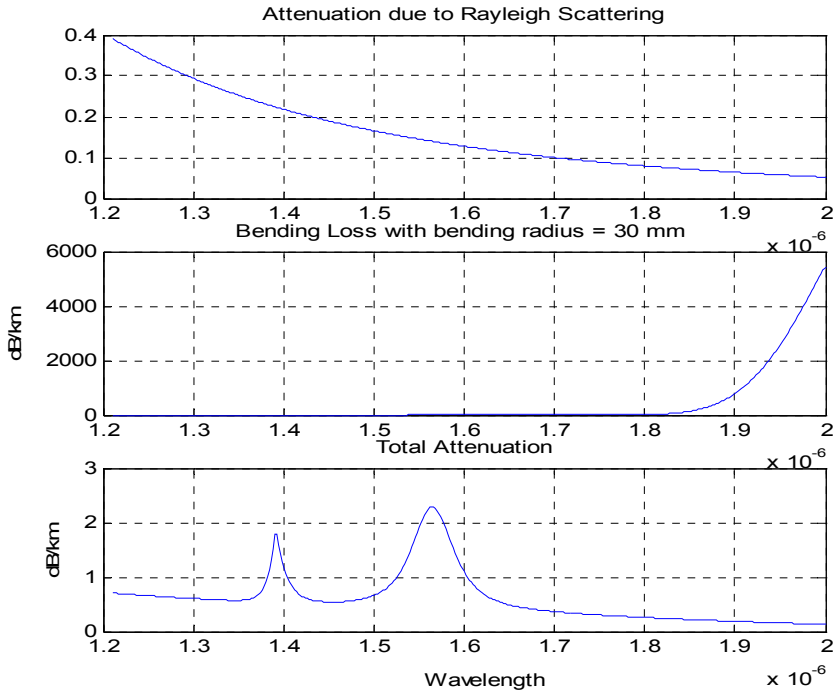
Figure V-30: Attenuation of W-fibre (Profile 2) designed for compensation of high slope NZ-DSF

The draw back in the design for anomalously negative dispersion is the increase of the attenuation. However, based on (V-8), the length of this DCF fibre is very short, whose total insertion loss will not abruptly rise. As comparison, the commercial DCF module produced by Siemens has total insertion loss of 10 dBm.

Profile 3

Core radius a (μm)	Inner-cladding radius b (μm)	Core RI (n_1)	Inner-cladding RI (n_2)	Outer-cladding RI (n)
1.176	2.2344	1.4562 (7.9% Ge-doped)	1.4208 (5.05% F-doped)	1.427172

Table V-6 Fibre properties of profile 3

Dispersion (ps/nm.km)	Dispersion Slope (ps/nm^2.km)	RDS (nm^{-1})	Attenuation (dB/km)	FOM	λ_{C11} (μm)	Effective Area (μm^2)	Critical curvature (mm)
-600.24	-14.536	0.02422	2.07	316.37	1.0835	5.586	8.17

Table V-7 Fibre parameters of profile 3

The profile in Table V-6, gives the design parameters to be : *R = 1.9 and δ = -0.18*, which also implies the infinite cut-off wavelengths and the completely guided mode within the core. Hence, the designed fibre does not experience the leaky mode.
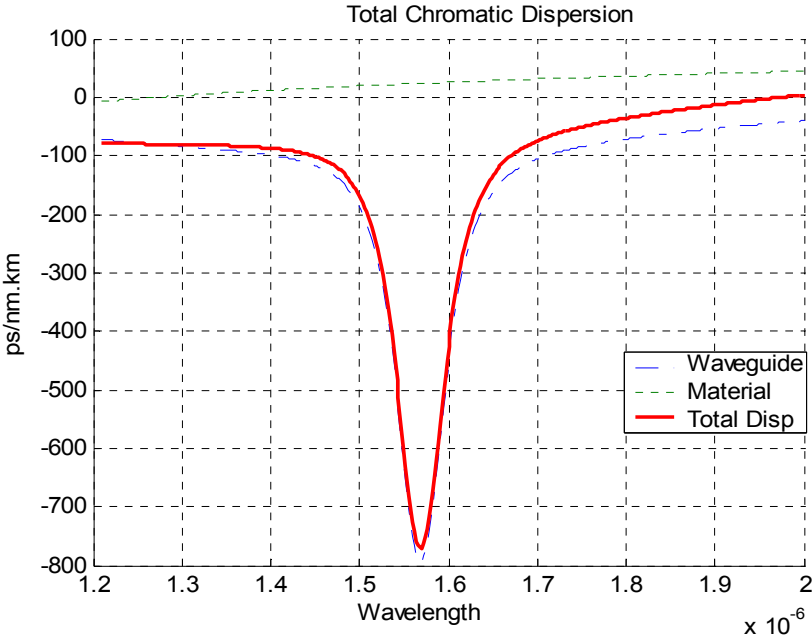
Figure V-31: Large negative Chromatic Dispersin of W-fibre (Profile 3) designed for compensation of NZ-DSF
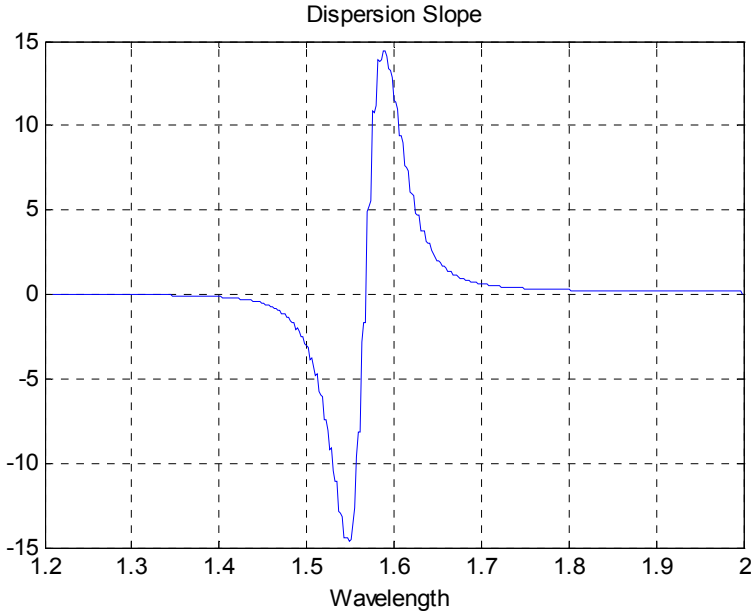
Figure V-32: High Dispersion Slope of W-fibre (Profile 3) designed for compensation of high slope NZ-DSF
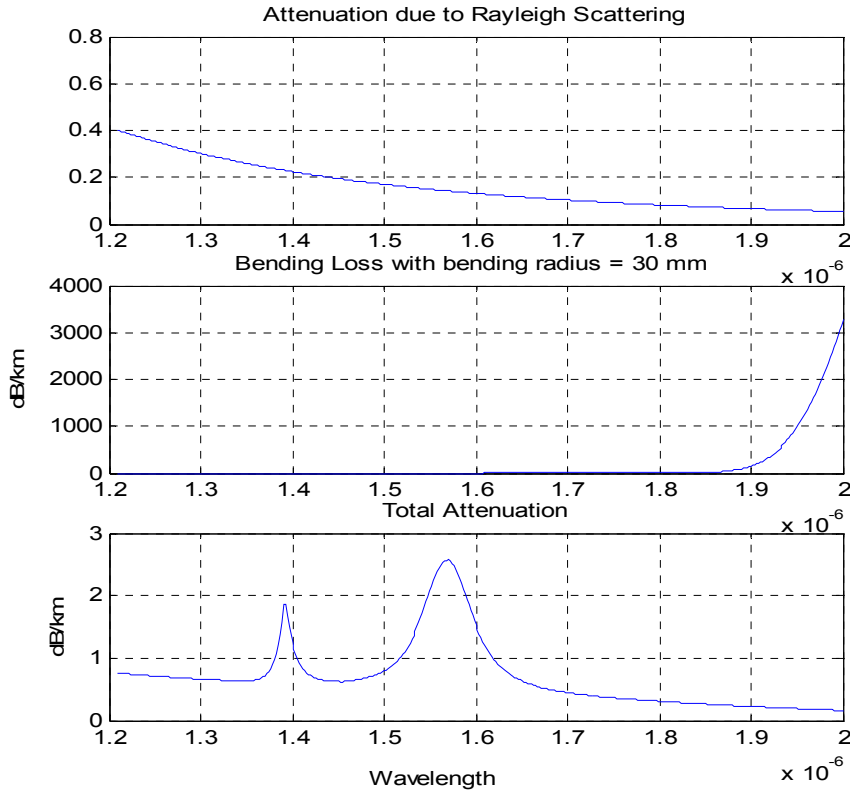
Figure V-33: Attenuation of W-fibre (Profile 3) designed for compensation of high slope NZ-DSF

Profile 4

Core radius a (μm)	Inner-cladding radius b (μm)	Core RI (n_1)	Inner-cladding RI (n_2)	Outer-cladding RI (n)
1.14	5.13	1.4487 (3.1% Ge-doped)	1.4208 (5.05% F-doped)	1.4239

Table V-8 Fibre properties of profile 4

Dispersion (ps/nm.km)	Dispersion Slope (ps/nm^2.km)	RDS (nm^{-1})	Attenuation (dB/km)	FOM	λ_{C01} (μm)	λ_{C11} (μm)	Effective Area (μm^2)	Critical curvature (mm)
-632.37	-17.329	0.0274	2.163	324.14	1.8218	7.6225	6.98	17.66

Table V-9 Fibre parameters of profile 4

The profile in Table V-4, gives the design parameters to be : *R = 4.5 and δ = -0.11*, which meets the condition of (V-16) for the mode starts leaky and finite cut-off wavelength. However, according to the relatively large ratio of radii (R), the leaky mode is expected to be less abruptly changed.
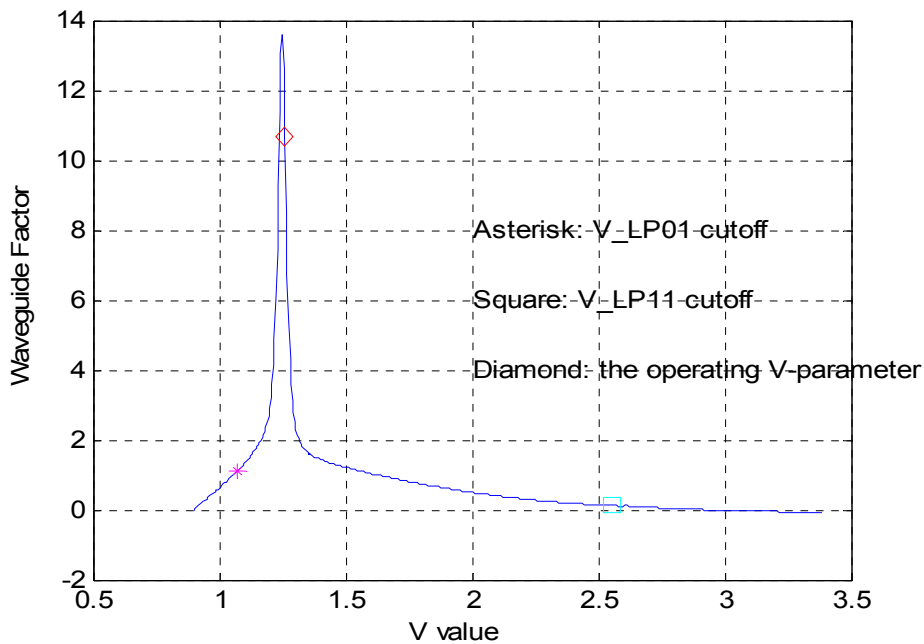
Figure V-34: Waveguide Parameter vs V-values of W-fibre (Profile 4) designed for compensation of high slope NZ-DSF
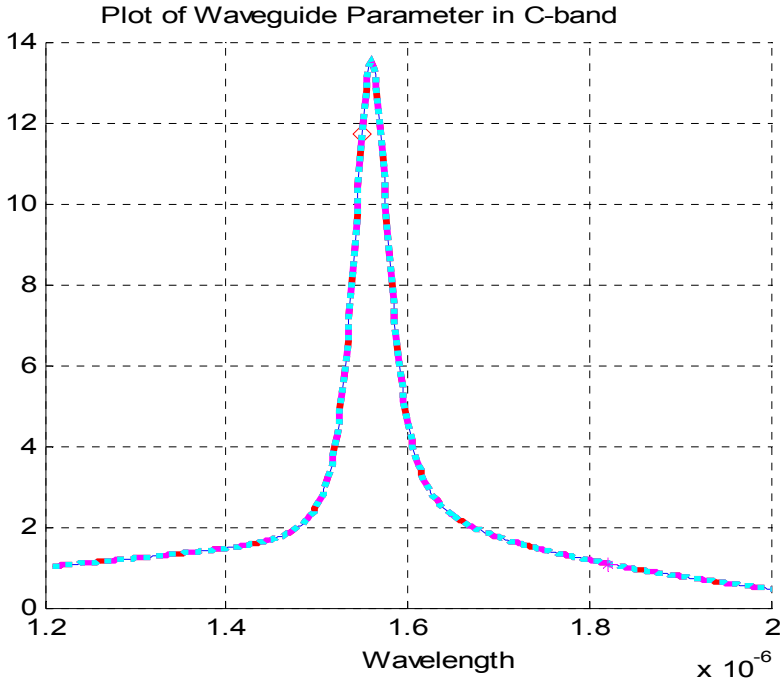
Figure V-35: Waveguide Parameter vs wavelengths of W-fibre (Profile 4)
designed for compensation of high slope NZ-DSF
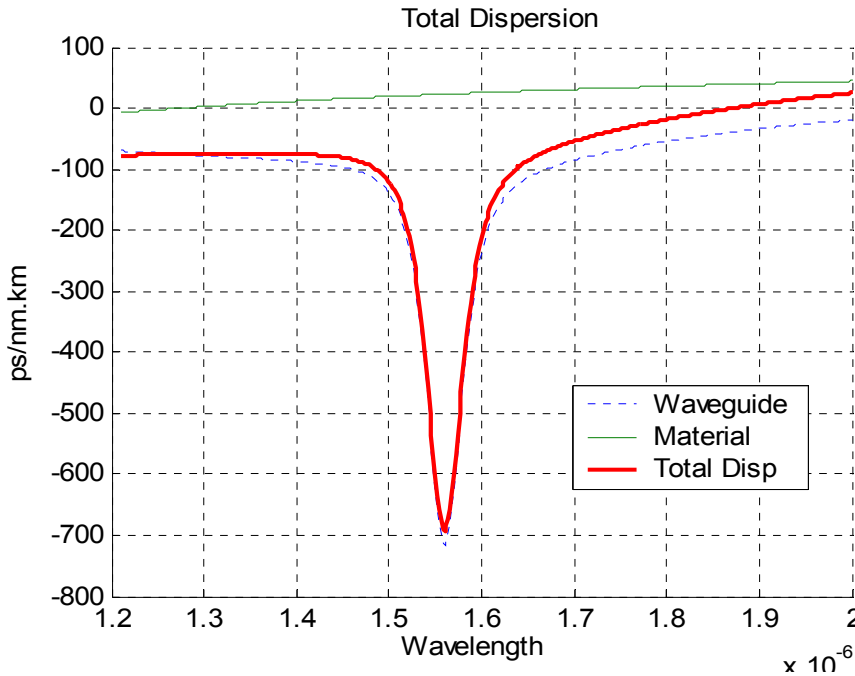
Figure V-36: Total Chromatic Dispersion of W-fibre (Profile 4)
designed for compensation of high slope NZ-DSF
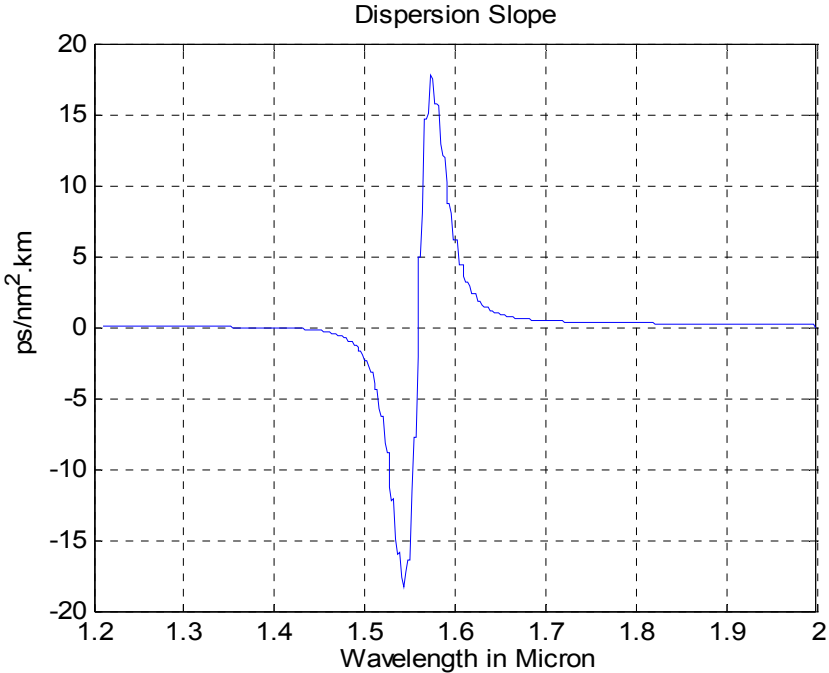
Figure V-37: Dispersion Slope of W-fibre (Profile 4)
designed for compensation of high slope NZ-DSF
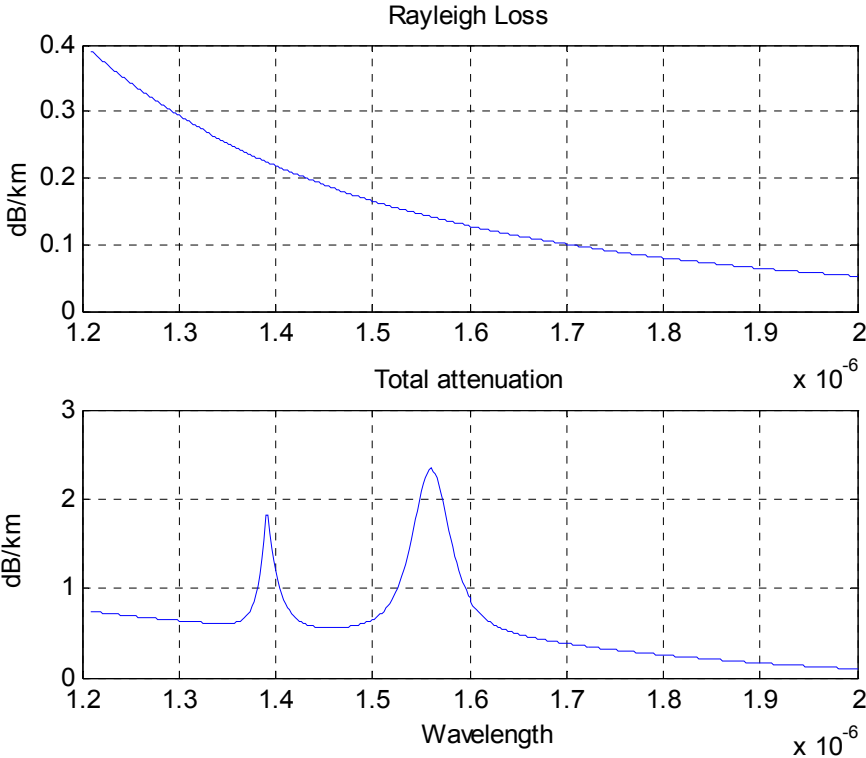
Figure V-38: Total Attenuation of W-fibre (Profile 4)
designed for compensation of high slope NZ-DSF

B.7 Design Methodology of Double Clad or W-shaped Fibre

- The design can be started considering the selection of either Δ_1, Δ_2, δ, a, b, or b/a. Since n_1 is known, setting Δ_1 will change n_2. If n_2 is also set, the tuning of Δ_1 or δ will lead to the variation of n.   Similarly, a change in the ratio b/a leads to changing b for a known radius a.

- It is best to design on the Vd^2Vb/dV^2 curve firstly based on a careful selection of δ and b/a. This combination is also needed to be considered for the cut-off V values of LP01 and LP11 modes. The V_{C01} and V_{C11} are shown on the curve of the waveguide factor with the asterisk and the square marker respectively. When the LP_{11} or LP_{01} cut-offs are properly determined to fall in the window of the wavelength spectrum being considered, C-L band, this then leads to the curve of the waveguide factor versus the range of operating wavelengths.

- The fibre properties included dispersion slope, attenuation, cut-off wavelength, spot-size, the FOM, the RDS and the critical curvature for bending loss evaluation can all be obtained.

- The draw-backs of W-fibre are the high attenuation, high sensitivity due to microbending loss and the shortage of freedom design control parameters, which gives W-fibre a low design flexibility and tolerance. Multiple-Clad fibres such as Triple-Clad fibre can cope with the problems. They provide higher design freedom degree by providing larger number of design parameters. The analysis and design steps of optical fibres with tripple cladding regions is presented in this section so that a complete design platform for dispersion compensation based on in-line optical fibres is available for DWDM system designers. A new and simple method has been developed for the approximation of Waveguide Dispersion Parameter Curves (ref: paper has been submitted).

C. Triple-Clad Fibre

The motivation in a design of triple clad fibre are in terms of the improvement of the fibre profile which has seven degrees of freedom to optimize the important fiber parameters compared with four in W-fibre. More control parameters gives more flexibility to obtain a good design. Large anomalous negative dispersion and high dispersion slope can be more easily achieved using this profile than in W-fibre. The problem facing the multi-clad such as triple-clad and quad rupture-clad fibres is that the LP_{02} mode can exist. [5, 24]

C.1 Profile Construction
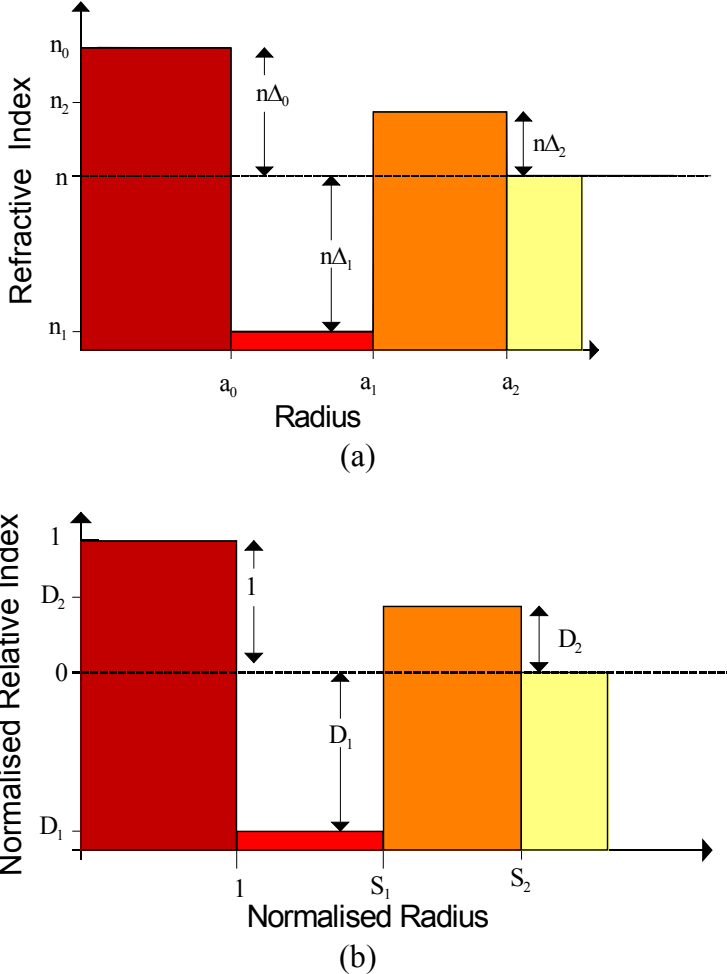
Figure V-39: RI profile of a triple-clad fibre (a) non-normalised index profile, and (b) normalised profile

The non-normalised and normalised RI profiles of a triple-clad step-index fibre is shown schematically in Figs 1(a) and 1(b) respectively. a_i - the ith outer radius, n_i - the RI of the *i-th* layer and n – the RI of the uniform cladding. The RI of the ith layer relative to that of the uniform cladding is thus given by [42, 43]:

$$\Delta_i = \frac{n_i - n}{n} \qquad\qquad \text{(V-37)}$$

The normalised outer radius is also defined as

$$S_i = \frac{a_i}{a_0} \qquad\qquad \text{(V-38)}$$

The normalised relative index of the *i-th* layer is then given by

$$D_i = \frac{\Delta_i}{\Delta_0} \qquad\qquad \text{(V-39)}$$

with $S_0=1$ and $D_0=1$. It is convenient to express the degrees of freedom in terms of the structural parameters a_0, S_1, S_2, n_0, D_1, D_2 and n.

A MATLAB design platform has been developed. The V-dependent parameter representing D_W are numerically determined. Seven fibre parameters that affect the performance of the triple clad fibres are: core radius (a_0), first cladding radius (a_1), second cladding radius (a_2), core index (n_0), first cladding index (n_1), second cladding index (n_2) and outer cladding index (n) are used as the degree of freedom in the designs.

C.2 Waveguide Parameters of Triple-Clad Profile Fibre

The transverse propagation constants of the guided lightwaves **u/a** and **v/a** in the core and cladding regions respectively are formulated for the core and the fist and second cladding layers (corresponding respectively to subscript i where i=0..2) of the triple-clad index profile fibres as

$$u_i = a_i \sqrt{k^2 n_i^2 - \beta_i^2} \qquad\qquad \text{(V-40)}$$

$$v_i = a_i \sqrt{\beta_i^2 - k^2 n^2} \qquad\qquad \text{(V-41)}$$

where β_i with are the propagation constants of the guided waves in the core, the first and second cladding layers are given by

$$\beta_i = \sqrt{k^2\left(b_i(n_i^2 - n^2) + n^2\right)} \qquad \text{(V-42)}$$

Hence the normalised frequencies for all layers can be expressed as

$$V_i = a_i k \sqrt{n_i^2 - n^2} \qquad \text{(V-43)}$$

and the effective V of the multiple-clad fibre can be defined as

$$V_{eff} = ka_0 \sqrt{2n\left((n_0 - n_1) + (n_1 - n_2) + (n_2 - n)\right)} \qquad \text{(V-44)}$$

The spot size r_0 can be found analytically as [3, 28]

$$r_0 = \sqrt{\frac{a_0^2}{\ln V_{eff}^2}} \qquad \text{(V-45)}$$

The spot size can be approximated so that not only the minimum dispersion is achieved but also the requirement for maximum effective area is satisfied.

The radial modal intensity distribution $I(r)$ is given by

$$I(r) \cong \exp\left(\frac{-1}{2}\left(\frac{r}{r_0}\right)^2\right) \qquad \text{(V-46)}$$

The waveguide dispersion factors of different fibre layers can be obtained from (6) as:

$$D_{wi} = -\left(\frac{n_i - n_{i+1}}{\lambda_c}\right) V_i \frac{d^2(V_i b)}{dV_i^2} \qquad \text{(V-47)}$$

where the generic normalised waveguide dispersion coefficient is $Vd^2(Vb)/dV^2$. For triple-clad fibres we have the following three normalised waveguide dispersion parameters

$$\frac{V_i d^2(V_i b)}{dV_i^2} = 2\left(\frac{u_i}{V_i}\right)^2 \left\{ K_i(1 - 2K_i) + \frac{2}{v_i}(v_i^2 + u_i^2 K_i)\sqrt{K_i}\left(K_i + \frac{1}{v_i}\sqrt{K_i} - 1\right)\right\} \qquad \text{(V-48)}$$

with

$$K_i = \frac{BESSELK_1(v_i)}{BESSELK_0(v_i)}$$

where $BESSELK_i$ is the ith order modified Bessel functions. Finally, using the superposition position the total dispersion of multiple-clad fibres is obtained as:

$$D_{TOT} = D_M + D_{W0} + D_{W1} + D_{W2}$$

(V-49)

C.3 Triple Clad Fibre With Fluorine Doped Claddings

In an attempt to improve the parameters of the compensating fibre, we tried doping the claddings with Fluorine instead of Germanium. F-doped silica fibres were described as having well defined step core without any dip, and having low attenuation. The relationship used to determine the level of dopant concentration *d%* required to realise a given refractive index *n(λ,d)* of the F-doped claddings was [37] and [44]

$$\frac{d}{d_0} = \frac{n(\lambda,d) - n(\lambda,0)}{n(\lambda,d_0) - n(\lambda,0)}$$

(V-50)

where d_0 is a reference doping level, and is specified in table 2 as 1% for material I with index *n(λ,d₀)*, and *n(λ,0)* is the undoped pure silica index.

C.4 Approximation of Waveguide Dispersion Parameter Curves

Fig.V-40

shows the complete shape of the waveguide parameters as given in (20) and the approximated curve for its right half where the V-parameter range is fallen into the design range of SMFs. Fig.V-41 shows three Vd2(Vb)/dV2 exact curves as represented by (V-48). Neither simple approximation nor exact representation of Vd2(Vb)/dV2 curves has been found in published literatures. Most published works [42, 43] and the developed algorithm in Ref[45] are far too complicated for design process, particularly at the design inception stage. Therefore, we propose in this section an algorithm to predict the behaviour of $Vd^2(Vb)/dV^2$ in the following steps:
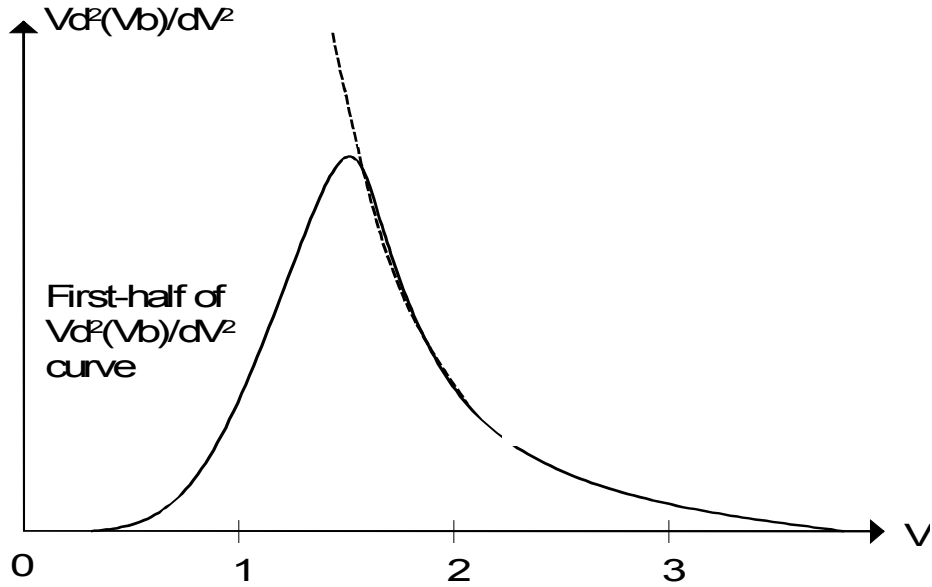
Figure V-40 $Vd^2(Vb)/dV^2$ complete curve, dotted line is obtained from (V-48)

STEP 1: Approximate the right half of the exact $Vd^2(Vb)/dV^2$ curves as given by *Eq.V-48* by a simple analytical expression with an error of less than 2% for 1<V<3 [4]. Inspecting a number of a family of $Vd^2(Vb)/dV^2$ curves [13, 21, 45] shown in *Fig V-41*, the peaks follow a simple cubic equation given by

$$\left(V \frac{d^2 (Vb)}{dV^2} \right) = V^3$$

(V-51)
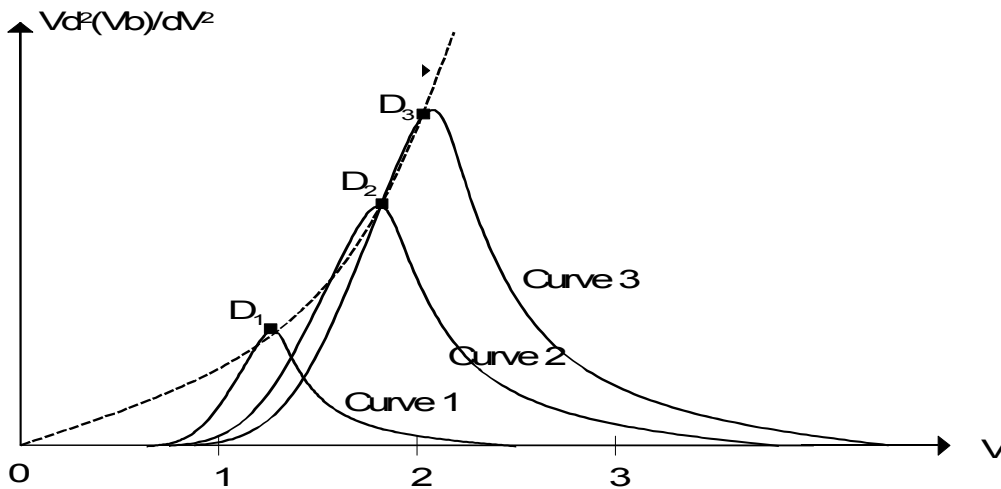
Figure V-41 $Vd^2(Vb)/dV^2$ family curves

Thus, the intercepting point **D**(Dx,Dy) in Fig. V-42 is the corresponding peak of one of the curves. A correction factor, mainly the constant of the cubic equation can be used to modify Eq.V-51 , if required. Higher order polynomial is unnecessary in this case.
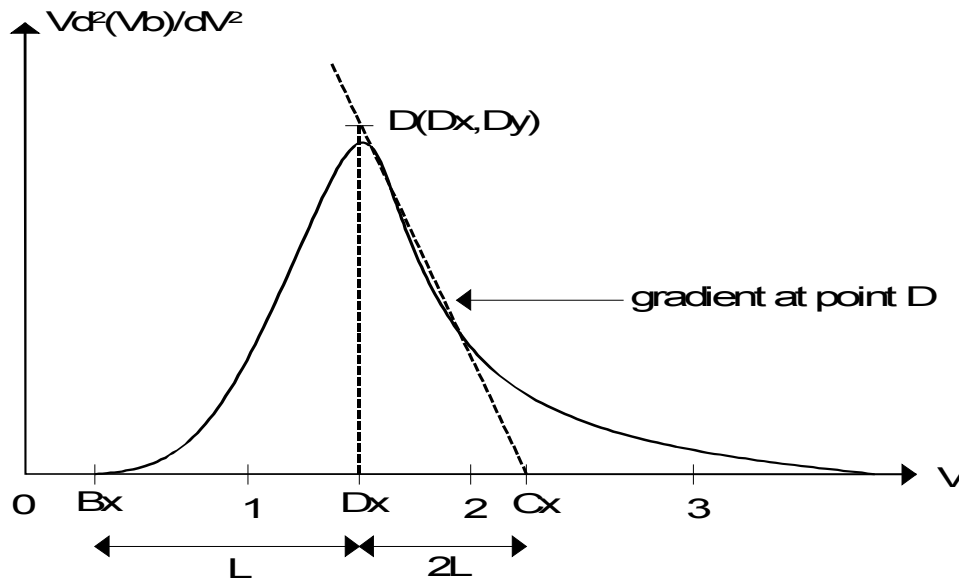
Figure V-42 The intersection point D and the approximated $Vd^2(Vb)/dV^2$ curve.

STEP 2: Referring to the point **D**(D_x, D_y) in Fig. V-42 , we could find the gradient at that point and hence the point Cx given by

$$Cx = Dx - \frac{Dy}{\left(\frac{d}{dV} \left(\frac{Vd^2 (Vb)}{dV^2} \right)_{at(Dx,Dy)} \right)}$$

(V-52)

STEP 3: Having found the location of **C**(Cx,0) we could predict point **B**(Bx,0), that is the cutoff point of $Vd^2(Vb)/dV^2$ curve as

$$Bx = Dx - \frac{1}{2} \left(Cx - Dx \right)$$

(V-53)

STEP 4 Now considering the curve from point **B** to point **D**, additional points are to be introduced to obtain a desired shape. Likewise, a few points are selected to represent the curve in the right-half of the $Vd^2(Vb)/dV^2$ curve. We found that ten points to represent the $Vd^2(Vb)/dV^2$ curve would be adequate. Having obtained these significant points, the task is

59

interpolating them to form a smooth curve. *Spline interpolation* method has been adopted for this purpose.

STEP 5: As we are using the $Vd^2(Vb)/dV^2$ curve to find the waveguide dispersions defined in *(V-48)* the curves as shown in Fig. V-41 can be represented by a general mathematical expression as a function of wavelength. Thus, a polynomial of 9th order given by (V-55) and (V-56) has been chosen for this purpose.

For single-mode, the normalised frequency is given by,

$$V_i = 2.405\left(\frac{\lambda_{c_i}}{\lambda}\right)$$
(V-54)

where λ_{ci} is the cutoff wavelength of ith region.
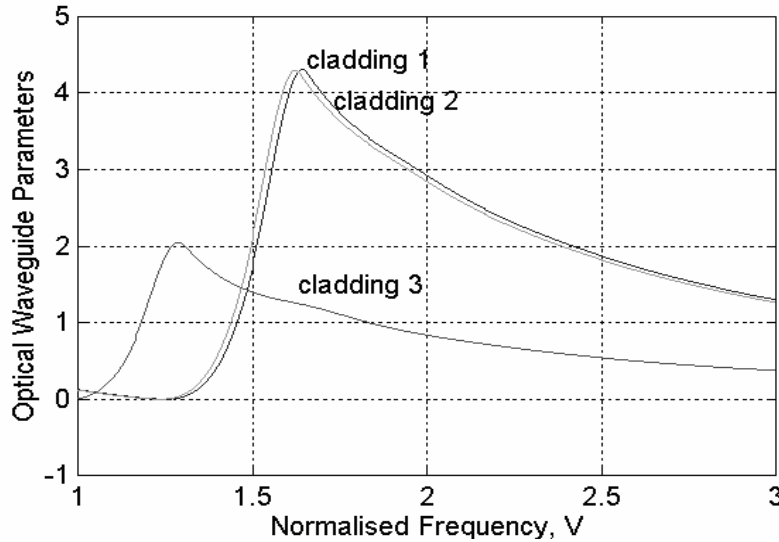
Figure V-43   The optical waveguide parameter curves for optical fibres with three cladding types.

Hence, a *9-th* order of $Vd^2(Vb)/dV^2$ polynomial can be approximated by,

$$V\frac{d^2(Vb)}{dV^2} = P_0 + P_1\left(\frac{2.405\lambda_c}{\lambda}\right) + P_2\left(\frac{2.405\lambda_c}{\lambda}\right)^2 + P_3\left(\frac{2.405\lambda_c}{\lambda}\right)^3 + ... + P_9\left(\frac{2.405\lambda_c}{\lambda}\right)^9$$
(V-55)

$$V\frac{d^2(Vb)}{dV^2} = \sum_{m=0}^{9} P_m\left(\frac{2.405\lambda_c}{\lambda}\right)^m$$
(V-56)

where $P_0, P_1, P_2, ..., P_9$ are the polynomial constants obtained by *polyfiting of MATLAB*[46]

The above steps allow seven degrees of freedom for fibre designs. By analyzing the effect of each parameter we would be able to predict the changes of the dispersion factor and hence identify the main factors that would play a principal role for tailoring the dispersion.

There is a maximum of three zero dispersion points. The first and second zero dispersion points are approximately located in the two spectral windows at 1300 nm and 1550 nm.

C.5 Design Results

C.5.a.   Effect of Core and Cladding Radius on the Total Dispersion

Figs. V-45 to V-47   show the variations of core/cladding radii with respect to the total dispersion factor. We observe the following effects of the variation of the core/cladding radii on the dispersion factor over the entire 1300 nm to 1600 nm spectral region:

(i)   As the core radius, a_0, is increased the total dispersion curve is shifted upwards, at the same time the second zero dispersion point is shifted to higher wavelength region. Meanwhile, the first zero dispersion point remains unchanged and the third zero dispersion point gradually shifts to lower wavelength region. By analyzing the behavior of the dispersion curves of several simulated results, we obtain the maximum sensitivity of changes in a_0 to total dispersion is about 88.88 ps/(nm-km-μm).

(ii)   As the first cladding radius, a_1, is decreased the total dispersion curve shifts upwards. The maximum sensitivity due to incremental change in a_{1_1} to total dispersion is about 64.68 ps/(nm-km-μm).

(iii)   As the second cladding radius a_2 is decreased, the total dispersion curve shifts upwards, but the first zero dispersion point shifts to lower wavelength region, a maximum sensitivity due to incremental changes of a_2 to total dispersion in the fibre windows region of 0.99 ps/(nm-km-μm) is obtained.

PLOT OF MATERIAL, WAVEGUIDE AND TOTAL DISPERSION
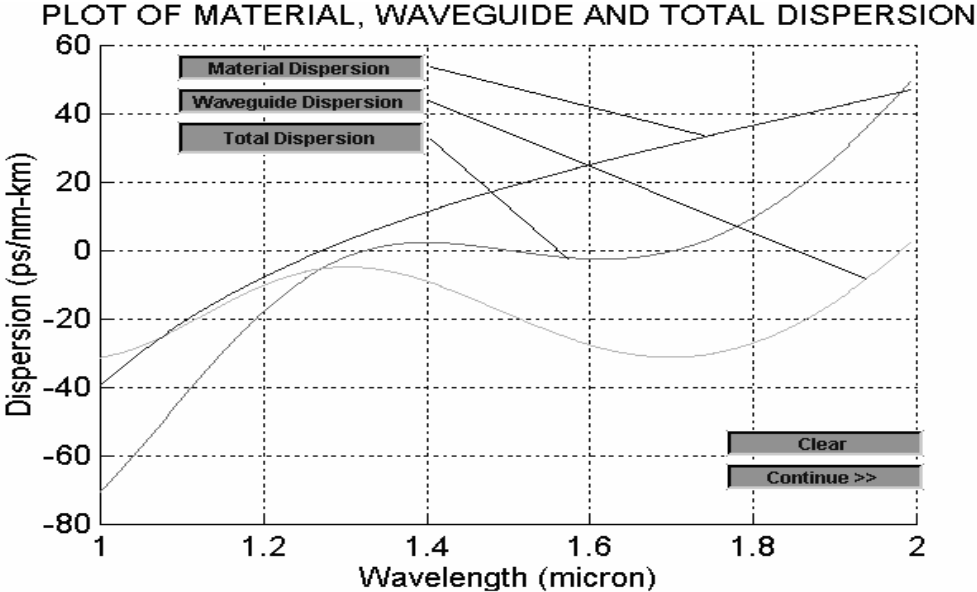
Figure V-44   Material, waveguide and total dispersion of 'type A' as the core material of a triple clad profile as a parameter

PLOT OF VARIOUS CORE RADIUS
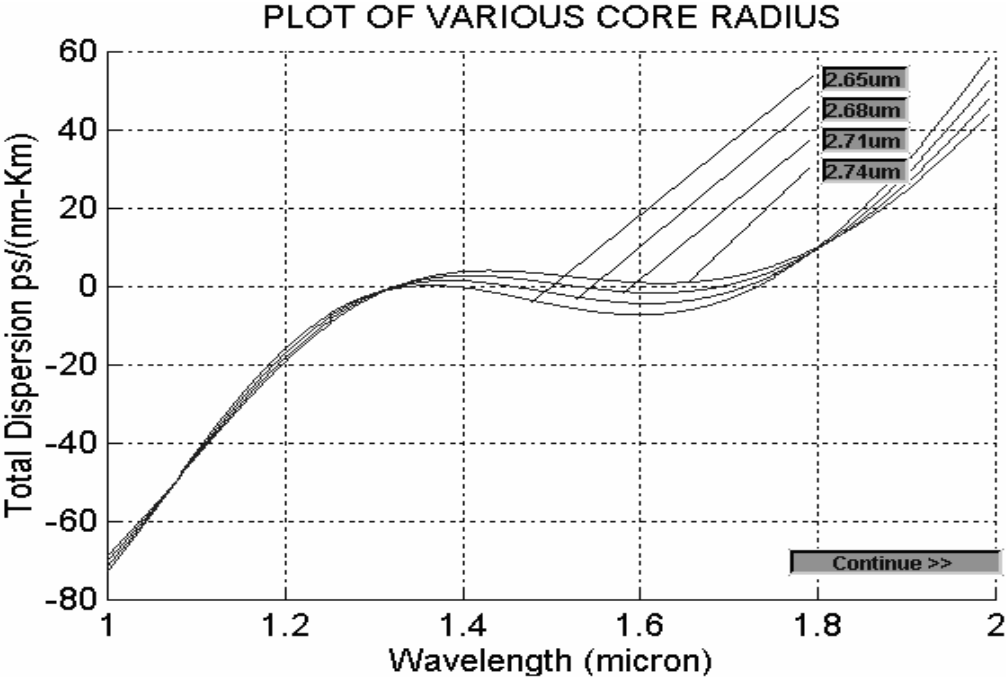
Figure V-45   Total dispersion factor versus wavelength with the core radius of the triple clad optical fibre as a parameter.
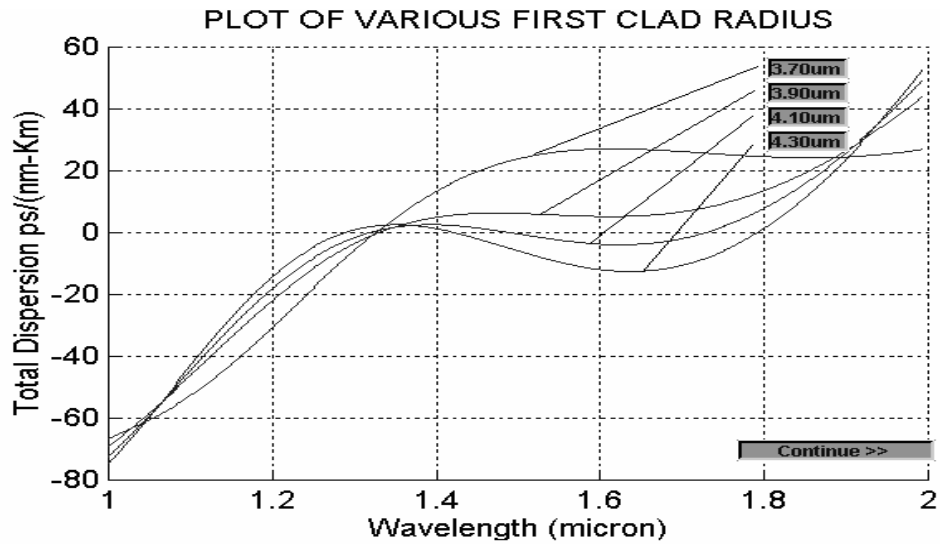
Figure V-46   Total dispersion factor versus wavelength with the first clad radius of the triple clad optical fibre as a parameter.
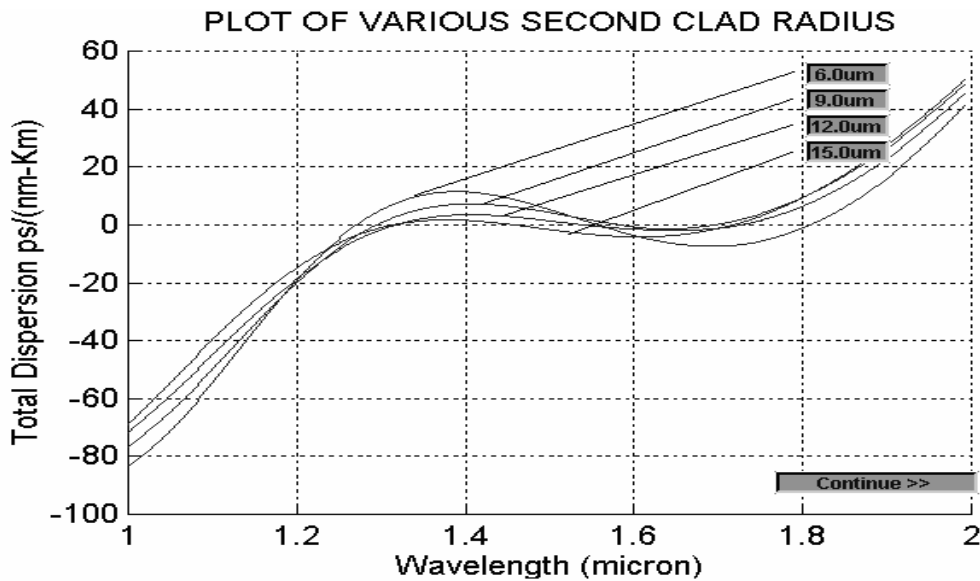
Figure V-47   Total dispersion factor versus wavelength with the second clad radius of the triple clad optical fibre

Therefore it can be concluded that the change in core radius, a_0 is very sensitive to the total dispersion (i.e. 88.88 unit dispersion per μm) as compared to that of the outer radius of the second layer a_2. Thus for the triple-clad fibre the selection of a_0 is very critical to achieve a specific non-zero dispersion factor. The sensitivity of each core radius is compared with respect to that of the second cladding layer and tabulated in *Table V-10* that reconfirms that the

most sensitive factor is the central core radius. Thus the manufacturing tolerance of the fibre core radius must be controlled accurately as compared to those of the cladding layers.

	a_0	a_1	a_2
Normalised Sensitivity	89.7	65.3	1

Table V-10 Normalised sensitivity comparison of core, first and second cladding radius

C.5.b.   *Effects of Refractive Indices of thecladding layers on the total dispersion*

Figs V-48 to V-51 show various curves representing the ratio of the core and cladding refractive indices versus the total dispersion parameter. The following effects of each core/cladding radius on the total dispersion factor can be noted:

(i)   As the core RI, n_0, is reduced, the total dispersion curve shifts upwards. A maximum sensitivity of incremental changes in n_0 to fibre total dispersion is 50,000 ps/(nm-km) per unit RI is obtained.

(ii)   When the first cladding RI, n_1, is increased the total dispersion curve shifts upwards but the first zero dispersion point shifts to higher wavelength region. A maximum sensitivity of incremental changes in n_1 to total dispersion is 59,200 ps/(nm-km) per unit RI is obtained.

(iii)   As the second cladding RI, n_2, is decreased the total dispersion curve shifts upwards but the first zero dispersion point shifts to lower wavelength region. Meanwhile, the second zero dispersion point remains almost unchanged. A maximum sensitivity of incremental change in n_1 to total dispersion of 6666 ps/(nm-km) per unit RI is obtained
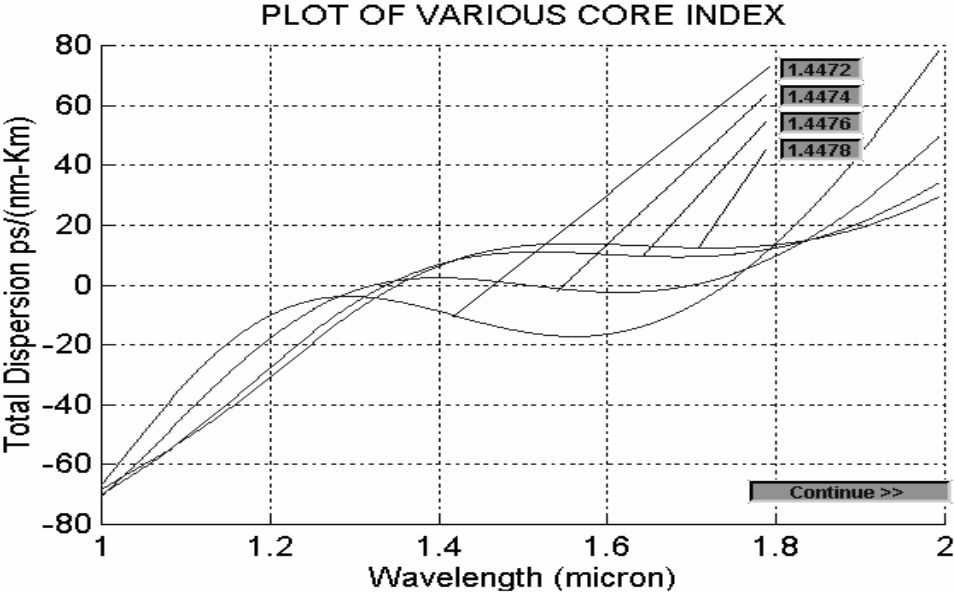
Figure V-48   Total dispersion factor versus wavelength with   the core RI of the triple clad optical fibre as a parameter.
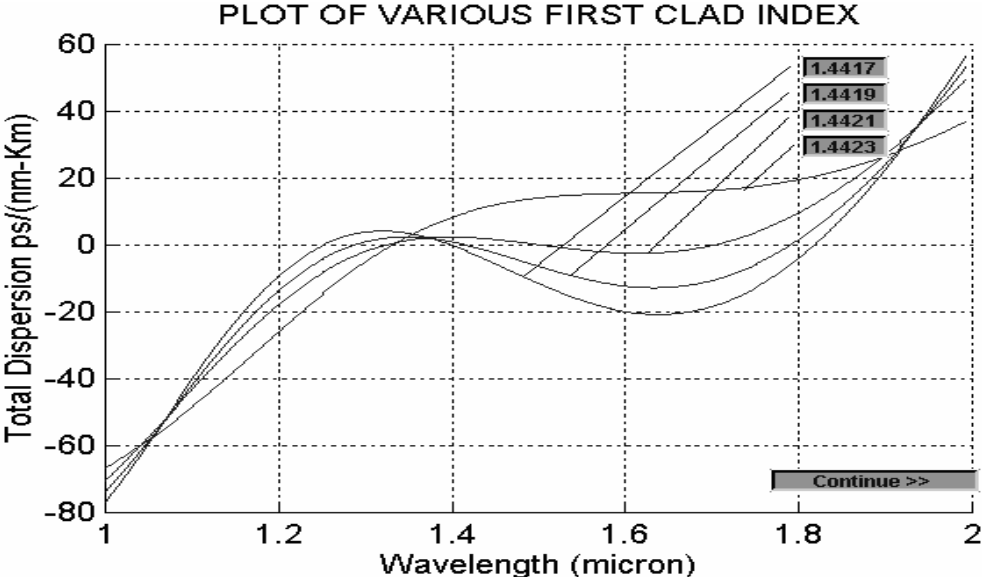
Figure V-49   Dispersion factor versus wavelength with the first cladding RI of triple clad profile as a parameter.
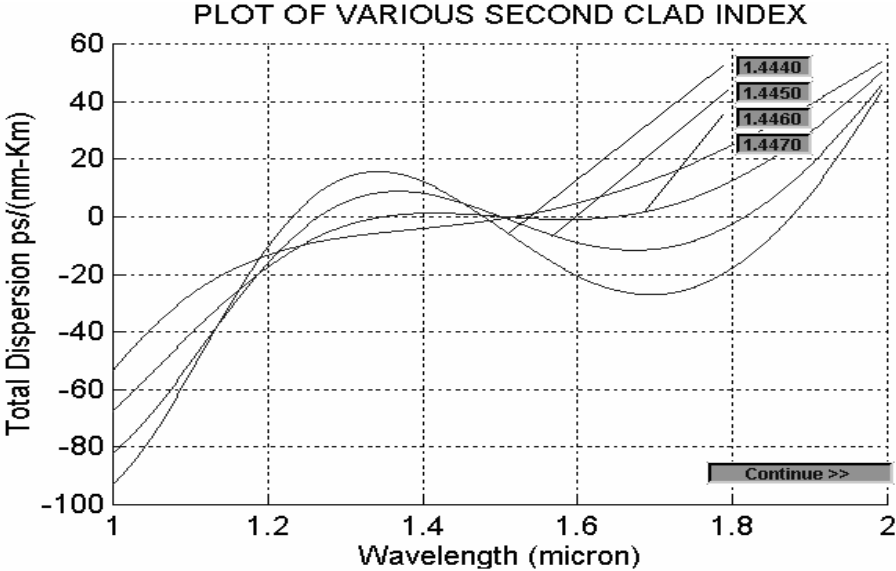
Figure V-50 Total dispersion factor as a function of the second cladding RI of the triple clad profile
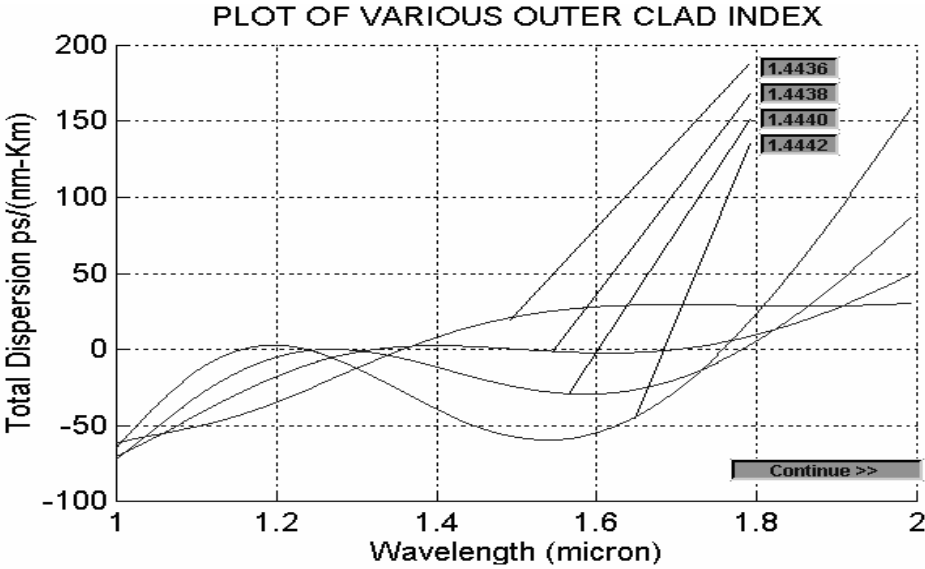
Figure V-51   Total dispersion parameter varies with variation of the outer cladding RI of the triple clad profile.

(iv) As the outer cladding RI, n, is decreased the total dispersion curve shifts upwards but the first and second zero dispersion points are shifted to higher wavelength region. We obtain a maximum sensitivity of changes in n_1 to fibre total dispersion of about 142,850 ps/(nm-km) per unit RI.

We thus conclude that changes in outer cladding RI, n is sensitive to the total dispersion (i.e.142,850 unit dispersion per unit RI) compared to the n_2. Hence selecting n is very critical in the design of triple-clad step-index optical fibres. The normalised sensitivity of the refractive indices of the core and the cladding layers with respect to the RI of the third cladding layer n_2 is tabulated in Table V-11. This layer is chosen for normalization due to its closeness to the cladding outer most cladding layer. It shows clearly that the outer most cladding layer is the most sensitive.

	n_0	n_1	n_2	n
Normalised Sensitivity	7.50	8.88	1.00	21.43

Table V-11   Normalised sensitivity comparison of core, first, second and the RI of the outer most cladding region.

Ref [47] has addressed the strong impact of third cladding on the characteristics of DCF, especially Waveguide Dispersion and the dispersion can be achieved on a wide range. This conforms with the previous remarks stated above.

C.6 Effect of Doping Concentration on the Total Dispersion

Fig. V-52 indicates that increasing doping concentration would shift the total dispersion curve down slightly. The change is minute. An estimate change of 0.5 unit dispersion per unit concentration is measured. Thus the doping concentration in the core region does not play a major role in the flattening of the total dispersion curve.

Hence, the doping concentration would thus now be the last factor to be considered for the design of triple-clad step-index fibres. This factor contributes significantly to the fibre attenuation.
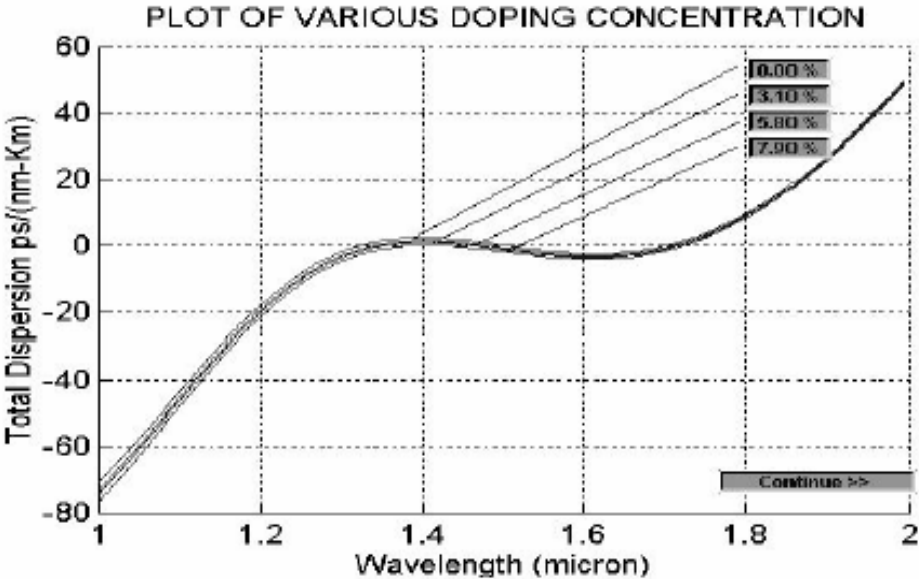
Figure V-52   Total dispersion factor varies with variation of doping concentration of the triple clad profile

In summary, the design of multi-clad DCF fibres have been thoroughly investigated and discussed in the last two sections. The design methodology and the effects of the fibre parameters on the properties and characteristics of the DCF fibres have been shown. Section VI discusses about the design of DCF for discrete/lumped Raman amplification (DCF-DRA). A new, simple but comprehensive method for designing a single-pump DCF-DRA has been developed.

VI. Fiber Design for Raman Amplification

A. Non-linear Effects

The non-linear effects can be classified into two categories based on stimulated scattering and intensity-dependent properties of the fibre. The first category is due to the scattering effects of the interaction of light waves with molecular vibrations in silica medium. Examples of this category are s*timulated Brillouin scattering* (SBS) and *stimulated Raman scattering* (SRS). The non-linear effects in the second category stem from the variation of refractive index due to its dependence on the intensity of the travelling signals. This category includes *four-wave mixing* (FWM), *self-phase modulation* (SPM) and *cross-phase modulation* (CPM). A fibre can be considered as a linear medium provided that the power of a signal traveling in an optical fiber is relatively small. The threshold power for non-linearity to occur can be estimated based on the non-linear coefficients and the loss profile of the fibre.

In modern optical communications, chromatic dispersion plays a key role in reducing the effects of nonlinearities where Nonzero dispersion fiber (NDF) being installed to new WDM systems set a clear example for this purpose where the Four Wave Mixing problem can be completely avoided.

- **Stimulated Brillouin scattering (SBS)**

SBS is created by the interaction between the incident light and the acoustic vibratin in the fibre. Similarly to SRS, SBS also generates the amplification for the signal at longer wavelengths or lower frequencies. However, unlike SRS, SBS depletes the transmitted signal by producing gain in the direction opposite to signal propagation, that is, back toward the source. SBS does not cause interaction between different wavelengths as long as the wavelength spacing is greater than 20 MHz, but can cause significant distortion within a single channel. The interaction gain bandwidth of SBS is much smaller than that of SRS.

- **Four-wave mixing (FWM)**

Four-wave mixing (FWM) induces new signals that appear as crosstalk to the existing signals. The phenomenon occurs when the signals travel at the same phase velocity in other words, there are no delays among them and the dispersion is approaching to zero. When signals propagate along the fibres at frequencies f_1, f_2, f_3, the non-linear interactions among these signals can result in FWM with the production of a new channel at

$$f_{FWM} = f_1 + f_2 - f_3 \qquad \text{(VI-1)}$$

The FWM effect is independent of the bit rate but is highly dependent on frequency channel spacing and it is reduced when dispersion is present. A commercial example is the NZ-DSF which is designed to let a small dispersion exist within the operating frequency or wavelength band.

- **Self-phase modulation (SPM)**

SPM arises due to the intensity-dependent characteristics of the fibre. The fluctuations in the optical power of a signal varies the refractive index property, and thus the propagation constant, which then leads to changes in signal phase. Different parts of a pulse, as a result, undergo different phase shifts, which cause pulse *chirping* and spectral broadening. The impairments due to SPM are significant mainly in high bit rate (over 10 Gb/s) systems.

- **Cross-phase modulation (XPM)**

The intensity dependence of the fibre refractive index can also lead to the XPM non-linear phenomenon. However, in this case, the total non-linear phase shift on a given channel is created due to the combined intensities of all transmitted channels, which may cause the cross-talk problem in WDM system. XPM becomes a problem if the wavelength channel spacing is relatively narrow(a few tens of GHz).

B. Stimulated Raman Scattering for Amplification

Stimulated Raman scattering (SRS) causes power to be transmitted from lower- wavelength channels to higher-wavelength channels, known as Stoke signals. The gain coefficient is a function of wavelength spacing. SRS occurs when the transmitted power of the channel exceeds a certain level, which is known as the threshold power. For a single-channel lightwave system, it has been shown that the threshold power P_{th} is given by [3]

$$P_{th} = \frac{16 A_{eff}}{k_P L_{eff} g_{R\_max}} \qquad \text{(VI-2)}$$

k_P is the polarization factor having the value between 1 when the polarizations between Stokes signal and pump are preserved and 1/2 when the polarizations are completely scrambled. $L_{eff} = [1 - \exp(-\alpha_P L)]/\alpha_P$ is the effective length of the fiber[30]. In the case of continuous-wave (CW) and quasi-CW conditions, the nonlinear interaction between the pump and Stokes waves of Stimulated Raman Scattering(SRS) is governed by the following set of two coupled equations:

$$\frac{dI_S}{dz} = g_R I_P I_S - \alpha_S I_S$$

$$\qquad \text{(VI-3)}$$

$$\frac{dI_P}{dz} = -\frac{\omega_P}{\omega_S} g_R I_P I_S - \alpha_P I_P$$

where $I_P, I_S, \alpha_P, \alpha_S, \omega_P, \omega_S$ are the intensity, the attenuation and frequency of pump and signal respectively.

The gain provided by Raman amplification can be obtained from the above equations. With the common assumption that the intensity of signal remains much smaller than the pump intensity, the Raman amplification gain can be expressed:

$$G_A = \exp(g_R P_0 L_{eff} / A_{eff}) \qquad \text{(VI-4)}$$

where $P_0 I_0 A_{eff}$ is the pump power; $L_{eff} = [1 - \exp(-\alpha_P L)]/\alpha_P$ is the effective length of the fiber.

One of the most important parameters for Raman amplification in any applications is the Raman effective gain coefficient, which is defined as

$$g_{eff}^{R} = \frac{g_R}{A_{eff}}$$ where g_R is the Raman Gain coefficient.

The effective Raman gain coefficient depends not only on the Raman gain coefficients itself but also on the effective area of the fiber. It hence leads to the significance of designing a fibre with small effective area in order to achieve high gain. In addition, flattening the Raman gain coefficient as much as possible is also a desirable need.

DCF fibre is an excellent gain medium for discrete Raman amplifiers [48] which have already been started to be widely deployed in the long-haul transmission systems. The advantages of Raman amplification using DCF fibre are to be discussed in the next section

B.1 Advantages of DCF as a lumped/discrete Raman amplifier (DRA):

- Due to high anomalous negative dispersion as designed in Part II, the deployed DCF can be just a few kms long, which also meets the requirement of Discrete Raman amplification.
- Small effective area and high Ge concentration gives higher Raman gain efficiency, which results in less Threshold Power to excite Raman Amplification.
- Gives additional flexibility in system.
- Saves space
- Potentially low cost.

It is also known that the threshold power is linearly proportional to the effective area.

$$P_{th} \propto \frac{\lambda A_{eff}}{2\pi n_{NL} L_{eff}} \tag{VI-5}$$

where n_0 = Refractive index of the fibre core at low optical power levels.

n_{NL} = the nonlinear refractive index coefficient which varies from 2.35×10^{-20} to approx. $3.2 \times 10^{-20} \text{m}^2/\text{W}$

P_{th} = Optical threshold power in Watts

Thus, a smaller value of A_{eff} gives smaller threshold power, i.e less power required to excite the SRS for amplification, hence less cost since the high power laser sources are expensive.

The A_{eff} parameter has been shown to be one of the most important properties of the DRAs. It is therefore of concern to point out the assumption and the equation implemented to find the effective area. The transverse modal profile was assumed to be approximately equal to that of the laser pump source. Besides, in the case of Gaussian assumption for the radial intensity distribution of the mode, the effective area for Raman amplification can be approximated as: [49, 50]

$$A_{eff}(\Delta \upsilon, \lambda_p) = \frac{A_{eff}(\lambda_s) + A_{eff}(\lambda_p)}{2} \qquad \text{(VI-6)}$$

where $\Delta \upsilon$ is the waveshift; λ_s and λ_p are signal and pump wavelengths respectively

$$A_{eff} = \pi \omega_{eff}^2 \qquad \text{(VI-7)}$$

B.2 Spectrum of Raman Amplification

The Stoke signals generated by SRS are shifted towards the longer wavelengths. The peak gain occurring at the first Stoke signal is about 100nm shift from the pump wavelength or about 440 cm^{-1} in wavelength number and approximately 13 THz shift in frequency domain.. The shape and the peak gain value varying with different amount of Germanium doping concentrations are illustrated in Fig. IV-1. It is shown that the Raman gain spectrum extends over 20-30 THz
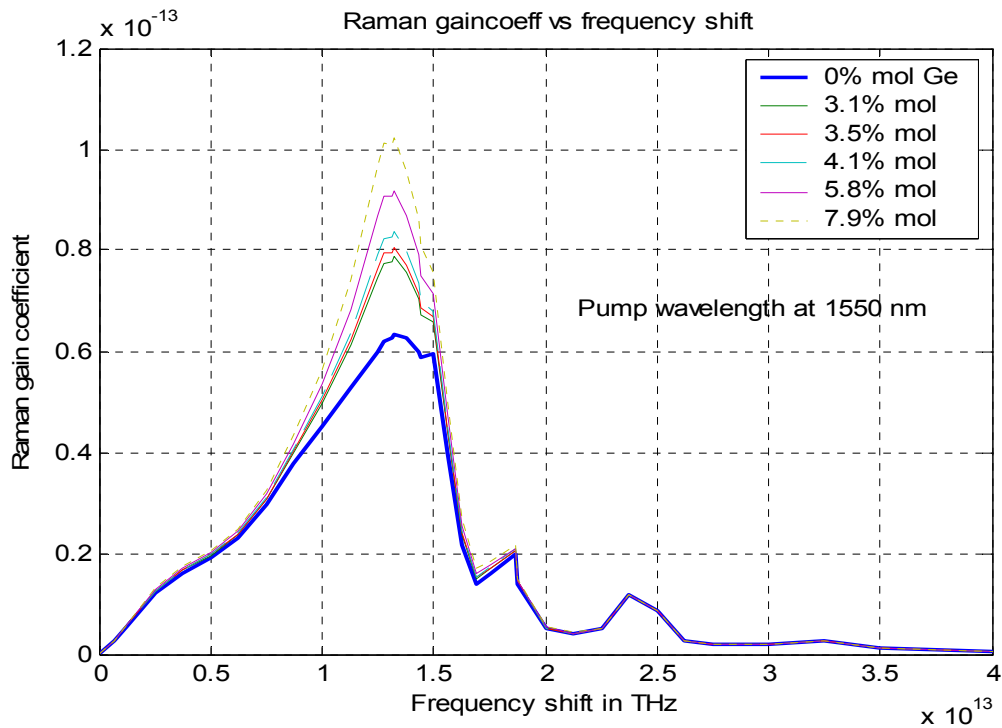
Figure VI-1: Spectrum of Raman Gain Coefficient with various
Germanium doping concentrations.

The Raman gain spectrum for pure bulk Silica with pump signal at 1.55 μm was achieved by segmenting the experimental graph obtained in Ref [51]. However, the actual Silica Raman gain spectrum used in the simulation is at the pump wavelength of 1.46 μm, which is utilized to amplify the signals operating in C-band. Thus, scaling of the Raman gain is required. It is important to note that the Raman gain spectrum is inversely proportional to the pump wavelength.

B.3 Key Equations to obtain Germanium-doped Raman gain spectrum

Obtaining a precise Raman gain is very significant in order to give good computational results of the discrete/lumper Raman amplifier using DCF fibre. From Ref.[52],[53] and [54], the method of predicting Raman gain spectrum with a certain amount of GeO_2 doping concentrations are obtained. The linear regression curve has been introduced. The linear relation between the RI and the Germanium doping concentrations has also been compared with [14] and illustrated as follows:
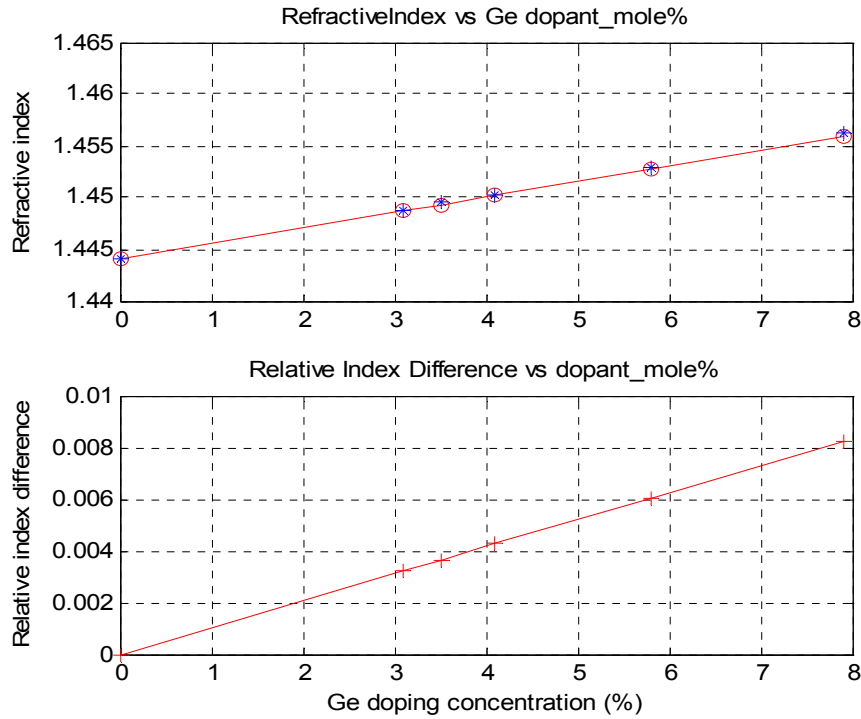
Figure VI-2: Linearity of refractive index with Germanium doping concentration

In *Fig.IV-2*, the RI corresponding to different Ge-doped concentrations follows a linear equation and verified with the actual RIs obtained from the Sellmeier 's coefficients.

The spectral profile of Raman gain spectrum $g(\Delta f)$ can be expressed as follows [53]

$$g(\Delta f) = \frac{\sigma_0(\Delta f)\lambda^3}{c^2 h n(\Delta f)^2} \tag{VI-8}$$

where Δf is the frequency-shift between the pump and the first Stoke signal ; n is the refractive index and $\sigma_0(\Delta f)$ is zero-Kelvin Raman cross-section [54, 55], which is defined as

$$\sigma_0(x_{GeO_2,}\Delta f) = \left[1 + C(\Delta f) \times x_{GeO_2}\right] \times \sigma_0(x_{SiO_2,}\Delta f) \tag{VI-9}$$

where $C(\Delta f)$ is the Linear Regression Coefficients, which has the profile:
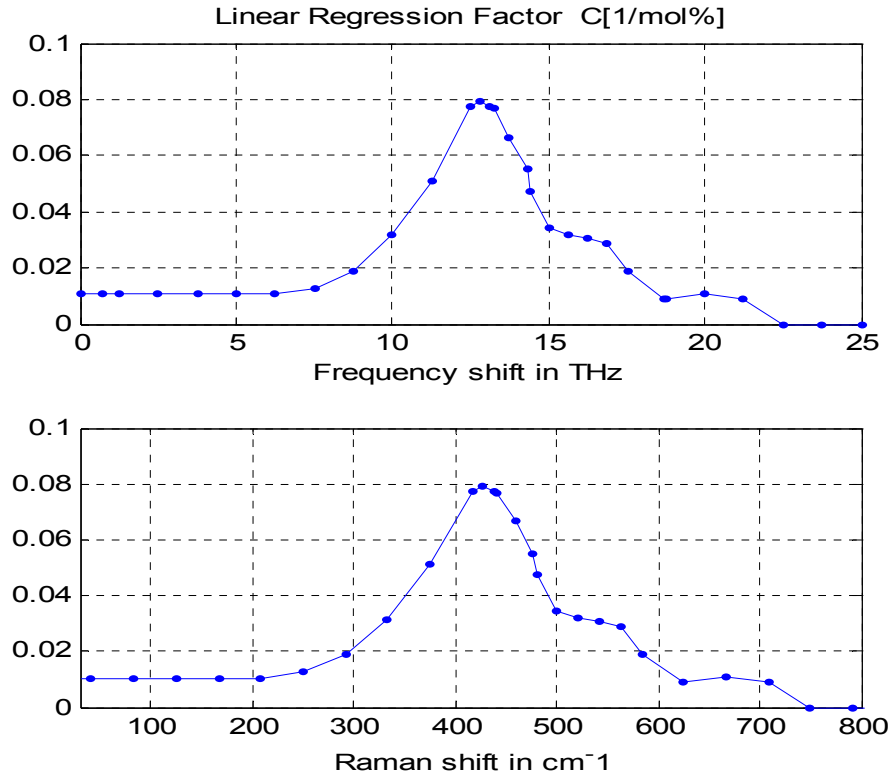
Figure VI-3: Linear Regression Factor

From the above equations, the Raman Gain coefficients of a particular GeO_2 doping concentration can be achieved from the Raman spectrum of pure silica

$$g(x_{GeO_2}, \Delta f) = \left[1 + C(\Delta f) \times x_{GeO_2}\right] \times g(x_{SiO_2}, \Delta f) \times \left(\frac{n_{Si}}{n_{Si-Ge}}\right)^2 \qquad \text{(VI-10)}$$

for a relatively small amount of GeO_2 doping concentration on pure silica, the difference between two refractive indices is negligible. Therefore, the Raman gain spectrum utilized in the simulation can be implemented as follows :

$$g(x_{GeO_2}, \Delta f) = \left[1 + C(\Delta f) \times x_{GeO_2}\right] \times g(x_{SiO_2}, \Delta f) \qquad \text{(VI-11)}$$

where $\Delta = \dfrac{n_{core} - n_{clad}}{n_{core}}$

This approach for the Raman gain is implemented in the simulation.

B.4 Design Methodology for DCF - DRAs

The technique focuses on single pump to avoid the interactive interferences between the pumps with the asymptotic approximation for Raman Gain within C-band (30 nm bandwidth). The insight of this technique is discussed in detail.

From the Refs. [45, 56], the idea of an algorithm to design a DCF for controlling the Raman gain is sought.

- Defining the normalized far-field RMS spot size $\bar{\omega} = \dfrac{\omega_0}{a}$ where $\bar{\omega} = \dfrac{2\displaystyle\int_0^\infty \psi^2(R)RdR}{\displaystyle\int_0^\infty \left[\psi'(R)\right]^2 RdR}$

where R = r/a is the normalized distance with respect to the core radius

- $\bar{\bar{\omega}}$ places a lower bound on the microbending loss [57] and useful for calculations of the splice loss due to small offsets. More importantly, it was proven to be directly related to the measurable root-mean square (RMS) width of the far-field spot size [58].

The relation existing between this normalized far-field RMS spot size and the waveguide dispersion has been presented In Ref [45]:

$$\frac{d(bV)}{dV} - b = \frac{4}{V^2\varpi^2} \tag{VI-12}$$

where b(V) is the normalized propagation constant.

The equation is then rearranged to be:

$$\varpi^2 = \frac{4}{V^2\left[\dfrac{d(bV)}{dV} - b\right]} = \frac{4}{V^2\left[\left(V\,^{db(V)}\!\big/_{dV} + b\,^{dV}\!\big/_{dV}\right) - b\right]} \tag{VI-13}$$

Hence, the equation can be simplified to be:

$$\varpi^2 = \frac{4}{V^3 \times \dfrac{db(V)}{dV}} \tag{VI-14}$$

Moreover,

$$b(V) = \left(1.1428 - \frac{0.996}{V}\right)^2 \tag{VI-15}$$

The relative error is less than 2% for 1<V<3.

$$\frac{db(V)}{dV} = 2 \times \left(1.1428 - \frac{0.996}{V}\right) \times \frac{0.996}{V^2} \tag{VI-16}$$

From *Eq. VI-14* and *VI-16*, it can be derived that

$$\varpi^2 = \frac{4}{2.27646V - 1.984} \tag{VI-17}$$

Therefore, the spot size can be calculated as:

$$\varpi_0{}^2 = \frac{4 \times a_{eff}^2}{2.27646V - 1.984} \tag{VI-18}$$

Thus the effective area is

$$A_{eff} = \pi \varpi_0{}^2 = \frac{4 \times \pi a_{eff}^2}{2.27646V - 1.984} \tag{VI-19}$$

In the case of Gaussian assumption for the radial intensity distribution of the mode, the effective area for Raman amplification can be approximated as: [49, 50]

$$A_{eff}(\Delta f, \lambda_p) = \frac{A_{eff}(\lambda_s) + A_{eff}(\lambda_p)}{2} \tag{VI-20}$$

The effective Raman gain

$$g_{eff} = \frac{g_{Raman}}{A_{eff}(\Delta f, \lambda_p)} \tag{VI-21}$$

As known,

$$V = \frac{2\pi}{\lambda} a n_2 \sqrt{\frac{n_1 - n_2}{n_2}} = \frac{2\pi}{\lambda} a n_2 \sqrt{2\Delta} \tag{VI-22}$$

Defining the variable:

$$X = a n_2 \sqrt{2\Delta} \quad \text{Thus, } V = \frac{2\pi}{\lambda} X \tag{VI-23}$$

❖ *The X-variable is the key parameter which gives the options for the design of DCF-DRAs. The solutions of X-variable are derived from (VI-24) – (VI-26).*

- In order to control the flatness of effective Raman gain over 30 nm bandwidth of C-band, we may simply control the values of the two ends which are located at 1530 nm and 1560 nm. In this method, the Raman gain within the C-band operating wavelength is asymptotically approximated.
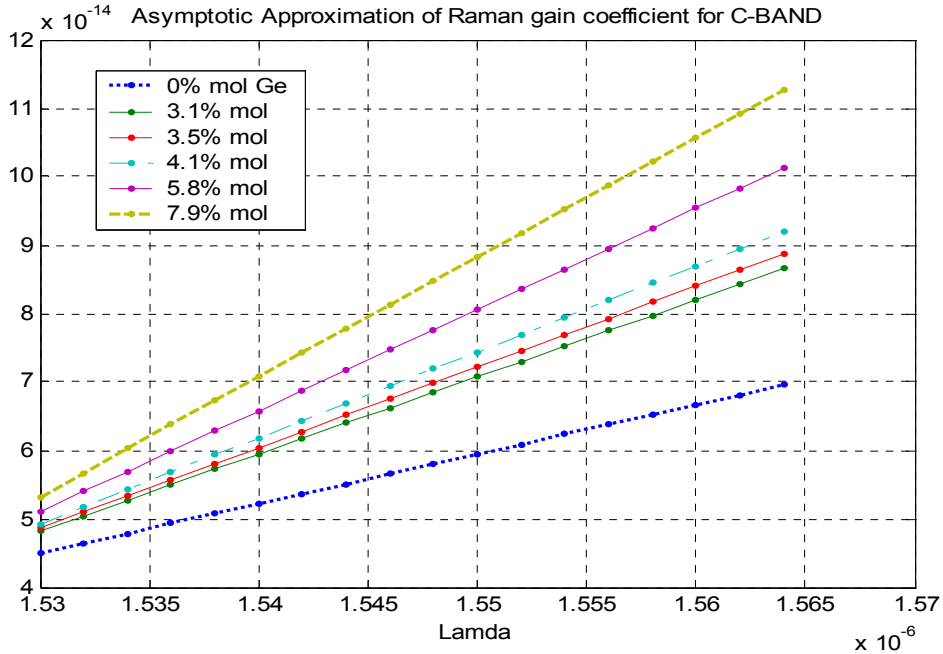
Figure VI-4: Asymptotic approximation of Raman gain within C-band

- In the other hand, since the known curves of the spot size and hence the effective area are hyperbolic, the effective Raman gain can not be perfectly flattened and a level of gain tilt is expectedly to exist and considered to be the ripple created by the single pump. The value of the tilt or the curvature of the effective gain are optimally determined depending on the feasibility of the design solutions for DCF.

- Defining the gain tilt to be K_{tilt} and manipulating the two ends of the effective Raman gain, which is:

$$g_{eff\_1560} = K_{tilt} g_{eff\_1530} \tag{VI-24}$$

$$\frac{g_{R\_1560}}{A_{eff}(\Delta f)_{1560}} = K_{tilt} \frac{g_{R\_1530}}{A_{eff}(\Delta f)_{1530}} \tag{VI-25}$$

The equation showing the control technique for the effective Raman gain of DRAs over the C-band is formulated as follows:

$$\frac{g_{R\_1560}\left(\dfrac{2.27646\times 2\pi}{\lambda_{1560}}X - 1.984\right)}{\left(\dfrac{2.27646\times 2\pi}{\lambda_{1560}} + \dfrac{2.27646\times 2\pi}{\lambda_{pump}}\right)X - 2\times 1.984} = K_{tilt}\frac{g_{R\_1530}\left(\dfrac{2.27646\times 2\pi}{\lambda_{1530}}X - 1.984\right)}{\left(\dfrac{2.27646\times 2\pi}{\lambda_{1530}} + \dfrac{2.27646\times 2\pi}{\lambda_{pump}}\right)X - 2\times 1.984}$$

$$(VI\text{-}26)$$

- Rearranging the above equation, a quadratic equation is obtained and hence the solutions can be derived. These solutions are correspondent to various amount of doping concentrations of Germanium in the core. The solution determines the gain tilt of the effective single-pump Raman gain and is then used for the design of an appropriate DCF profile of this DCF-DRA.

B.5 Design Steps:

- Since $x = an_2\sqrt{2\Delta}$, it can be seen that a solution of x may give various options for the design according to different combination of the values of the core radius (a) and the inner cladding RI (n_2). In our design, n_1 is known as it is the core material with a specific Germanium doing concentration.

- From the solution derived above, the core radius and the RI of the core and the inner-cladding have been found. These parameters of DCF are utilized for controlling and estimating the effective Raman gain of the DRAs. However, these design solutions are only selected when they also show a feasible design to achieve a good DCF profile. This can be obtained based on the consideration of the normalized frequency V-value.

- The unknown design parameters are then optimized to achieve a good compensation scheme for simultaneously compensating the dispersion and the dispersion slope.

- The method can also be inversely used to estimate the gain tilt when the profile of DCF fibre has already been aware. By knowing the values of normalized frequencies V-values at 1.53 μm and 1.56 μm, the derived equation above can now be utilized for the calculation of the gain tilt.

B.6 Design Results

Profile 5 gives a good design for a DRA using DCF fibre. The gain tilt obtained is within the acceptable range and the DCF with high RDS and FOM is capable for compensation of high RDS transmission fibres. The profile parameters are described in Table VI-1 and the simulated results of are expressed in Table VI-2.

Core radius a (µm)	Inner-cladding radius b (µm)	Core RI (n_1)	Inner-cladding RI (n_2)	Outer-cladding RI (n)
1.31	2.751	1.4487 (3.1% Ge-doped)	1.4208 (5.05% F-doped)	1.42554

Table VI-1: Profile 5 for designing DCF – DRAs.

Gain Tilt (dB)	Dispersion (ps/nm.km)	Dispersion Slope (ps/nm^2.km)	RDS (nm^{-1})	Attenuation (dB/km)	FOM	λ_{C11} (µm)	Effective Area (µm^2)	Critical curvature (mm)
1.382	-300.65	-3.2379	0.01077	1.1672	257.59	0.80356	**6.9617**	11.77

Table VI-2: Design results of properties of profile 5

The graphical results are demonstrated in Fig.VI-5 to Fig.VI-12. The achieved results such as the Dispersion value, RDS, FOM, Attenuation ..etc are compared to those reported in [59], [60] and [61].
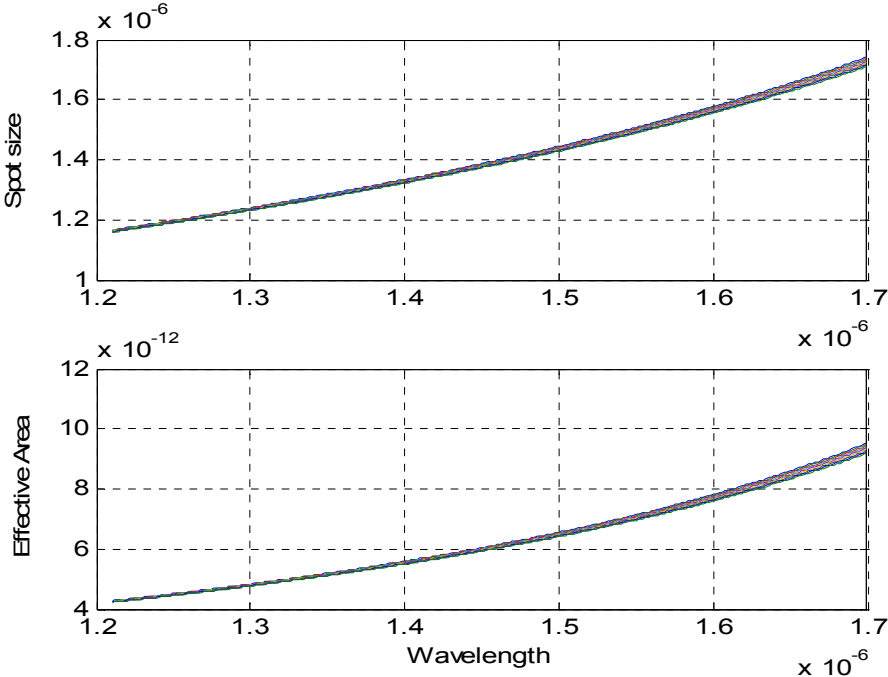
Figure VI-5: Effective Area of profile 5
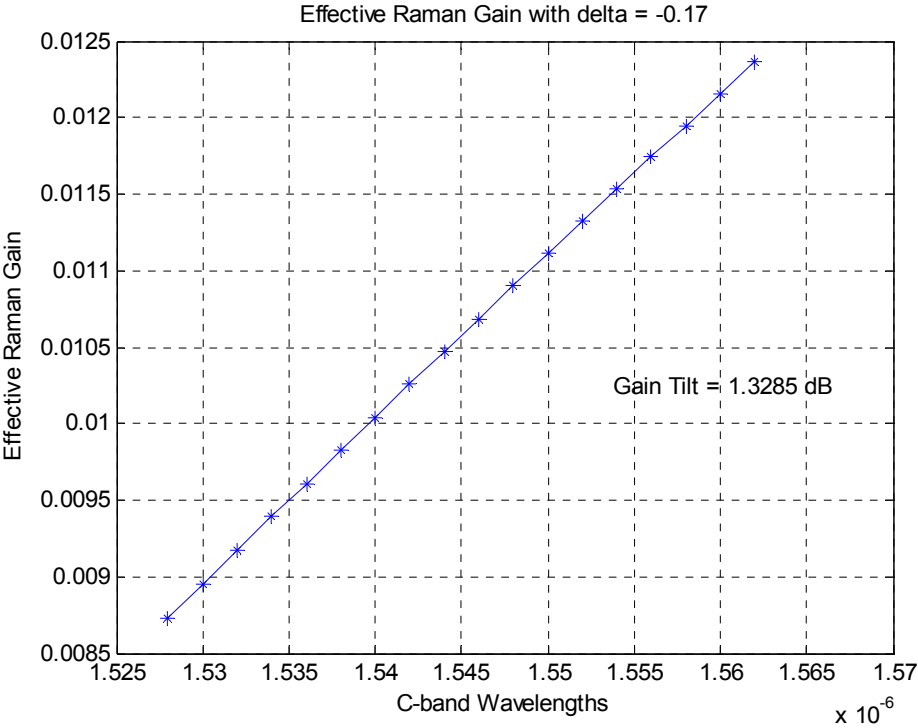
Figure VI-6: Effective Raman gain of profile 5

The gain tilt = 1.382 dB obtained in the Simulation as the result of the design of DCF whereas the predicted value *Ktilt* for solving the equation is 1.615 dB. The achieved results are compared to those reported in [59] and [60], in which the reported gain ripple of the DRAs are 2.3 dB and 1.2dB respectively**.**

- The slight difference in the values between the predicted and the simulated gain tilt has validated this fast, simple and relatively accurate way for designing DRAs on DCF fibre with single pump scheme. The DRAS utilizing multiple pump scheme can be developed from this methods by considering the gain tilt caused by each individual pump and superimposing the gain total. It is believed that the gain ripple in the multi-pump DRAs when properly designed is considerably reduced

- Comparing the properties of the designed DCF to those reported in to those reported in [59], [60] and [60], the obtained dispersion and dispersion slope hence RDS value are comparable and even relatively higher than those. However, the designed results need to be practically tested to claim the better performance.
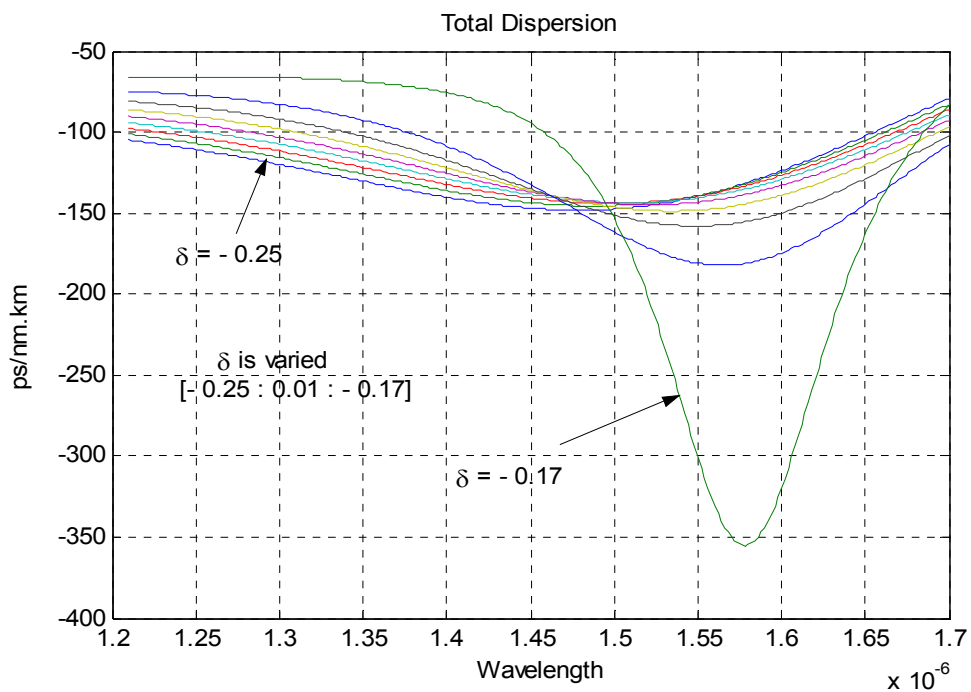
Figure VI-7: Total Chromatic Dispersion of profile 5

83
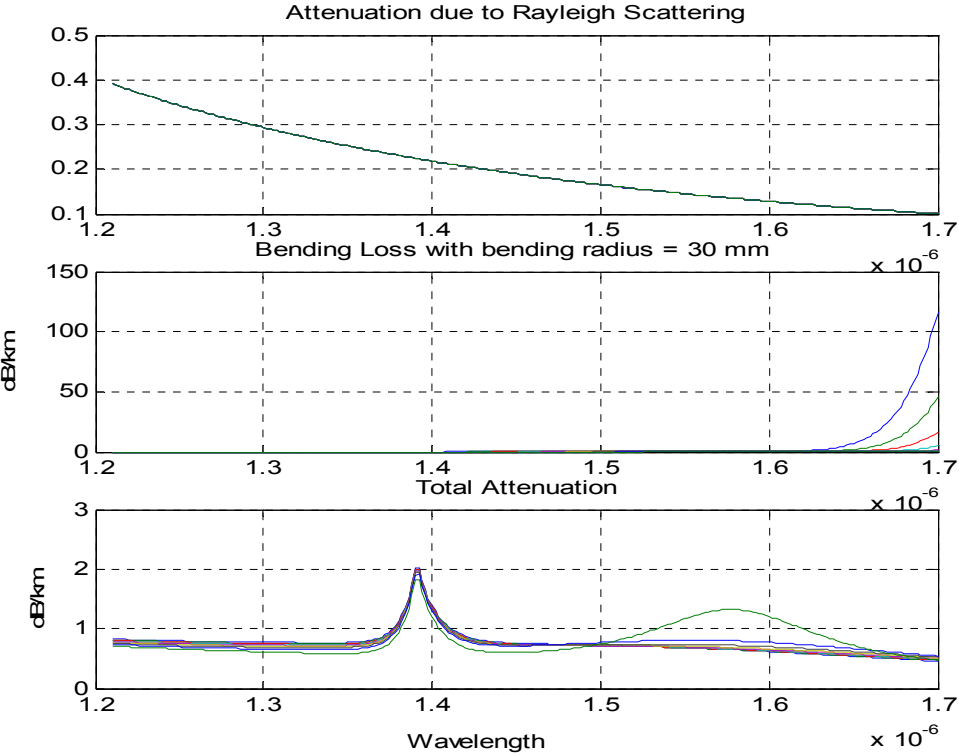
Figure VI-8: Total Attenuation of profile 5
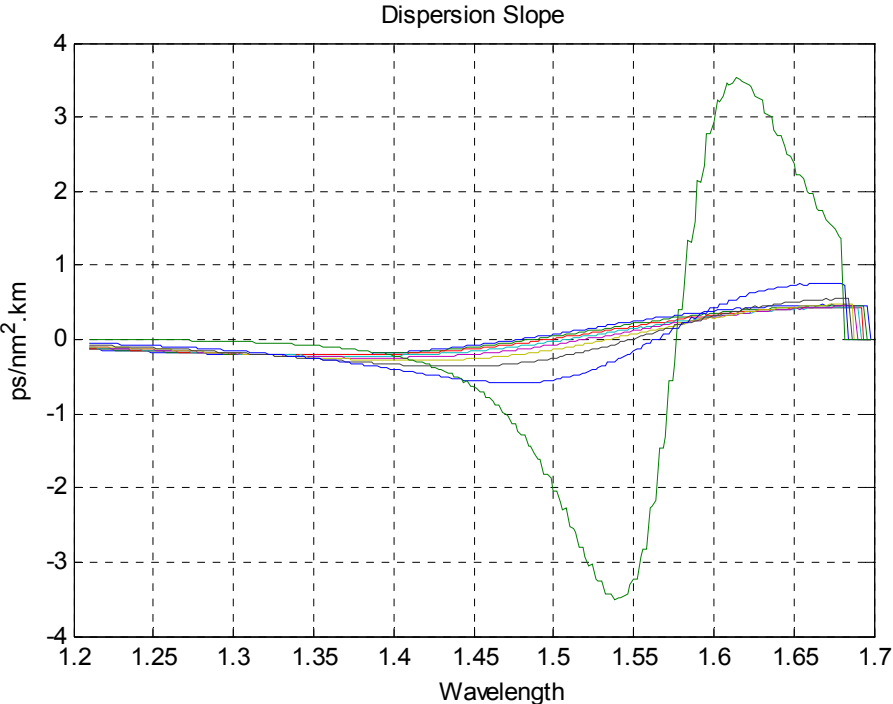
Figure VI-9: Dispersion Slope of profile 5
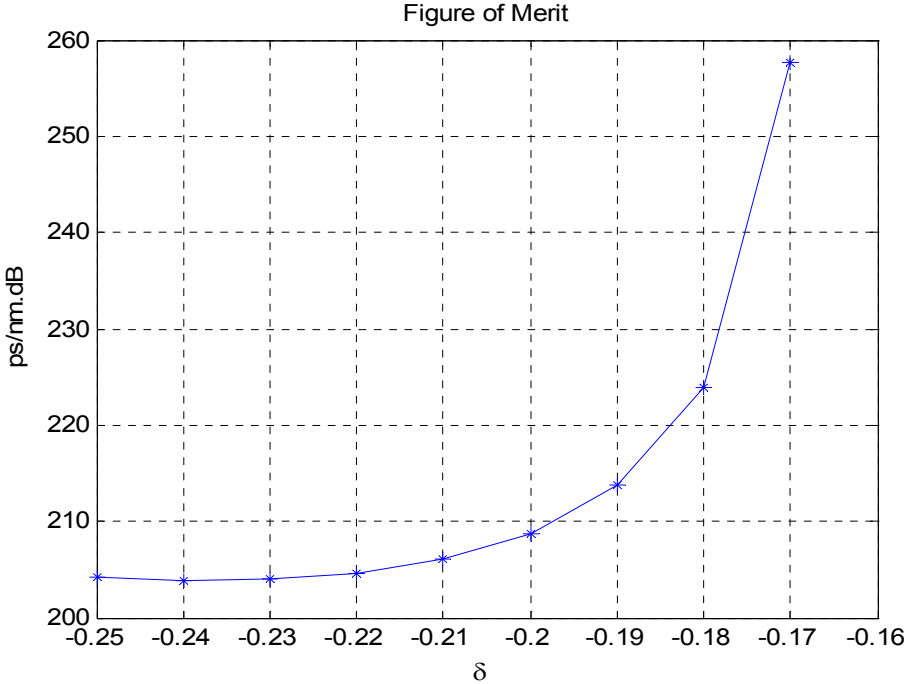
Figure VI-10: Figure of Merit of profile 5
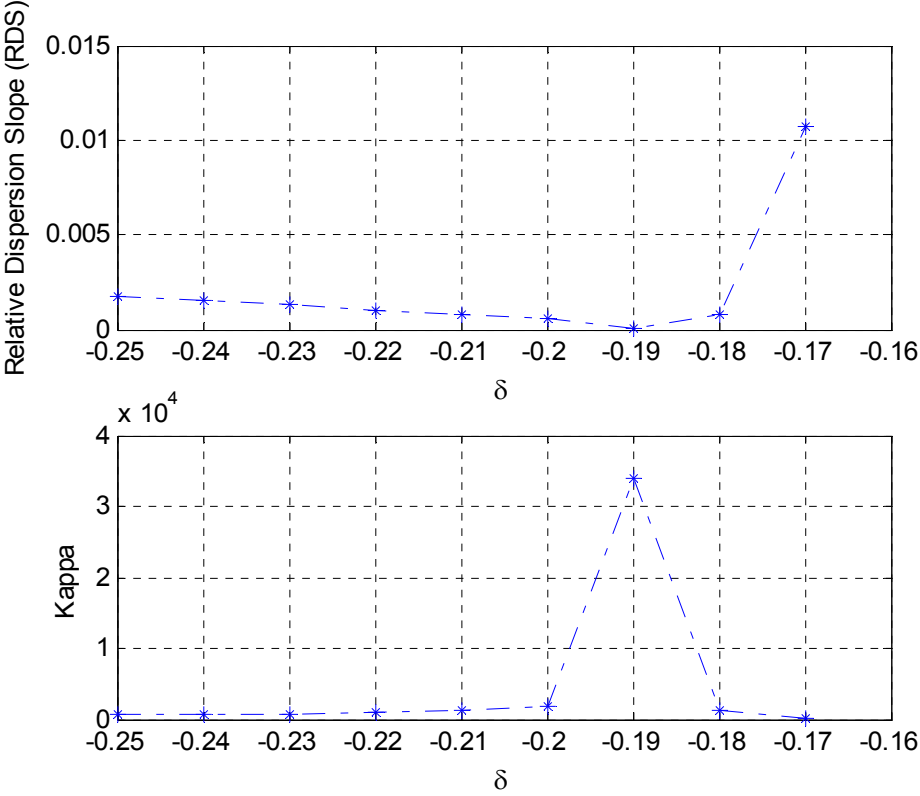
Figure VI-11 Relative Dispersion Slope and Kappa of profile 5
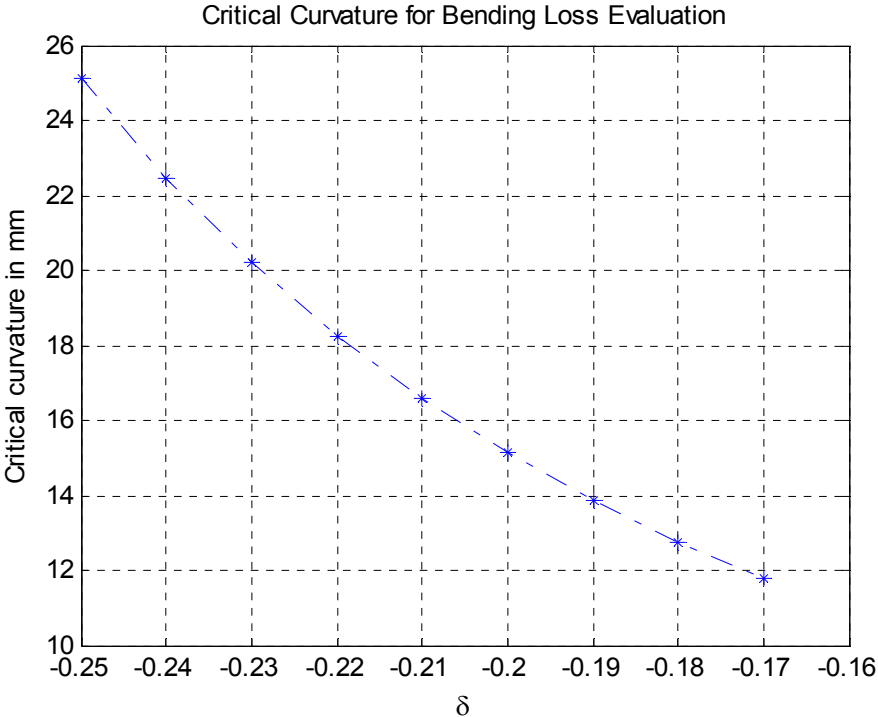
Figure VI-12 Radii of Critical Curvature of profile 5

In summary, a new and fast method for predicting and controlling the effective Raman gain of the DCF - DRAs has been successfully developed. The value of the effective Raman gain and especially its gain tilt caused by a single pump can be fast predicted. The obtained results have been compared to the reported data. The developed significantly reduces the complexity of numerical simulation and enables a simple but accurate second-order approximation for the effective Raman gain.

However, more efforts are needed to improve the currently developed technique so as to involve the effects of multi-pump sources on the effective Raman gain and predict its gain ripple which is created by the superimposition of those sources.

VII. Concluding Remarks

This technical report has comprehensively shown the design of profile-modified SI single mode fibre for dispersion compensation purpose that is critical to the scheme of dispersion management in ultra-long haul and high capacity modern DWDM optical systems. The

conventional SI fibre is added with multi- outer claddings in which the inner cladding profile is depressed with an amount of doped-Fluorine to have a low refractive index. The special characteristic MC-DCF gives anomalously high negative chromatic dispersion that is utilized in upgrading the currently installed systems. The DCF is designed to compensate not only for dispersion but also for higher-order dispersion or dispersion slope.

The ESI method and the enhancement method in approximating the dispersion have been addressed. The comprehensive analysis and design methodology or W-profile or double-clad fibre has been addressed in detail in section IV. The simulation results of the key required characteristics or properties of the DCF have also been achieved. Several profiles of the DCF designed for compensating the dispersion of SSMF and for high-slope NZ-DSF have also been recorded. Besides, Raman amplification on DCF has been increasingly become a critical demand in the system. . A quadratic relationship between dispersion and gain and gain tilt has been formed to permit the optimization of the design of DCF for Raman amplification. Therefore the design technique for discrete Raman amplifiers has been accomplished and a new and fast method for predicting and controlling the effective Raman gain of the DCF - DRAs has been developed in section V.

In conclusion, the detailed design of MC-DCF and DCF-DRAs have been comprehensively discussed. The future works involve the investigation of dispersion impacts in different photonic modulation formats in long-haul ultra-high speed optical transmission systems using the designed DCF as DRA and the role of dispersion impairments in photonic signal processing systems such as phased-controlled array antenna designed using photonic band-gap techniques.

VIII.   References

[1]   L. E. Nelson, Zhu, B & et al, "High-Capacity, Raman-Amplified Long-Haul Transmission and the Impact of Optical Fiber Properties," presented at Proceeding of SPIE, vol 5247, 2003.

[2]   S. N. Knudsen, "Design and Manufacture of Dispersion Compensating Fibres and Their Performance in Systems," *OFC*, 2002.

[3]   G. P. Agrawal, *Fiber-optic communications systems*, 3rd ed: John Wiley & Sons, 2001.

[4]   J. B. Jeunhomme, *Single Mode Fibre Optics, Principles and Applications*, 2nd ed ed: Marcel Dekker Pub, 1990.

[5]   E. Basch, E., (Editor in Chief), *Optical-Fiber Transmission*, 1st ed: SAMS, 1987.

[6]   R. Sammut, A., & Ghatak, A., K., *Opt. Quantum Electron.*, vol. 10, pp. 475-482, 1978.

[7]   C. Millar, "Direct Method for determining Equivalent Step Index profiles for monomode fibres," *Elect. Lett*, vol. 17, pp. 458-460, 1981.

[8]   F. Martinez, & Hussey,C.D., "ESI Determination from Mode-Field Diameter and Refractive Index Profile Measurements on single-mode Fibres," presented at IEE Proceeding, vol 135, Pt.J, June 1988.

[9]   H. Matsumura, & Suganuma, T., "Normalisation of Single-Mode Fibers having an arbitrary Index Profile," *Appl. Opt.*, vol. 19, pp. 3151-3158,1980., 1980.

[10]   X. Zhang, & Tian, X., "Analysis of Waveguide Dispersion Characteristics of WI- and WII-type Triple-Clad Single-Mode Fibers," Nov 2002.

[11]   A. Monerie, "Propagation in Doubly Clad Single Mode Optical Fibres," *IEEE J. Quant. Elect*, vol. vol QE-18., pp. 535-542, April 1982.

[12]   Y. Fang, "Equivalent Step-Index-fiber Method for Multicladding Fibers," *J.Lightwave Tech*, vol. 11, Oct 1993.

[13]   L. N. Binh, "Design guidelines for ultra-broadband dispersion flattened optical fibres with segmented core index profile," Dept. Elect. Comp. Syst. Eng, Monash Uni. Tech.Rept.No.ECSE14   -   2003, http://www.ds.eng.monash.edu.au/techrep/reports/post2003index.html.

[14]   L. N. Binh, "Optical Fibres for Ultra-High Capacity Communications Systems and Networks - ECE4405/5405 NOTES," Monash University, Australia, Melbourne July 2001.

[15]   M. Hirano, A. Tada, T. Kato, M. Onishi, Y. Makio, M. Nishimura, "Dispersion Compensating Fibre over 140 nm-Bandwidth," *Proc. 27th ECOC, Th.M.1.4*, pp. 494-495.

[16]   K. Thyagrajan, R.K.Varshney, P.Palai, A. K. Ghatak, and I.C. Goyal,, "Novel design of a dispersion compensating fibre," *IEEE Photonics Tech Lett*, vol. 8, pp. 1510-1512, Nov-1996.

[17]   A. Safaai-Jazi, and J.J.Lu, "Analysis and Design or Multi-Clad Single Mode with Three -Zero-Dispersion Wavelengths," presented at IEEE Proc., SouthEastcon, 1989.

[18]   G. Auge, Brehm, C., Heunhomme, L., and Sergent, L.C, "Parametric Study of Depressed Inner Cladding Single-Mode Fibers," *J. Lightwave Tech*, vol. LT-3, August 1985.

[19]   J. A. Antos, and smith, D.K, "Design and Characterization of Dispersion Compensating Fiber Based on the LP_{01} Mode," *J.Lightwave Tech*, vol. 12, October 1994.

[20]   B. J. Ainslie, and Day, C.R, "A review of Single-Mode Fibers with Modified Dispersion Characteristics," *J. Lightwave Tech*, vol. LT-4, August 1986.

[21]   L. N. Binh, and S.V. Chung, "A generalized approach to single-mode dispersion-modified optical fiber design," *Opt. Eng*, 1996.

[22]   Y. Liu, Da Silva V. L., Antos A. J. Bhagavatula, Chowdhury, D. Q., and Newhouse, M. A, "Single-mode dispersion shifted fibers with large effective area for amplified systems," presented at Postdeadline paper PD-2-9, Hong Kong, June 1995.

[23]   C. D. Poole, J.M. Wiesenfeld, D.J. DiGiovanni and A.M. Vengsarkar, "Optical fiber-based dispersion compensation using higher order modes near cut-off," *IEEE J. Lightwave. Tech*, vol. 12, pp. 1746-1758.

[24]   B. J. Ainslie, & Day, C.R., "A Review of Single-Mode Fibers with Modified Dispersion Characteristics," *J.Lightwave Tech*, vol. LT-4, pp. 967-979, Aug 1986.

[25]   J. Irven, Harrison, A.,P., & Smith C.,R., *Elect. Lett*, vol. 17, 1981.

[26]   B. J. Ainslie, & Day, C.R., & et al, *Elect. Lett*, vol. 15, pp. 411, 1979.

[27]   P. L. Francois, "Tolerance Requirements for Dispersion Free single-Mode Fiber Design: Influence of Geometrical Parameters, Dopant Diffusion and Axial Dip.," *IEEE J. Quant. Elect*, vol. QE-18, October 1982.

[28]   A. W. Snyder, "Understanding Mono-mode Optical Fibers," *Proc. IEEE*, vol. 69, pp. 6-13, Jan 1981.

[29]   S. N. Knudsen, Nielsen, L., & Pedersen, M, "Optimisation of Dispersion Compensating Fibres for Cabled Long-Haul Applications," *Elect. Lett*, vol. 36, Oct 2000.

[30]   G. P. Agrawal, *Non-Linear Fibre Optics*, 2nd ed: Academic Press 1995, 2001.

[31]   N. Shibata, Kawachi,M., & Edahira, T., "Optical Loss Characteristics of High GeO_2 Content Silica Fibres," *Transactions of IECE*, vol. E65, pp. 120, 1980.

[32]   A. Antos, J., Hall, D., W., & Smith, D.,K.,, "Dispersion Compensating Fibre for Upgrading Existing 1310 nm Optimised Systems to 1550 nm Operation," *OFC '93 Technical Digest*, pp. 204-205, 1993.

[33]   S. Kawakami, & Nishida, S, "Characteristics of a Doubly Clad Optical Fiber with a Low-Index Inner Cladding," *IEEE J.of Quantum Elect,*, vol. QE-10(12), pp. p. 879 - 887., 1974.

[34]   M. Monerie, "Analytical Approximation for W-Type Fibre Propagation Parameters," *Elect. Lett*, vol. 18, pp. 386-388, April 1982.

[35]   M. Monerie, "Fundamental-Mode Cutoff in Depressed Inner Cladding Fibres," *Elect. Lett*, vol. 18, July 1982.

[36]   L. N. Binh, D.L. David, & K.Y. Chin, "Wavelength Division Multiplexed Optical Communication Systems and Networks (WDM-MOCSS)," Monash University - Clayton, Australia, Department of Electrical and Computer Systems Engineering, Laboratory for Optical Communications and Applied Photonics 1997.

[37]   C. D. Poole, et al.,, "Broadband Dispersion Compensation by using the High Order Spatial Mode in a Two Mode Fibre," *Optics Letters*, vol. 17, pp. 985-987, 1992.

[38]   Y. Akasaka, Sgizaki, R., et al - (Furukawa Electric Co.Ltd, Japan), "High-Dispersion-Compensation Ability and Low Non-Linearity of W-shaped DCF," *OFC Technical Digest*, 1996.

[39]   F. Weling, "The Design of Dispersion Flattened Single-Mode Fibers," *Philips Research Laboratories*, 1988.

[40] H. Rudolph, D., & Neumann E.,G., "Approximations for the Eigenvalue of the Fundamental Mode of a Step Index Glass Fibree Waveguide," *Nachrichten Techn. Z.*, vol. 29, 1976.

[41] V. Srikant, "Broadband Dispersion and Dispersion Slope Compensation in High Bit Rate and Ultra-Long Haul Systems," *Optical Society of America, (OCIS codes: General)*, 2000.

[42] Y. a. H. C. D. Li, "Triple-clad single-mode fibers for dispersion flattening," *Opt. Eng*, vol. vol. 33, pp. 3999-4005, 1994.

[43] Y. Li, C.D.Hussey, and T.A. Birks, "Triple-clad single-mode fibers for dispersion shifting," *IEEE J. Lightwave Tech*, vol. LT-11, pp. 1812-1819, 1993.

[44] G. Cancellieri, *Single mode optical fibers*, 1st ed. Italy: Uni of Ancona, 1991.

[45] S. V. Chung, "Simplified analysis and design of single mode optical fibers," Monash University, Australia, 1987.

[46] MathWorks Inc., *MATLAB high performance numeric computation*, Aug. 1982.

[47] X. Zhang, & Tian, X., "Analysis of Waveguide Dispersion Characteristics of WI- and WII-type Triple-Clad Single-Mode Fibers," *Optics & Laser Technology*, vol. 35, pp. 237-244, November 2002.

[48] P. B. Gaarde, "Raman Amplification and Dispersion Compensation," presented at Conference of Advances in Raman-Based, High-Speed Photonics: Raman Amplifiers, Data Transmission, and Signal Processing, Los Alamos National Laboratory , USA, Feb 2003.

[49] W. P. L. Urquhart, P.J, "Effective Core Area for Stimulated Raman Scattering in Single-Mode Optical Fibres," *IEE Proceedings*, vol. 132, Pt. J, Aug 1985.

[50] K. Rottwitt, Bromage, J., & et al, "Scaling for the Raman Gain Coefficient: Applications to Germanosilicate Fibers," *J.Lightwave Tech*, vol. 21, pp. 1652-1662, July 2003.

[51] P. S. Andre᾽, Correia, R., & et al, "Raman Gain Characterisation in Standard Single Mode Optical Fibres for Optical su\imulation Purposes," *Optica Applicata*, vol. XXXIII, pp. 560-573, 2003.

[52]   K. Yuhong, "Calculations and Measurements of Raman Gain Coeffcients of Different Fiber Types," in *Department of Electrical Engineering*: Virginia Polytechnic Institute and State University, Dec 2002.

[53]   S. T. Davey, & et al, "Optical Gain Spectrum of GeO_2-SiO_2 Raman Fiber Amplifiers," *IEE Proceedings*, vol. 136 pT.j, pp. 301-304, Dec 1989.

[54]   F. Galeener, Mikkelsen, J.C. & et al, ""The Relative Raman Cross Sections of Vitreous SiO_2, GeO_2,B_2O_3 and P_2O5"," *Appl. Phys. Lett*, vol. 32, 1978.

[55]   N. Shibata, Horigudhi, M., & Edhario, T., "Raman Spectra of Binary High-Silica Glasses and Fibers Containing GeO_2, P_2O_5 and B_2O_3," *J. Non-Crystalline Solids*, vol. 45, pp. 115-125, 1981.

[56]   P. Sansonetti, "Modal Dispersion In Single-Mode Fibres: Simple Approximation Issued from Mode Spot Size Spectral Behaviour," *Elect. Lett*, vol. 18, July 1982.

[57]   K. Petermann, & Kuhne, R., "Upper and Lower Limits for the Microbending Loss in Arbitrary Single-Mode Fibres," *J.Lightwave Tech*, vol. LT-4, pp. 2-7, 1986.

[58]   C. Pask, "Physical interpretation of Petermann 's strange spot size for single-mode fibres," *Elect. Lett*, vol. 20, 1984.

[59]   G. L. Nielsen, Qian,Y., and et al, "Module for Simultaneous C+L-band Dispersion Compensation and Raman Amplification," *Optical Society of America*, vol. OCIS codes: (060.2360); (060.2320), 2002.

[60]   M. Wandel, Kristensen, P., & et al, "Dispersion Compensating Fibers for Non-Zero Dispersion Fibers," *Optical Society of America, (OCIS codes: 060.2280; 060.2230)*, 2001.

[61]   K. Aikawa, Suzuki, R., & et al, "High Performance Dispersion and Dispersion Slope Compensating Fiber Modules for Non-zero Dispersion Shifted Fibers," *Fujikura Technical Review*, 2003.

[62]   R. Minasian, & Alameh,K., "Photonic Signal Processing - Invited Paper," *supported by Australian Research Council, CSIRO and Australian Photonics CRC*, 2001.

IX. Appendix

Sellmeiere Constants	Gemanium Concentration, C (mole %)							
	0 (pure silica)	3.1	3.5	4.1	5.8	7.0	7.9	13.5
G_1	0.6961663	0.7028554	0.7042038	0.68671774	0.7088876	0.6869829	0.7136824	0.73454395
G_2	0.4079426	0.4146307	0.4160032	0.43481505	0.4206803	0.44479505	0.4254807	0.42710828
G_3	0.8974794	0.8974540	0.9074049	0.89656582	0.8956551	0.79073512	0.8964226	0.82103399
λ_1	0.0684043	0.0727723	0.0514415	0.072675189	0.0609053	0.078087582	0.0617167	0.08697693
λ_2	0.1162414	0.1143085	0.129160	0.11514351	0.1254514	0.11551840	0.1270814	0.11195191
λ_3	9.896161	9.896161	9.896156	10.002398	9.896162	10.436628	9.896161	10.48654

Table IX-1 Sellmeier's constants forGeO2 -doped materials